P-04-155

Forsmark site investigation

Petrophysical surface data Stage 2 – 2003 (including 2002)

Hans Isaksson, Håkan Mattsson, Hans Thunehed
Mikael Keisu, GeoVista AB

September 2004

Svensk Kärnbränslehantering AB
Swedish Nuclear Fuel
and Waste Management Co
Box 5864
SE-102 40 Stockholm Sweden
Tel 08-459 84 00
+46 8 459 84 00
Fax 08-661 57 19
+46 8 661 57 19

ISSN 1651-4416
SKB P-04-155

Forsmark site investigation

Petrophysical surface data
Stage 2 – 2003 (including 2002)

Hans Isaksson, Håkan Mattsson, Hans Thunehed
Mikael Keisu, GeoVista AB

September 2004

Keywords: Petrophysics, Gamma-ray spectrometry, Anisotropy, Magnetic susceptibility, AMS, Density, Porosity, Resistivity, Induced polarisation, AP PF 400-02-11; 400-02-47, Field note no Forsmark 30 (2002) and 32 (2003).

Abstract

This report presents all petrophysical surface data collected during 2002 and 2003. The purpose of petrophysical measurements is to gain knowledge of the physical properties of different rock types. This information is used to increase the understanding of geophysical measurements and to support the geological mapping.

The work comprises statistical processing and evaluation of results from the 2002 petrophysical sampling and gamma ray spectrometry measurements on outcrops, compiled with new results from further sampling and measurements in 2003. The analyses were made with respect to rock type characteristics and the geographical distributions of the measured properties. Tables summarizing the different petrophysical properties for each rock group are the main result of the work. The properties are:

- Volume susceptibility.
- Q-value.
- Density.
- Porosity.
- Resistivity.
- Induced polarisation.
- Potassium content.
- Uranium content.
- Thorium content.
- Natural exposure rate.

A special study on the anisotropy of magnetic susceptibility (AMS) of rocks is presented. The AMS method gives 3D-oriented information related to deformational rock fabrics.

Data from the magnetic susceptibility measurements carried out during the geological mapping in 2002 and 2003 have also been compiled and evaluated.

Field work has included petrophysical rock sampling (handheld diamond drilling) and in situ gamma-ray spectrometry measurements on outcrops and soil.

Sammanfattning

Denna rapport presenterar petrofysiska data insamlade på markytan under år 2002 och 2003. Syftet med att insamla petrofysiska data är att få information om bergarternas (och i viss mån jordarternas) geofysiska egenskaper och därmed bättre kunna tolka den geofysiska informationen geologiskt.

Arbetet har omfattat sammanställning, statistisk bearbetning och utvärdering av petrofysiska data från 2002 och 2003 års undersökningar. Resultaten är noggrant kopplade till olika bergarter och/eller bergartsenheter samt till den geografiska fördelningen. En sammanfattande tabell med petrofysiska parametrar för olika bergarter utgör ett viktigt resultat från undersökningarna. Parametrarna är:

- Volym susceptibilitet.
- Q-värde.
- Densitet.
- Porositet.
- Resistivitet.
- Inducerad polarisation.
- Kaliumhalt.
- Uranhalt.
- Toriumhalt.
- Totalstrålning.

En särskild studie har omfattat magnetisk susceptibilitetsanisotropi (AMS). AMS ger tredimensionell information om bergarternas deformationsmönster.

Data från magnetiska susceptibilitetsmätningar som utförts i samband med den geologiska karteringen år 2002 och 2003 har också sammanställts och utvärderats.

Fältarbete har omfattat petrofysisk provtagning av berg med hjälp av handhållen borrmaskin samt in situ mätningar med gammaspektrometer på hällytor och på jord.

Contents

1 Introduction

This document reports *petrophysical surface data, stage 2 (2003)* which is one of the activities performed within the site investigation at Forsmark. The work was conducted according to activity plan AP PF-400-02-11 and AP PF-400-02-47 (SKB internal controlling documents), by GeoVista AB; Hans Isaksson, Håkan Mattsson and Hans Thunehed. Mikael Keisu has been responsible for the final delivery of data.

The work carried out in this stage, stage 2, comprises all petrophysical data collected during 2002 and 2003. Previous work, stage 1, comprised collection and interpretation of petrophysical data during 2002.

Field work has included petrophysical rock sampling and in situ gamma-ray spectrometry measurements on outcrops and soil.

2 Objective and scope

The purpose of petrophysical measurements is to gain knowledge of the physical properties of different rock types. This information is used to increase the understanding of geophysical measurements and to support the geological mapping.

The work comprises statistical processing and evaluation of results from the 2002 petrophysical sampling and gamma ray spectrometry measurements on outcrops /1 and 2/, compiled with new results from further sampling and measurements in 2003. The analyses were made with respect to rock type characteristics and the geographical distributions of the measured properties. Data from the magnetic susceptibility measurements carried out during the geological mapping in 2002 and 2003 /3 and 4/ are also included in the report. A special study on the anisotropy of magnetic susceptibility (AMS) of rocks is presented. The AMS method gives 3D-oriented information related to deformational rock fabrics.

In some figures, contour maps based on interpolation methods of petrophysical parameters are presented. In some cases, the interpolation of petrophysical data is questionable, but it is performed in this report in order to better visualize the spatial variations in the data. Detailed variations in these contour maps should be ignored.

3 Input data and geological coding

3.1 Sample collection and in situ measurements

In total, during 2002 and 2003, 553 bedrock samples were collected with a portable drill machine at 128 locations and on 139 rock objects, see also Figure 3-1. Corresponding figures for 2003 were 162 rock samples, 44 locations and 45 rock objects, respectively. The samples were oriented with magnetic and sun compasses /1/. Measurements of the magnetic susceptibility, remanent magnetization and anisotropy of magnetic susceptibility (AMS), density, porosity, electric resistivity and induced polarization were carried out at the Division of Applied Geophysics, Luleå University of Technology.

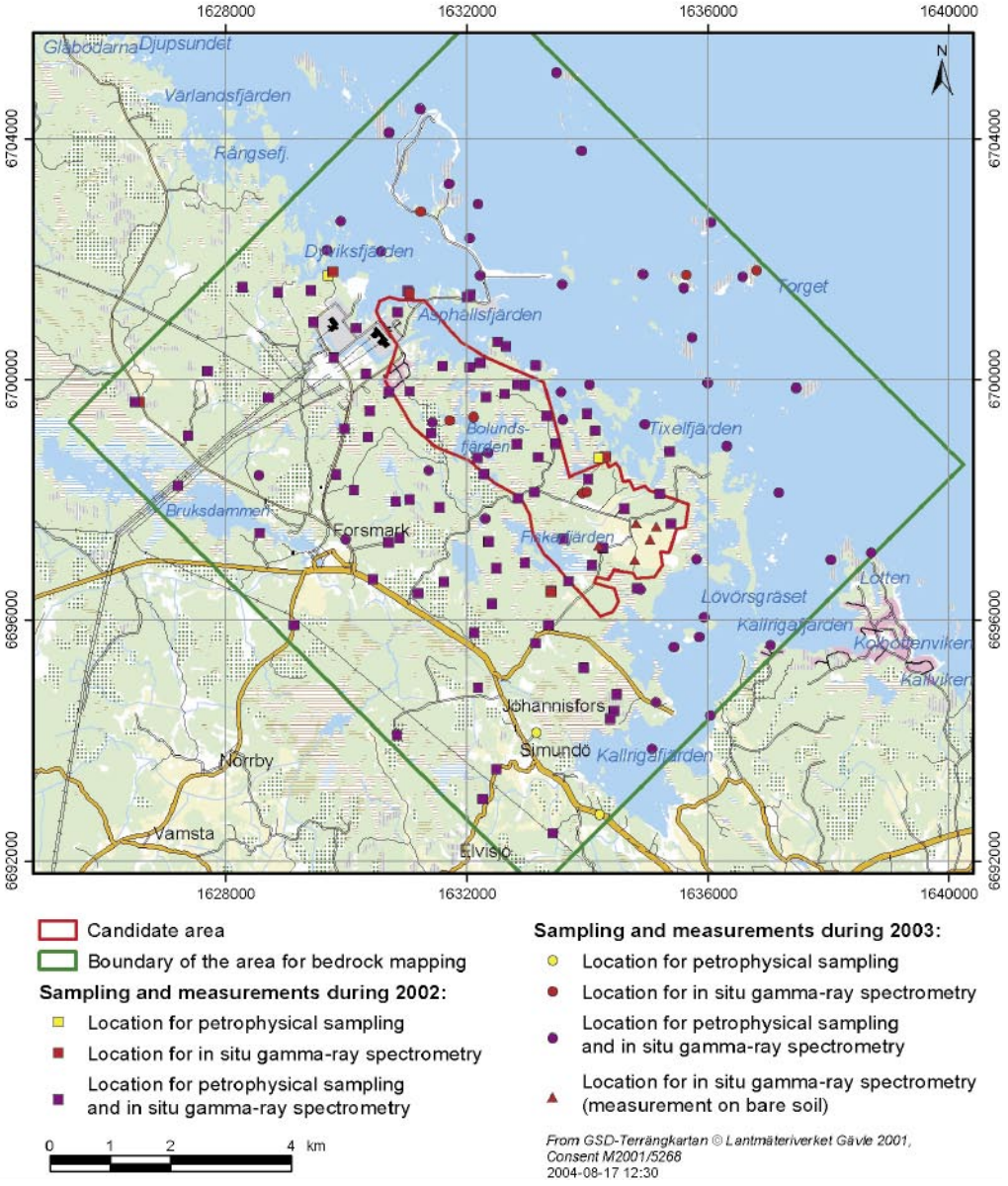

Figure 3-1. *Geographical distribution of locations for petrophysical sampling and in situ gamma-ray spectrometry measurements, for both 2002 and 2003.*

In total, 652 measurements of natural gamma radiation with a portable gamma-ray spectrometer were performed in situ on outcrops at 135 locations and on 169 rock objects, see also Figure 3-1. Corresponding figures for 2003 were 241 measurements, 48 locations and 56 rock objects, respectively. In addition, 14 measurements were carried out on 4 locations of bare soil in the Storskäret area. The final compilation of measurements on bare soil also includes another 7 measurements on 1 location used as a calibration spot for the helicopter borne geophysical survey /5/, see Appendix 5.

The equipment used and the execution of sampling, petrophysical laboratory measurements as well as the in situ gamma-ray spectrometry measurements during 2003 are the same as for 2002, described in /1/. A description on sample identification and a photographic documentation of the core samples from 2003 are available in Appendix 4. The corresponding documentation for 2002 is available in /1/.

3.2 Data processing

The following laboratory measurements have been carried out: magnetic susceptibility, remanent magnetization, anisotropy of magnetic susceptibility (AMS), density, porosity, electric resistivity and induced polarization. Measurements of natural gamma radiation with a portable gamma-ray spectrometer were performed in situ on outcrops and in a few cases on bare soil. A description of the collection of samples, laboratory measurement techniques, sample and data handling and the performance of in situ gamma-ray spectrometry measurements is given in /1/. Each sampling (measurement) location was assigned an identity code “PFMXXXXXX” (where XXXXXX is a serial number) followed by a rock order number, which corresponds to the location identity code and the rock order number used for the bedrock mapping /3, 4/. The rock order number is followed by a specimen number, which separates the different drill cores (samples) collected at each location.

The selection of sampling (measurement) locations was performed in co-operation with the responsible geologist. The geological coding system follows the Preliminary site description, Version 1.1 /6/. Each rock sample was classified according to this system, also presented in Table 3-1.

The field geologists who performed the bedrock mapping carried portable instruments for in situ measurements of the magnetic susceptibility /3, 4/. Normally, eight readings were taken on each rock type at the observed outcrops, which has created a unique database of 1,832 locations and 3,254 individual rock objects covering a large part of the Forsmark area. A compilation of this data is presented in Chapter 9.

Table 3-1. Code table for the different rock groups.

Rock Group (SGU)	Code (SKB)	Composition (and grain size)
		Name (IUGS/SGU)
A1	103076	Dacite and andesite, metamorphic.
A1	106000	Sedimentary rock, metamorphic.
A2	109014	Magnetite mineralization associated with calc-silicate rocks.
A3		Veined gneiss.
A4	108019	Calc-silicate rock (skarn).
A5	109010	Pyrite-pyrrhotite-chalcopyrite-sphalerite mineralisation.
A2	109014	Magnetite mineralisation associated with calc-silicate rock.
B1	101004	Ultramafic rock (olivine-hornblende pyroxenite).
B2/B3	101033	Diorite, quartz diorite and gabbro, metamorphic.
B4	102017	Amphibolite.
B5/B6	101054	Tonalite and granodiorite, metamorphic.
B7	101056	Granodiorite, metamorphic.
B8/B9	101057	Granite and granodiorite, metamorphic, medium-grained (the most common rock type in the candidate area).
B10	101058	Granite, metamorphic, aplitic.
	111051	Granitoid, metamorphic.
C	101051	Granodiorite, tonalite and granite, metamorphic, fine- to medium-grained.
D1	111058	Granite, fine- to medium-grained.
D2/D3	101061	Pegmatitic granite, pegmatite.

4 Density and magnetic properties

Different rock types vary in composition and this leads to variations in their petrophysical properties. The rock density and magnetic properties (susceptibility and remanence) are therefore often used as supportive information when classifying rocks. These properties are important for the interpretation of geophysical data and they also constitute input parameters when modelling gravity and magnetic data.

4.1 Data processing

In order to get a better picture of the data and to increase the possibility to compare different data sets and data from different rock types, a number of sub-parameters are often calculated from the density, the magnetic susceptibility and the magnetic remanence. Two such sub-parameters are the silicate density and the Q-value (Königsberger ratio). The silicate density /7/ provides an estimation of the rock composition and is calculated by correcting the measured total density for the content of ferromagnetic minerals (e.g. magnetite and pyrrhotite) by use of the magnetic susceptibility. The Q-value /8/ is the quotient between the remanent and induced magnetization:

$$Q = \frac{M_R}{M_I} = \frac{M_R}{KH} = \frac{M_R \mu_0}{KB}$$

where

M_R = Remanent magnetization intensity (A/m),

M_I = Induced magnetization (A/m),

K = Magnetic susceptibility (SI),

H = Magnetic field strength (A/m),

B = Magnetic flux density (T),

μ_0 = Magnetic permeability in vacuum ($4\pi\ 10^{-7}$ Vs/Am).

The Q-value thus indicates the contribution of the remanent magnetization to the measured anomalous magnetic flux density and is therefore an important parameter when interpreting and modelling ground and airborne magnetic data. The Q-value is also grain size dependent and indicates what ferromagnetic minerals that is present in the rock.

In this investigation the so called density-susceptibility rock classification diagrams (see for example Figure 4-1) were used. The Y-axis in these diagrams displays the magnetic susceptibility on the left hand side and the estimated magnetite content to the right. It has been shown that for rocks in which the magnetic susceptibility is primarily governed by magnetite, there is a fairly good correlation between the magnetic susceptibility and the magnetite content /9/. However, the scatter is relatively high so predictions of the volume-percent magnetite in rocks based on the magnetic susceptibility should be used with caution. The silicate density curves are based on equations from Henkel 1991 /7/, and the average densities of each rock type originate from Puranen 1989 /10/. The diagram should be read in the way that if a rock sample plots on, or close to, a “rock type curve” it is indicated

that the rock should be classified according to the composition of this rock type. Since there is often a partial overlap of the density distributions of different rock types, there is always a certain degree of uncertainty in the classification. A sample plotting in between, for example, the granite and granodiorite curves should thus be classified as granite to granodiorite.

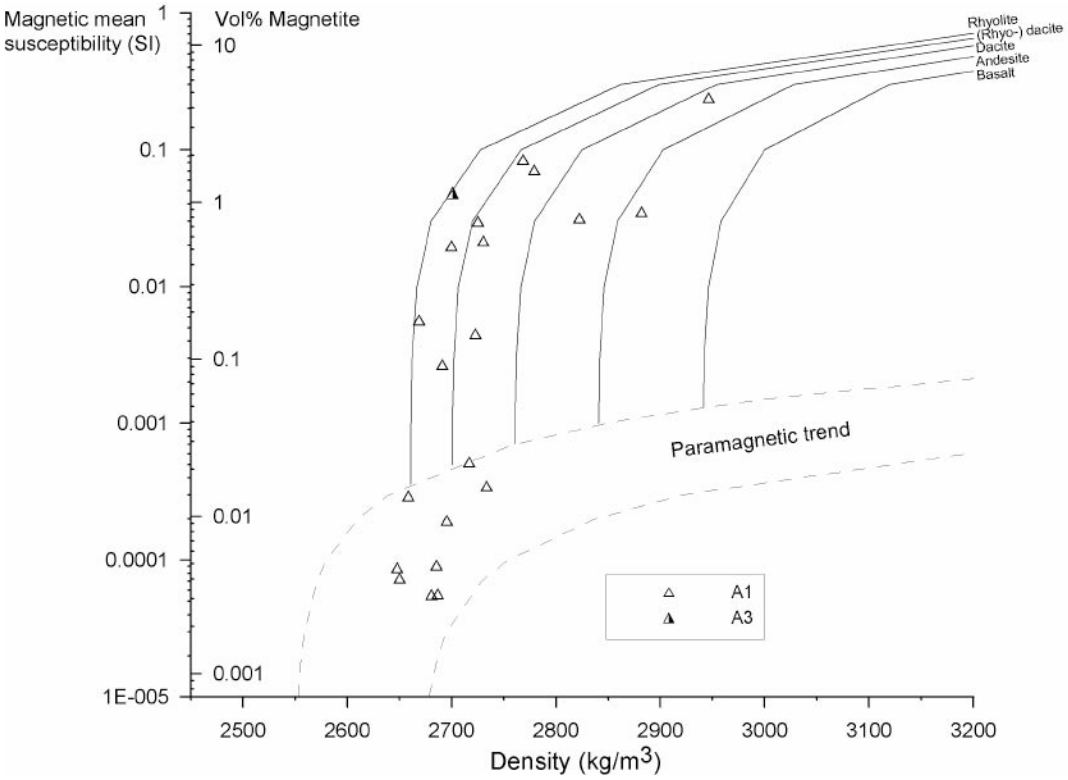

a) Rock group A (A2 excluded)

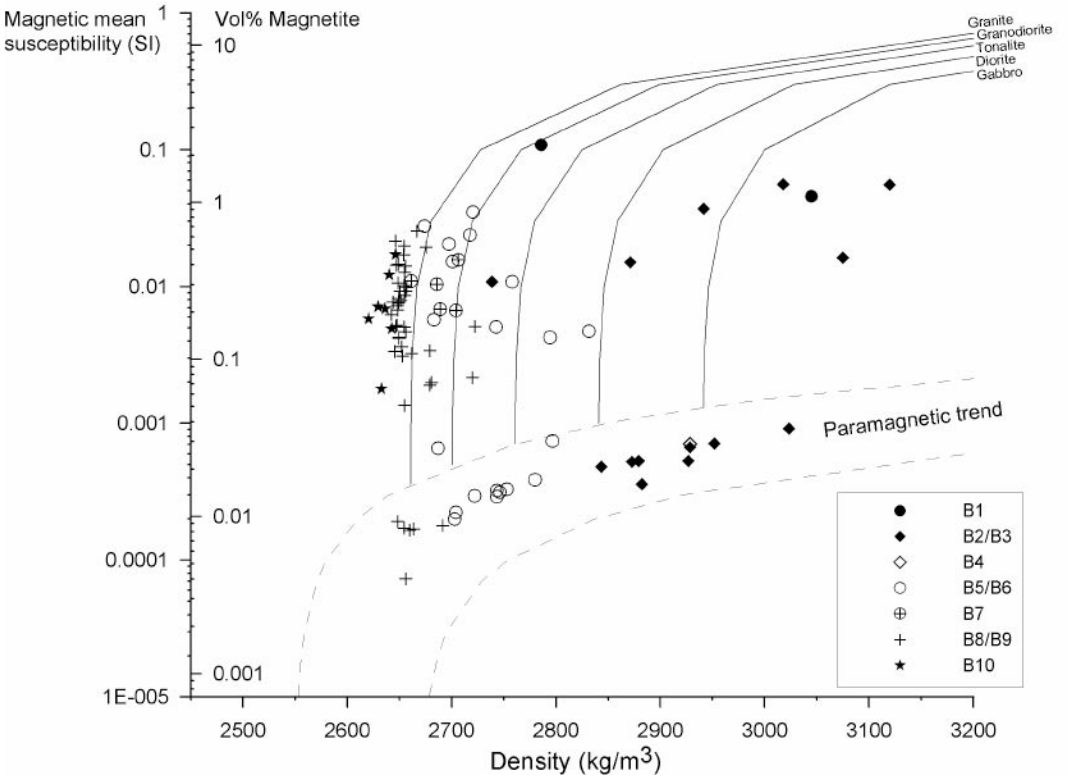

b) Rock group B

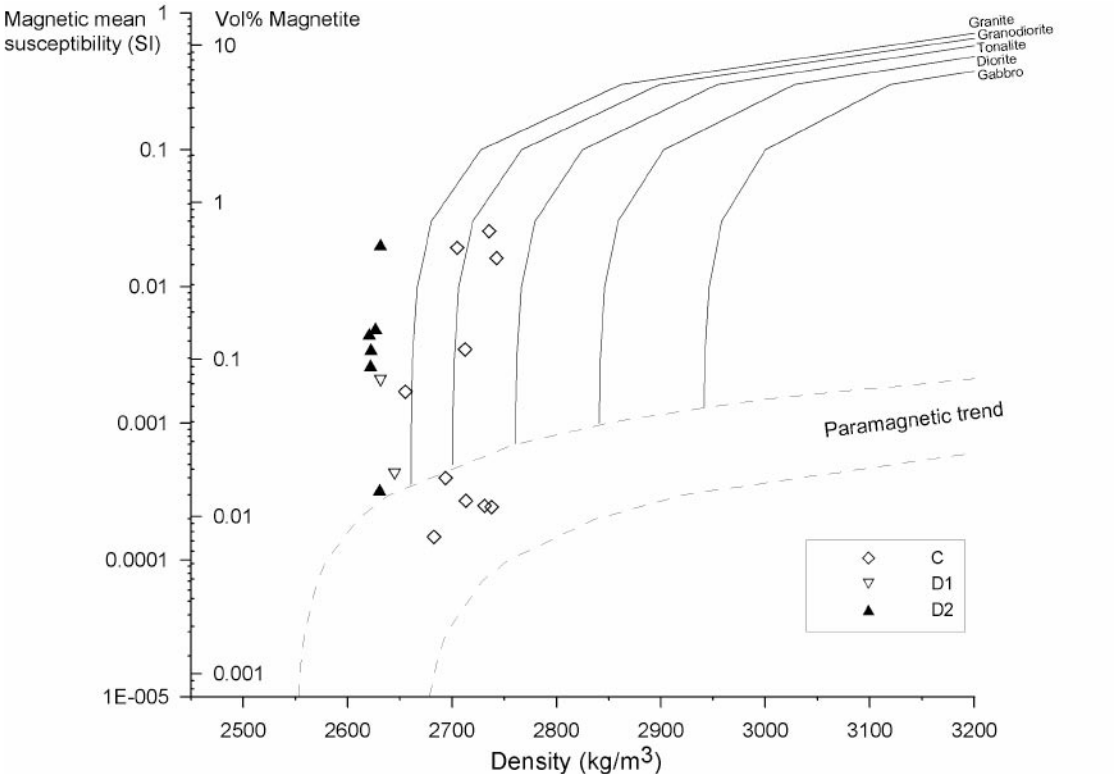

c) Rock groups C and D

Figure 4-1. *Density-susceptibility rock classification diagrams for the rocks of the Forsmark area. See the text for explanation.*

4.2 Results

The classification of the volcanic rocks, groups A1 and A3, indicates that a majority of the rocks should be classified as rhyolite or rhyodacite to dacite, see Figure 4-1a (group A2, Fe-rich mineralization, is excluded in the figure). The rock density of groups A1 and A3 averages at 2,730 kg/m^3 (Figure 4-2a). Three group A1 samples (sites PFM001221, rock order number 5, PFM001521 and PF001885) have significantly higher densities compared to the average value, and these classify as dacite to andesite in the rock classification diagram. The scatter in the susceptibility histogram of Figure 4-2 shows that the ferromagnetic content varies greatly within the volcanic rock group A1.

The diagram in Figure 4-1b indicates that the group B rocks vary greatly in mineral composition, ranging from leucocratic granite to ultramafic rocks. However, a majority of the rocks fall close to the granite and granodiorite classification curves. These are mainly rock samples from the groups B7, B8/B9 and B10. In the density histogram (Figure 4-2) there is a corresponding peak at c 2,670 kg/m^3. The B5/B6 samples show a large scatter, ranging in indicated composition from granite to diorite. Their average density is c 2,730 kg/m^3.The B2/B3 rocks mainly plot between the diorite and gabbro classification curves, having an average density of c 2,930 kg/m^3. The sample at PFM000233, with the density of 2,738 kg/m^3, constitutes an outlier. The meta-ultramafic rock at site PFM001201 (group B1) has suffered from alteration (serpentinization) which has lowered its density to a value corresponding to a granodiorite composition.

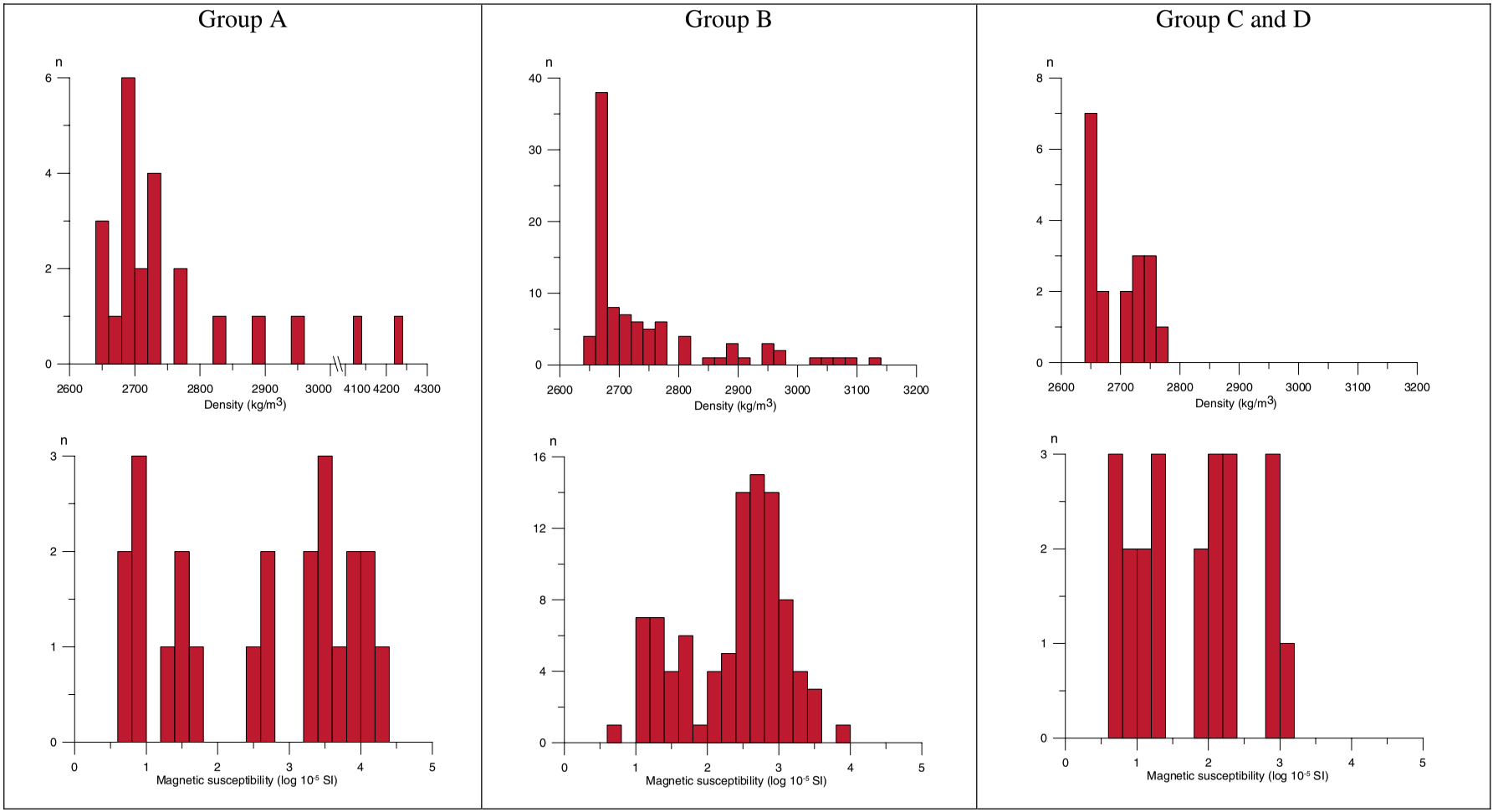

Figure 4-2. *Histograms showing the distribution of density and magnetic susceptibility of the rocks in the Forsmark area.*

There is an indication in Figure 4-1b that the metagranodiorite-metagranite to metagranite rock groups (B8/B9), the metatonalite to metagranodiorite rocks (groups B5/B6) and the metadiorite to metagabbro rocks (B2/B3) can be divided into two "magnetic subgroups", one group containing a fair amount (0.1–1 volume percent) of magnetite and the other containing no, or only a small amount, of ferromagnetic minerals. The grouping is also clearly visible in the susceptibility histogram of Figure 4-2. This may be important for future work involving for example modelling of magnetic data.

The quartz-rich felsic granitoids (group C) mainly classify as granodiorite rock, whereas the rocks of group D1 and D2 (granite and pegmatitic granite) generally have lower densities and are classified as leucocratic granite (Figures 4-1c and 4-2).

A contour plot of the geographical distribution of wet densities for the main rocks (rock order 1, group A2 excluded) in the Forsmark area is presented in Figure 4-3 (gridding performed with Surfer 8, ™ Golden Software, inverse distance to the power of 2, cell size = 200 m, search radius = 800 m). The data indicates that the candidate area is dominated by densities corresponding to granite (ranging from 2,625 kg/m^3 to 2,675 kg/m^3). An area of slightly higher densities, related to metatonalite rocks, crosscuts the north-eastern boundary of the candidate area. Along the south-western boundary of the candidate area there is a sharp density contrast and high density rocks are dominant in the area to the south and southwest. Also north and northwest of the candidate area the density is relatively higher.

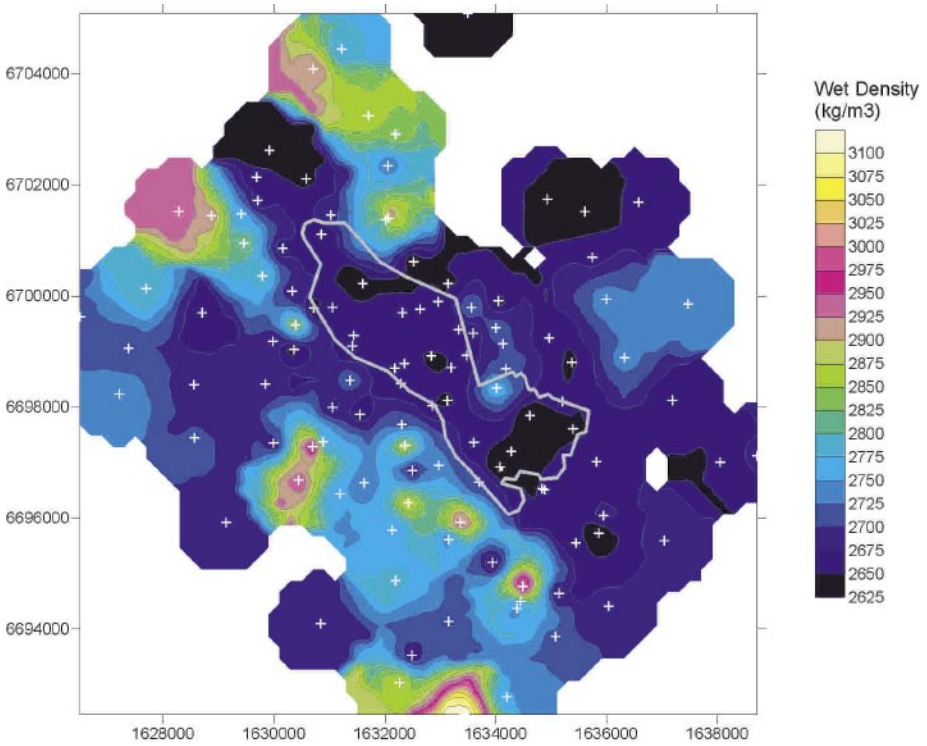

Figure 4-3. *Contour plot of wet density distribution for the main rocks (first order rock groups) in the Forsmark area. Mineralized rocks (group A2) are excluded. White crosses denote sampling locations. The candidate area is outlined with a white line.*

The geographical distribution of the main rock types classified on basis of the silicate density indicates that a vast majority of the sampled rocks within the candidate area, where the bedrock is mainly mapped as granite to granodiorite, classify as rocks with a composition corresponding to granite (Figure 4-4, gridding performed with Surfer 8, ™ Golden Software, inverse distance to the power of 2, cell size = 200 m, search radius = 800 m). There is a generally good agreement between the silicate density classifications and the geological classification (Figure 4-5). The high density rocks north and northwest of the candidate area mainly classify as diorite or gabbro, whereas the rocks to the southwest mainly classify as tonalite to diorite.

It is worth noting that the silicate densities of the metatonalite rock that crosscuts the north-eastern boundary of the candidate area, varies from 2,698 kg/m^3 to 2,780 kg/m^3, which may indicate fairly large compositional variations within this rock unit.

A majority of all measured rock samples have Q-values below 0.5, which indicates that magnetic anomalies mainly reflect the magnetization induced by the present earth magnetic field (Figure 4-6). However, the obtained Q-values are high enough to recommend that the direction and intensity of the remanent magnetization should be accounted for in modelling of magnetic data from the area. The Q-value data indicates that the remanent magnetization is mainly governed by magnetite or possibly hematite, whereas pyrrhotite most likely can be excluded, at least as a prominent remanence carrier. At three sites there are indications of extremely high Q-values; Q = 25.5 (metagabbro PFM000243), Q = 14.9 (Fe-mineralization PFM000336) and Q = 15.9 (Fe-mineralization PFM000446). The Q-value of the metagabbro (not shown in Figure 4-6b) is calculated using susceptibility and remanence intensity data from two different specimens within the site, which makes this result a bit uncertain. However, it is reasonable to believe that the Q-values of all the three rock types may be very high, which may have a significant effect on the shape and intensity of related magnetic anomalies. Such high Q-values may indicate the presence of pyrrhotite.

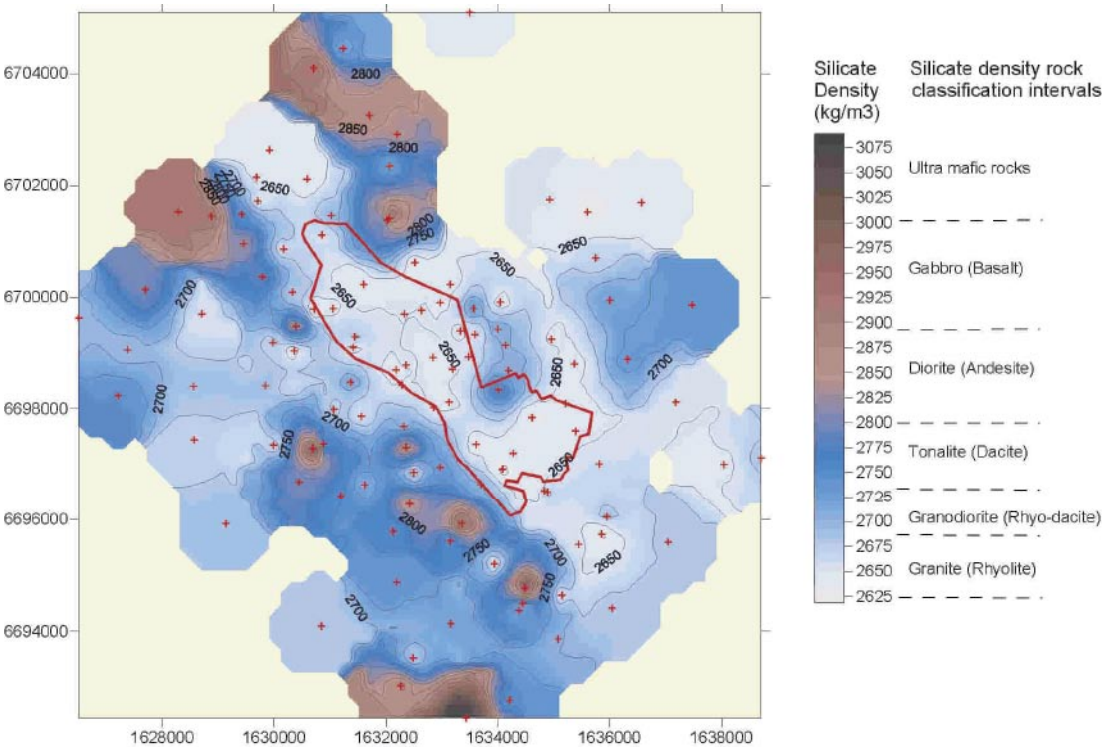

Figure 4-4. *Contour map of the silicate density for the main rocks (first order rock groups) in the Forsmark area (mineralized rocks (group A2) are excluded). Rock classification interval based on the silicate density are indicated to the right of the colour scale. Red crosses denote sampling locations. The candidate area is outlined with a red line.*

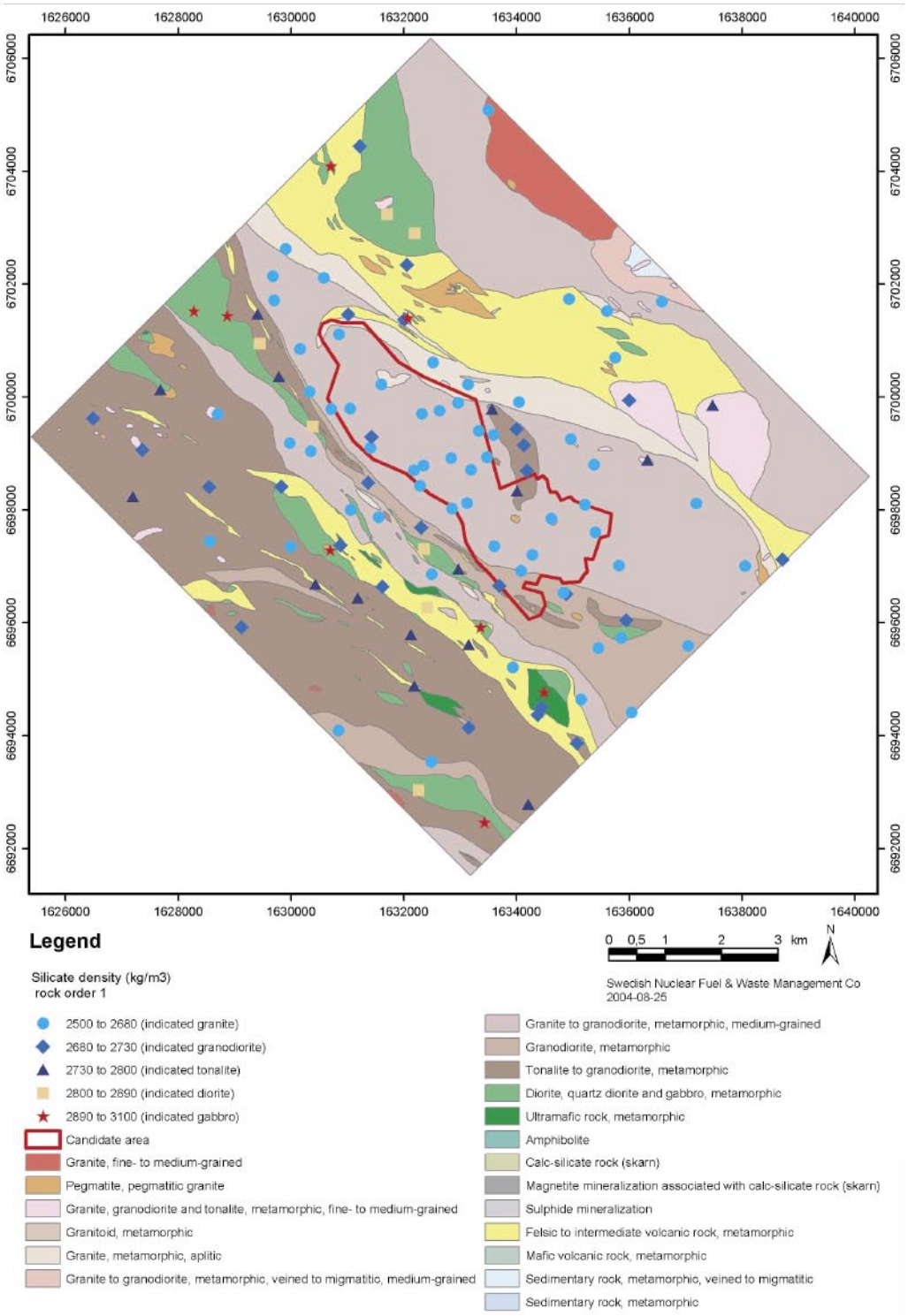

Figure 4-5. *Map showing sample locations and the silicate density rock classification at each location (first order rock groups, mineralized rocks (group A2) are excluded) plotted on the present bedrock map of the Forsmark area.*

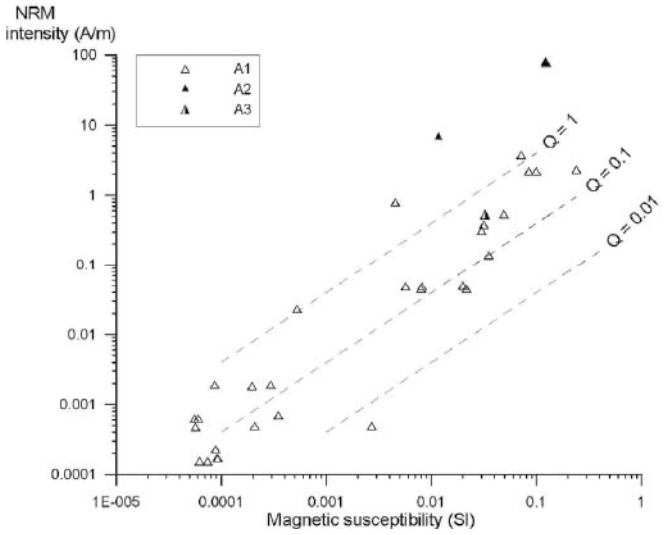

a) Rock group A

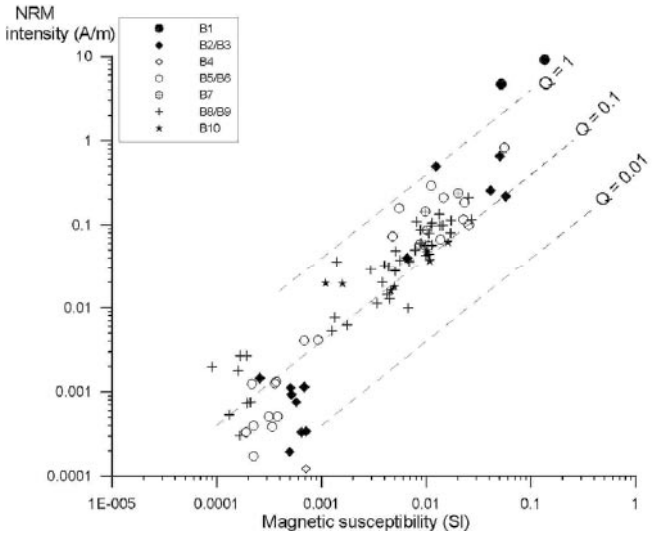

b) Rock group B

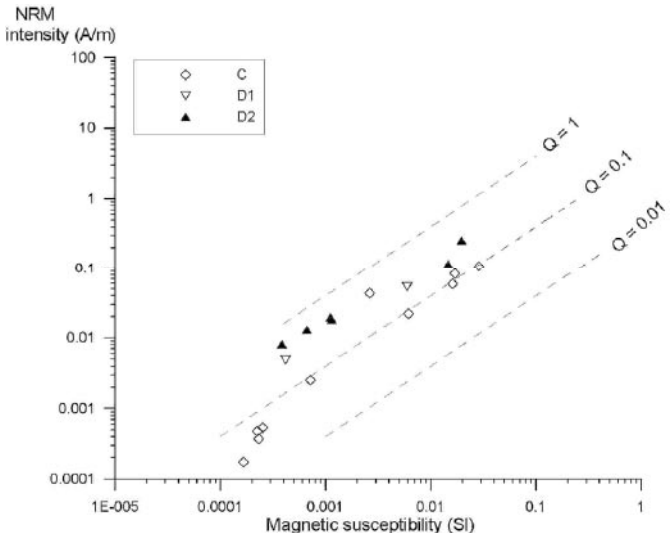

c) Rock groups C and D

Figure 4-6. *Natural remanent magnetization (NRM) intensity versus magnetic susceptibility for the rock from the Forsmark area. See the text for explanation.*

The diagram of natural remanence intensity versus magnetic susceptibility for the volcanic group of rocks (groups A1–A3, Figure 4-6a) indicates that the rocks have an inhomogeneous magnetic mineralogy. The varying susceptibility and remanent magnetization intensity is most likely related to variations in magnetite content in the rocks. This is also valid for the metagranodiorite to metagranite group (B8/B9). However, the high susceptibility specimens of the metatonalite to metagranodiorite rocks (B5/B6) and the metadiorite and metagabbro rocks (B2/B3) have higher Q-values than the low susceptibility specimens of each group respectively (Figure 4-6b). This suggests that the low and high susceptibility groups have different magnetic mineralogy, or that different grain sizes of magnetite govern their magnetizations. Both explanations given above of these groupings may be of importance for the understanding of the geology of the area. For example, all four sites within the metatonalite-metagranodiorite rock, previously mentioned, that crosscuts the north-eastern boundary of the candidate area have low Q-values and low susceptibilities, to be compared with the larger variance in silicate density in the same samples.

The group C granitoids have lower Q-values than the pegmatitic granite D2, but both these groups fall close to the general distribution of the group B rocks.

The geographical distribution of the Q-values is displayed in Figure 4-7 (gridding performed with Surfer 8, ™ Golden Software, inverse distance to the power of 2, cell size = 200 m, search radius = 800 m). Within the candidate area the Q-values are generally below 0.2. Higher Q-values are found northwest and southeast of the candidate area whereas rocks with lower Q-values tend to occur south and north of candidate area. Comparing Figure 4-7 with Figure 4-4 indicates that high density rocks generally have lower Q-values than more low density rocks.

The NRM-directions of the investigated rocks mainly show moderate to steep inclinations and scattered declinations, without any distinct signs of clustering (Figure 4-8a). However, significant groupings are found for some of the investigated rock groups, even though the mean directions generally are poorly defined (Figure 4-8b). The mean NRM-direction of unaltered rocks should fall close to the present earth field (PEF) direction, which is approximate declination = 358° and inclination = 72° in the investigated area. However, a majority of the rocks in the Forsmark area have suffered from plastic deformation and as indicated by Figure 4-8b, the mean directions of the rock groups B5/B6, B7, B8/B9 and B10 differ significantly from the PEF-direction. They are mainly oriented more towards southeast.

The large number of samples plotting in the south east direction, which is sub-parallel to the maximum strain indicated by the magnetic lineations (Figure 5-4), suggest that the NRM-directions are affected by the deformation of the rocks.

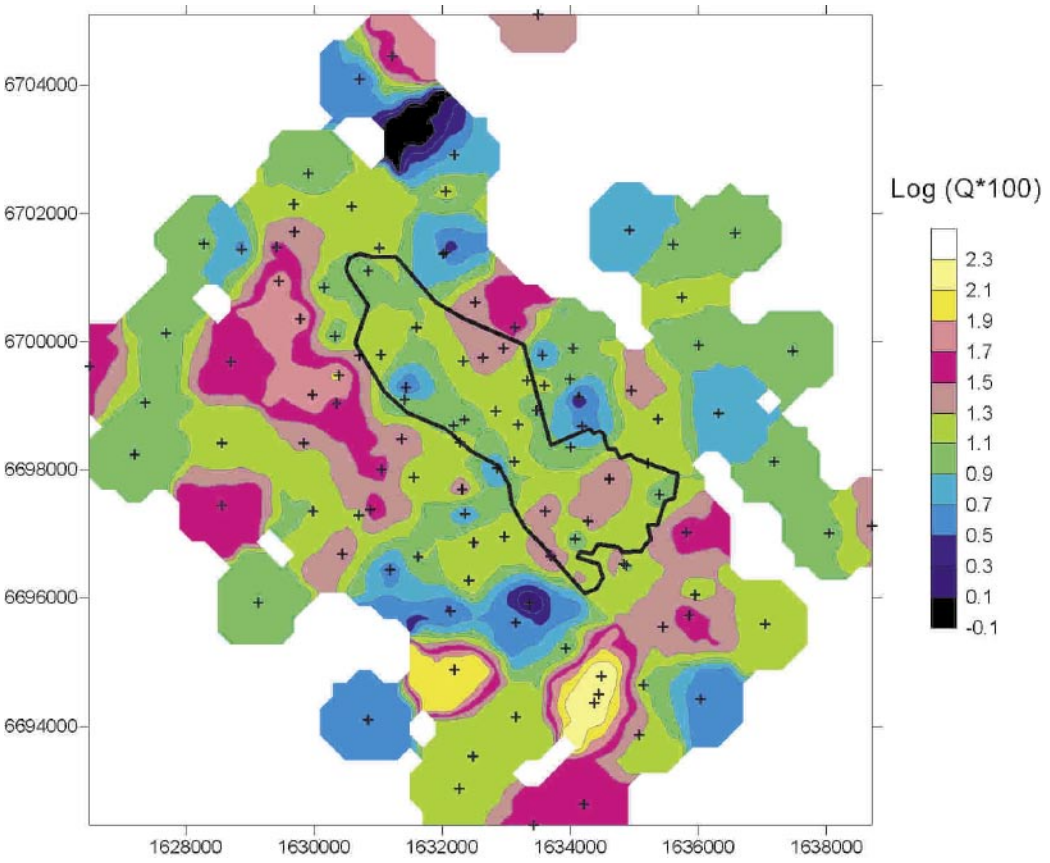

Figure 4-7. *Contour map of the logarithm of the Q-parameter (10^{-2}) for the main rocks (first order rock groups) in the Forsmark area (mineralized rocks (group A2) are excluded). Black crosses denote sampling locations. The candidate area is outlined with a black line.*

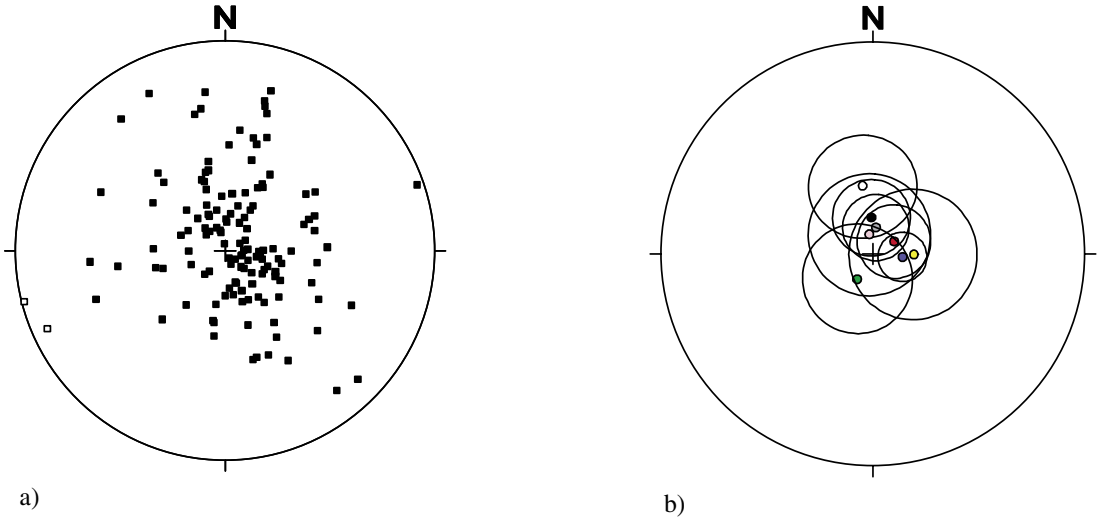

Figure 4-8. *a) Equal area projection diagram of NRM-directions from all measured rock samples in the Forsmark area (two samples have negative inclination, and these are denoted by open symbols). b) Equal area projection diagram of group mean NRM-directions for group A1 (black), B2/B3 (grey), B5/B6 (red), B7 (green), B8/B9 (blue), B10 (yellow), C (white) and D2/D3 (pink). The circles show the 95% cone of confidence of each mean direction respectively.*

4.3 Conclusions

The following conclusions are drawn based on the density and magnetic study:

- The results of the rock classification based on susceptibility-density diagrams are generally in good accordance with the geological rock classification. For most outliers, a reasonable explanation is found (e.g. alteration).
- The vast majority of samples collected within the candidate area have silicate densities that correspond to granite.
- The dominant rock types can be divided into a low and a high magnetic group. The two groups most likely reflect natural variations in magnetite content and no geographical clustering of any of the groups seem to occur.
- Q-values are below $Q < 0.5$ for a majority of the rocks.
- The NRM directions show scattered declinations and moderate to steep inclination. There is an indication that the NRM directions of the rock groups B5–B10 are affected by the plastic deformation of these rocks.

5 Anisotropy of magnetic susceptibility (AMS)

5.1 The method

The anisotropy of magnetic susceptibility (AMS) is a fairly unknown method and this paragraph gives a brief introduction to its origin and application. A more complete description of AMS can be found in, for example, /11/.

The magnetic anisotropy of rock forming minerals basically originates from two sources, the grain shape and the crystallographic structure /12/. Magnetite is ferromagnetic and carries strong shape anisotropy, whereas pyrrhotite and hematite are governed by crystalline anisotropy due to their antiferromagnetic origin. Paramagnetic minerals (e.g. biotite, hornblende) and diamagnetic minerals (e.g. quartz, feldspars) are also carriers of magneto-crystalline anisotropy. The orientation of the anisotropy of magnetic susceptibility coincides with the crystallographic axes for most rock forming minerals, and it is therefore possible to directly transfer “magnetic directions” to “tectonic directions” (foliation and lineation) measured in the field.

Since magnetite carries a very high magnetic susceptibility in comparison to most other rock forming minerals, even a low grade tends to dominate the magnetic properties, including the anisotropy of a rock. However, for e.g. “non-magnetic” granites the magnetic anisotropy is mainly governed by biotite and other paramagnetic minerals.

The magnetic susceptibility ***K*** is generally written as a constant of proportionality between the applied field ***H*** and the induced magnetisation ***M***. However, the susceptibility responds differently to different directions of the applied field. It is anisotropic and *K* can not be described as a simple scalar, but has to be written as a symmetric 3×3 tensor /13/:

$$\begin{bmatrix} M_x \\ M_y \\ M_z \end{bmatrix} = \begin{bmatrix} k_{11} k_{12} k_{13} \\ k_{21} k_{22} k_{23} \\ k_{31} k_{32} k_{33} \end{bmatrix} \begin{bmatrix} H_x \\ H_y \\ H_z \end{bmatrix}$$

where x, y and z stands for three perpendicular directions in a right handed co-ordinate system. The tensor *K* is termed the anisotropy of magnetic susceptibility (AMS) tensor (on matrix form). It is a symmetric tensor implying that

$$k_{12} = k_{21}; k_{13} = k_{31}; k_{23} = k_{32}$$

By the use of linear algebra it is possible to calculate the eigenvalues and the eigenvectors of K. The eigenvectors are termed principal directions (p1, p2, p3) and the eigenvalues principal susceptibilities K1 (or kmax), K2 (or kint), and K3 (or kmin), where K1 ≥ K2 ≥ K3. The principal susceptibilities can graphically be described by an ellipsoid, with K1 representing the long axis, K2 the intermediate and K3 the short axis (Figure 5-1).

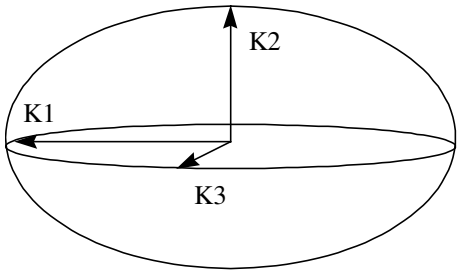

Figure 5-1. *The anisotropy ellipsoid, K1 = maximum axis, K2 = intermediate axis, K3 = minimum axis.*

The degree of anisotropy is usually characterised by P = K1/K3. The degree of foliation is F = K2/K3 and the degree of lineation is L = K1/K2. The shape of the anisotropy ellipsoid is defined by the shape parameter T, see below. For $-1 < T < 0$ the ellipsoid is prolate (cigar-shaped) and for $0 < T < 1$ the ellipsoid is oblate (disc-shaped). If T = 0 the ellipsoid is neutral.

$$T = \frac{2\ln K2 - \ln K1 - \ln K3}{\ln K1 - \ln K3}$$

The magnetic susceptibility indicates the volumetric content and type of magnetic minerals in a rock. For primary low-magnetic granitoids in which the susceptibility is carried primarily by iron-bearing silicates (biotite and hornblende), the susceptibility is proportional to the iron content and can be used as a petrography index /14/. If different rock types vary in mineralogy they may be identified by means of variations in their magnetic susceptibility. However, when dealing with altered or deformed rock types containing ferromagnetic minerals (e.g. magnetite, hematite or pyrrhotite) the link between the susceptibility and petrography is complex. Brittle deformation of rocks causes fracturing and in the vicinity of the fractures magnetite oxidizes to hematite, which decreases the magnetic susceptibility giving rise to low magnetic zones. Also plastic deformation affects the magnetic mineralogy but the result is more complex since the deformation may lead to a destruction of magnetite, but flowing of hydrothermal fluids may lead to a creation, recrystallization, of magnetite as well.

An unaltered rock carries a primary AMS fabric that corresponds to the rock type, its mineral composition and the environment in which it was created. Sedimentary rocks generally show an oblate shaped AMS ellipsoid orientated parallel to the bedding plane, thus with the minimum principal susceptibility axis orthogonal to the bedding. A lineation can be developed if the grains were deposited in a slope or in running water /5-1/, otherwise the K1 and K2 axes form a girdle pattern. AMS is a well-known indicator of the direction of magma flow in basic dykes and the method has been used in several studies to define flow fabrics (for example /15, 16 and 17/). Basic sills and dikes and basaltic lava flows usually carry a degree of AMS less than 10% and the fabric of sub horizontal sills reminds of that of sedimentary rocks. AMS has been applied to many granite plutons for kinematical reconstruction of their emplacement /18 and 19/. A primary magnetic fabric can generally be related to the shape of the intrusion /11/ and preferred orientations of feldspars (known as geological magma flow indicators) tend to be parallel to the magnetic foliation plane, for example /20/. If the magnetic foliation of a granite pluton is parallel to a regional foliation, the pattern may be due to large scale deformation.

The deformation of a rock produces strain that imposes a secondary magnetic fabric. A brittle deformation basically gives rise to rigid grain rotation and fracturing whereas a plastic deformation mainly causes changes of the grain shape that result in a tectonic foliation and lineation. Therefore, plastic deformation must be considered as the main producer of secondary magnetic fabrics. However, deformational AMS structures in two monzonite plutons that lack visible tectonic structures have been reported /21/. From the general theory of magnetic anisotropy follows that small changes of the distances between atoms, ions or crystal lattices are enough to change the anisotropy and therefore the magnetic susceptibility can be more sensitive to minor deformations not visible to the eye.

Attempts to connect the degree of anisotropy to the degree of strain are reported by for example /11, 21, 22 and 23/. Examples of good correlation have been found over a limited range of strain, but there are large problems to overcome, such as growth or recrystallisation of minerals. Also, measurements of the AMS reflect the properties of an entire rock and not just a specific grain fraction. In general, if the primary rock fabric is determined by AMS, if the degree of deformation is low and if there is no recrystallisation of minerals, it should be possible to determine the amount of strain by use of the AMS. However, these criteria are not easily achieved.

5.2 Data processing

The AMS analyses in Forsmark include results from 134 rock objects at 125 sites (529 specimens), and generally 4 drill cores were collected at each object. One specimen was cut from each drill core and the AMS measurements were performed, which produced four data readings per object. The four measurements on an individual rock object allow a calculation of mean directions of the principal AMS axes (called the site mean direction) and corresponding “site mean value” of the degree of anisotropy (P), degree of lineation (L), degree of foliation (F) and ellipsoid shape (T). When calculating the site mean values of the P, L, F and T parameters, the orientations of the ellipsoids of each specimen are taken into account. Vector addition is applied to the three susceptibility axes of the four specimens from the site, which results in a “site mean ellipsoid”. The site mean values of the anisotropy parameters thus give information of the site as a whole and are not just “simple” average values. According to statistical demands at least six measurements (specimens) are required for estimating uncertainty regions of the calculated mean directions. No such calculations were therefore performed. Instead, the data quality of each site was evaluated by visual inspection and site mean directions based on scattered specimen directions were rejected (about 10% of the data were rejected). At some sites, only two or three specimens gave measurable results and if the corresponding principal axes fell close to each other the mean direction was accepted as a site mean direction. If the principal directions of the specimens were far apart, no mean direction could be established, and the data were rejected.

5.3 Results

The average mean susceptibility of all measured rock specimens shows a distinct bimodal distribution, which indicates two populations of magnetic carriers (Figure 5-2a). The low-magnetic specimens average at c 50×10^{-5} SI, which suggests no, or very little, content of ferromagnetic minerals such as magnetite, hematite or pyrrhotite. The group of specimens with higher susceptibilities has an average value of c $1{,}000\times10^{-5}$ SI, which clearly indicates the presence of ferromagnetic minerals (most likely magnetite). Histograms of the susceptibility of different rock units (Figure 4-2) indicate that both low (10^{-4} SI) and high (10^{-2} SI) susceptibilities occur within the group of meta-granitiod (group B) rocks that dominate the bedrock of the investigated area.

The average degree of anisotropy is P = 1.33, which is a fairly high value, and about 60% of the specimens have a degree of anisotropy P > 1.2 (Figure 5-2b). This indicates that a majority of the investigated rocks have been affected by plastic deformation most likely related to the regional deformation and metamorphism of the area. However, a correlation

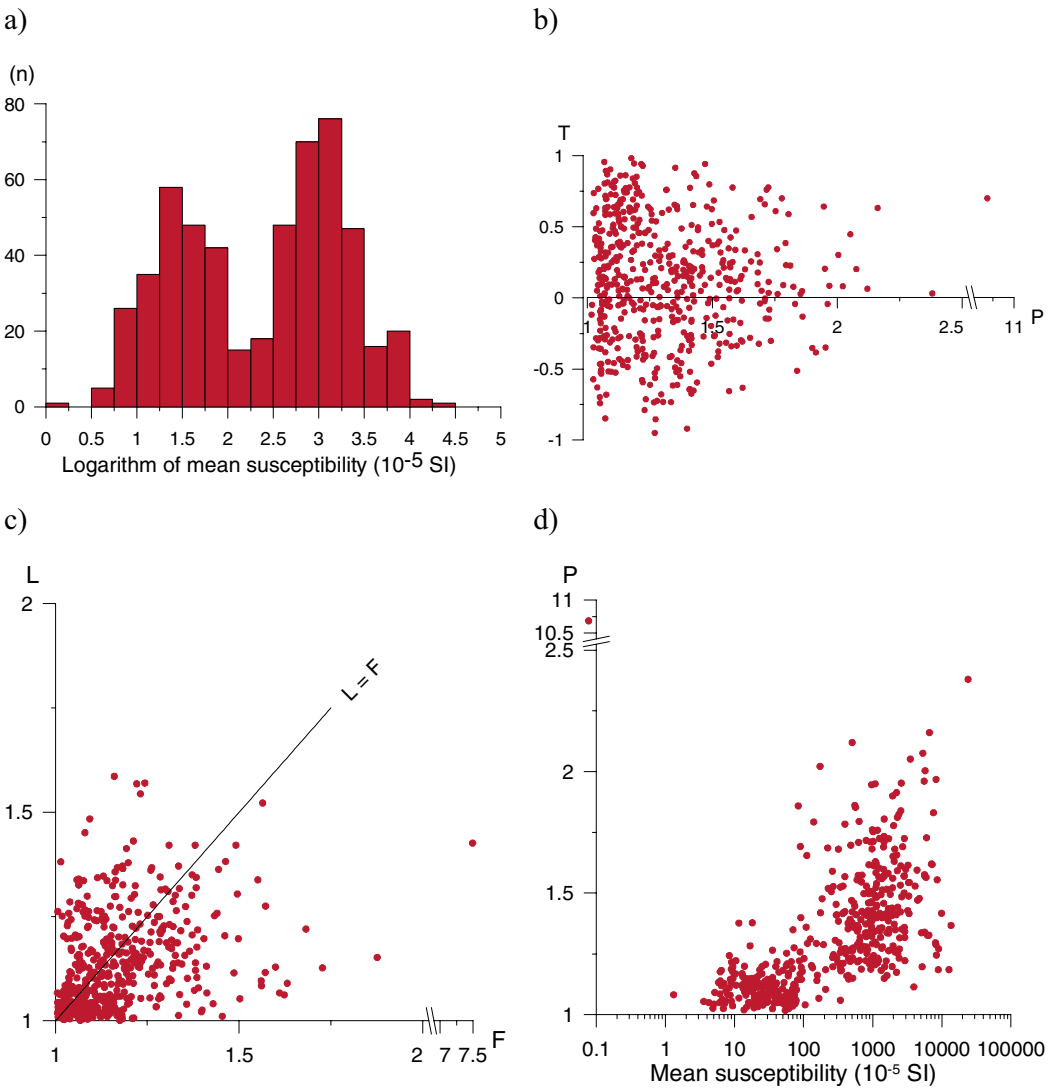

Figure 5-2. *Anisotropy of magnetic susceptibility parameters for individual specimens from all sampling sites. a) Histogram of the mean susceptibility, b) Shape parameter (T) versus degree of anisotropy (P), c) Degree of lineation (L) versus degree of foliation (F) and d) Degree of anisotropy (P) versus mean susceptibility.*

exist between the degree of anisotropy and the volume susceptibility, which indicates that the P-parameter is dependent (at least from a statistical point of view) on the concentration of magnetite and can not be directly connected to the degree of tectonic strain (Figure 5-2d). This correlation is also indicated in the site mean data and it is most likely related to an interaction between magnetite grains. Since there is a wish to identify areas within the site investigation area that have suffered from a high degree of deformation, an attempt was made to "correct" the degree of anisotropy for the dependence to the volume susceptibility.

The magnetite content, as well as the concentration of other magnetic minerals, is often rock type dependent. Therefore, only the group B rocks, with the exception of the mafic rocks (sub-groups B1, B2 and B4) were selected for the correction, which includes a total number of 84 sampling locations. It is assumed that the P-parameter depends on a linear combination of the two components grain shape and volume susceptibility, and a principal component analysis (PCA) is applied to the P-parameter and corresponding mean susceptibility data. By calculating eigenvectors and eigenvalues for the data it is possible to mathematically separate the two components from each other; one solely dependent on the volume susceptibility, the other independent of the susceptibility and, in theory, mainly dependent on the grain shape of the minerals. The geographical distribution of the "corrected" degree of anisotropy is presented as a contour plot in Figure 5-3a. The data broadly indicates that the rocks along the south western boundary of the candidate area, and further to the southwest, have moderate to high degree of anisotropy, in the central-eastern part there is domination of low anisotropy degrees and in the north-eastern part most rocks carry moderate degrees of anisotropy. The result suggests that the lowest strained rocks are found in the central and south-eastern part of the candidate area and the highest strained rocks occur southwest of the candidate area. In Figure 5-3b a contour plot of the ellipsoid shape parameter (T) is presented. The T-parameter shows no correlation to the mean susceptibility and has therefore not been altered. The rocks of the candidate area are dominated by weakly prolate (elongated) to neutral shaped ellipsoids, whereas the rocks to the southwest of the candidate area have AMS-ellipsoids dominated by weak to strong oblate (flattened) shapes. Oblate shaped ellipsoids (S-tectonites) seem to be related to rocks with a high degree of anisotropy.

An equal area projection plot of site mean directions of the minimum (poles to foliation) and maximum (lineation) AMS axes for all investigated sites shows a fairly uniform pattern (Figure 5-4). The minimum axes form a girdle pattern, however with a cluster in the northeast sub horizontal direction, and the maximum axes cluster in the southeast direction with moderate to steep dips. A general interpretation of the distribution of the AMS axes is that a majority of the rocks have suffered from a dominant NE–SW directed compressive deformation with a maximum strain in the southeast direction, dipping c 45°.

The division of the sampling sites into the four rock groups A, B, C and D (where A = Supracrustal rocks, B = Ultramafic, mafic, intermediate and quartz-rich felsic (granitoid) meta-intrusive rocks, C = Quartz-rich felsic (granitoid) meta-intrusive rock, fine- to medium-grained and D = Granite, pegmatitic granite, pegmatite) shows that the general AMS fabric seems to dominate also the individual A, B, C and D groups (Figure 5-5). The girdle distribution of the minimum axes (poles to foliation) is only distinctly present in group B (but indicated in group A) and it indicates a folded geometry. The estimated orientation of the fold axis defined from the average intersection point of the planes belonging to each of the poles falls at Declination = 132° and Inclination = 43° (red star in Figure 5-5). The magnetic lineation of group B are clustered and display a mean direction of Declination = 134° and Inclination = 50°, which indicates that the direction of the fold axis is parallel to the direction of the lineation.

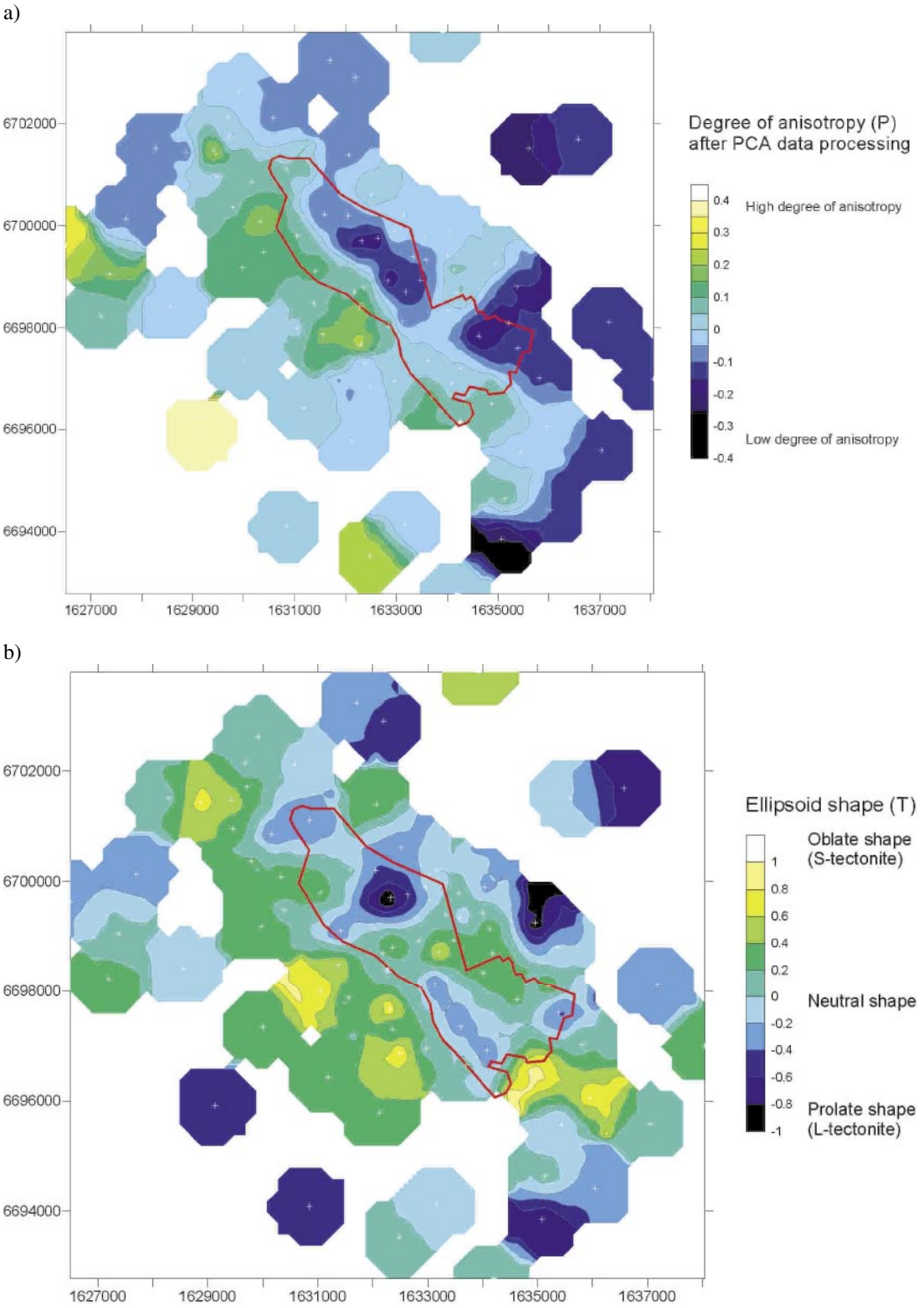

Figure 5-3. *Contour plots of a) normalized degree of magnetic anisotropy and b) ellipsoid shape parameter (T) of the rocks in the Forsmark area. The sampling locations are indicated by a white cross. See the text for explanation. The candidate area is outlined with a red line.*

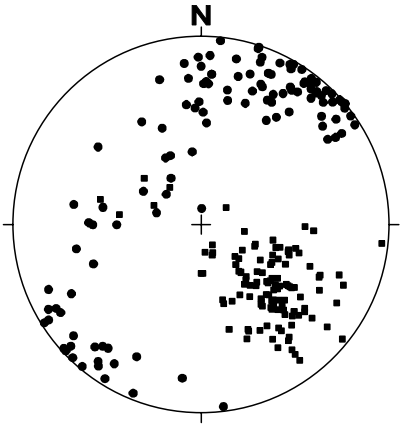

Figure 5-4. *Equal area projection plot of the site mean Kmax (lineation) and Kmin (pole to foliation) AMS axes for all investigated sites in the Forsmark area. Squares = lineation and dots = poles to foliation.*

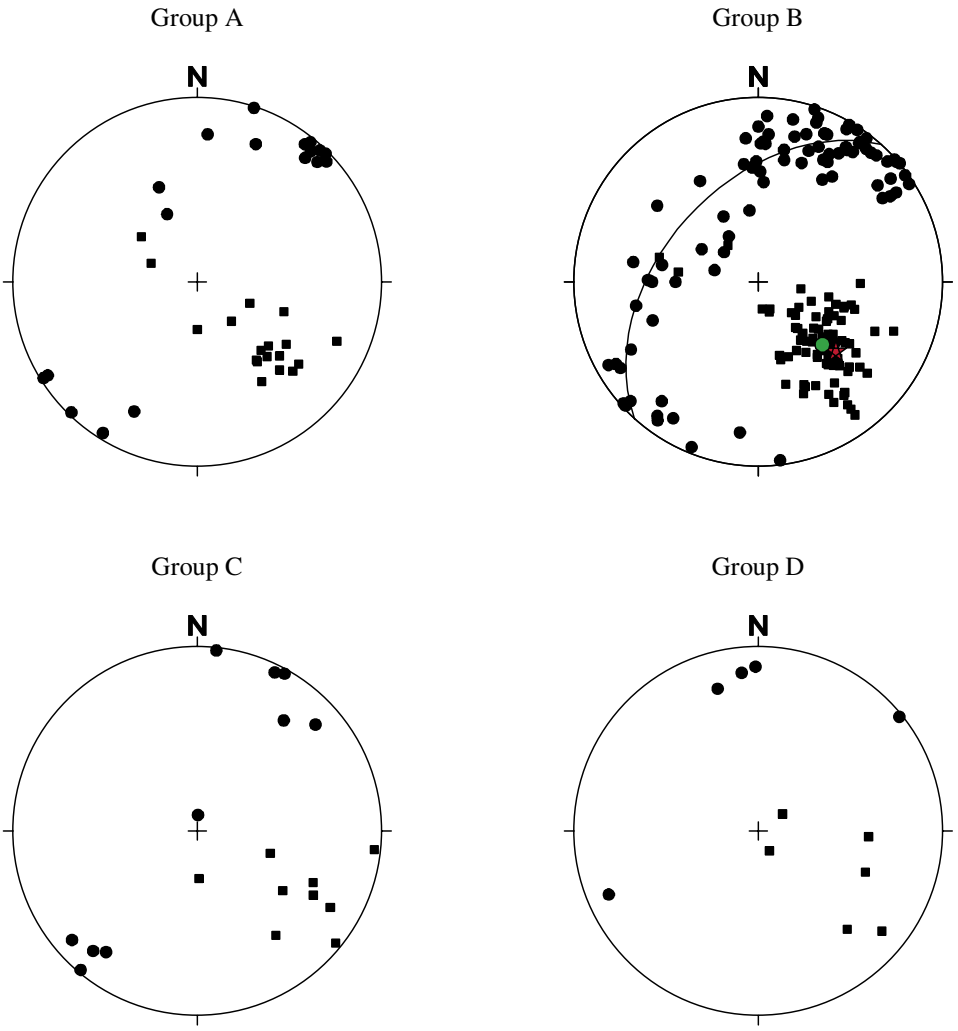

Figure 5-5. *Equal area projection plots of AMS lineation and poles to foliation for each of the four geological groups A, B, C, and D respectively (site mean data). Squares = lineation and dots = poles to foliation. The red star in the group B plot indicates the estimated fold axis estimated from the mean intersection point of the magnetic foliation planes. The green dot shows the mean magnetic lineation direction.*

The geographical distribution of the lineation and foliation plane orientations shows a consistent pattern (Figures 5-6 and 5-7). In the figures, the group A and B rocks are represented by black symbols and the groups C and D rocks are represented by red symbols. Plus-symbols indicate sites where no mean direction could be established. A majority of the lineations have a southeast directed orientation and they dip c 35°–65°. In the central part of the candidate area there is an obvious counter clockwise rotation of c 20°–30° of the lineation, which is most likely related to the fold geometry indicated by the orientation of the foliation planes (Figure 5-5).

In Figure 5-7 the geographical distribution of the foliation planes shows that the rotation occurs within the central and eastern part of the candidate area. The rotation affects both meta-granite rocks and the meta-tonalite rock at the north-eastern boundary. Apart from this indicated fold of the rocks the foliations display very consistent, mainly southeast oriented strike directions with mainly sub vertical dips toward southwest. The magnetic fabric agrees very well with the general structural rock fabric of the area as indicated by aeromagnetic and geological data.

Contour plots of the dip of the magnetic foliation planes (5-8a) and the dip of the magnetic lineation (5-8b) clearly shows that different parts of the bedrock have different structural orientations. The dip of the foliation planes in the vicinity of the indicated fold geometry (central part of the candidate area), including the metatonalite rock, are significantly shallower than for the rocks at most other sampling locations. The rocks surrounding the folded geometry mainly show moderately dipping foliations. Northeast, west and northwest of the candidate area the dip of the foliation planes become steeper (80–90°), but most far west the dips are slightly shallower. The magnetic lineation of the metatonalite rock is subhorizontal, and northwest of the metatonalite the lineation dips rather steep. Along the south-western boundary of the candidate area the magnetic lineation dips moderately and the rocks further to southwest show moderate to steeply dipping lineations. A majority of the rock sample collected northeast of the candidate area have subhorizontal lineations.

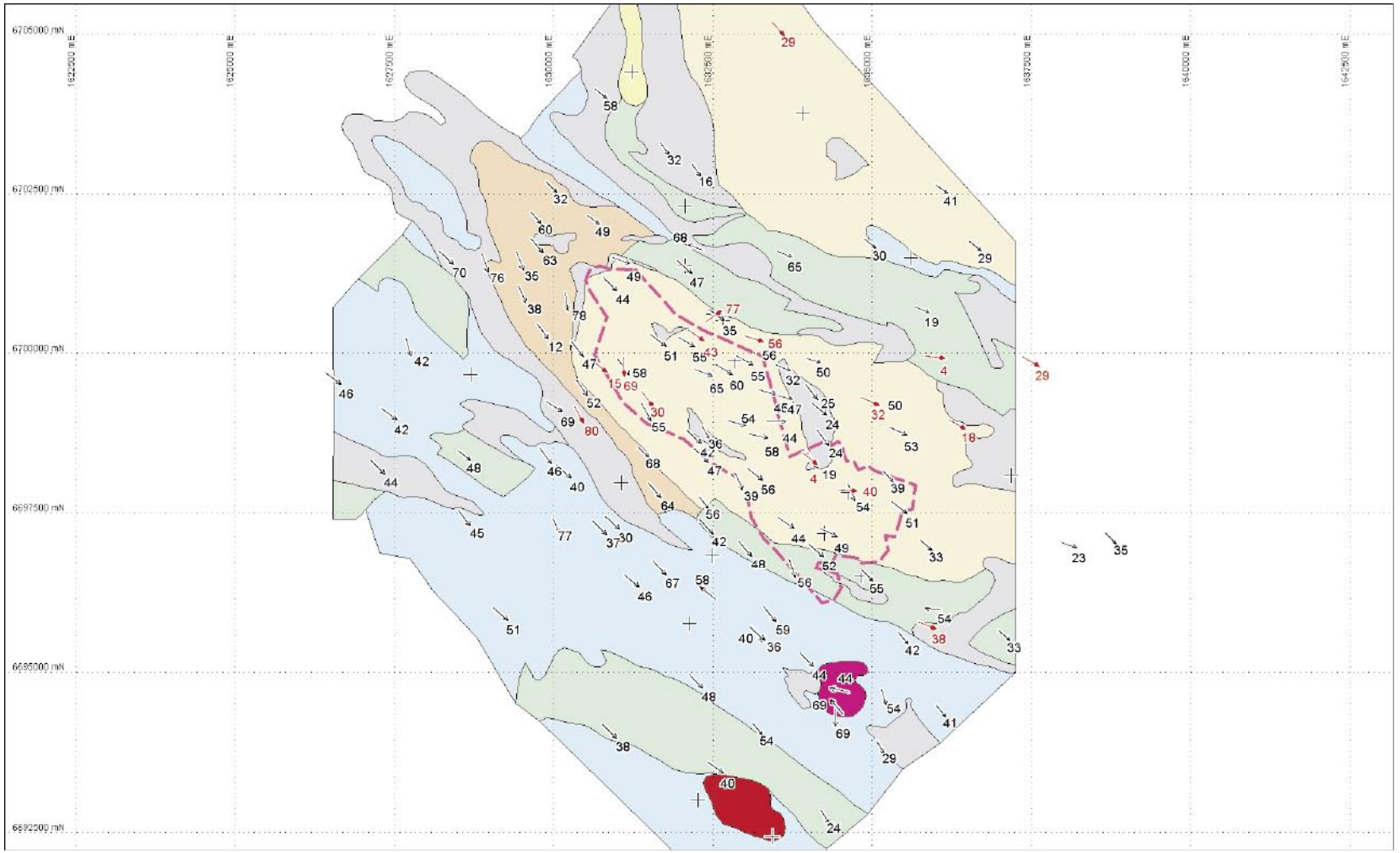

Figure 5-6. *Site mean magnetic lineation (strike and dip) of the rocks in the Forsmark area. See the text for explanation. The background information shows areas with different structural magnetic anomaly patterns (from /26/, Figure 4-5). The Forsmark candidate area is outlined with a dashed magenta line.*

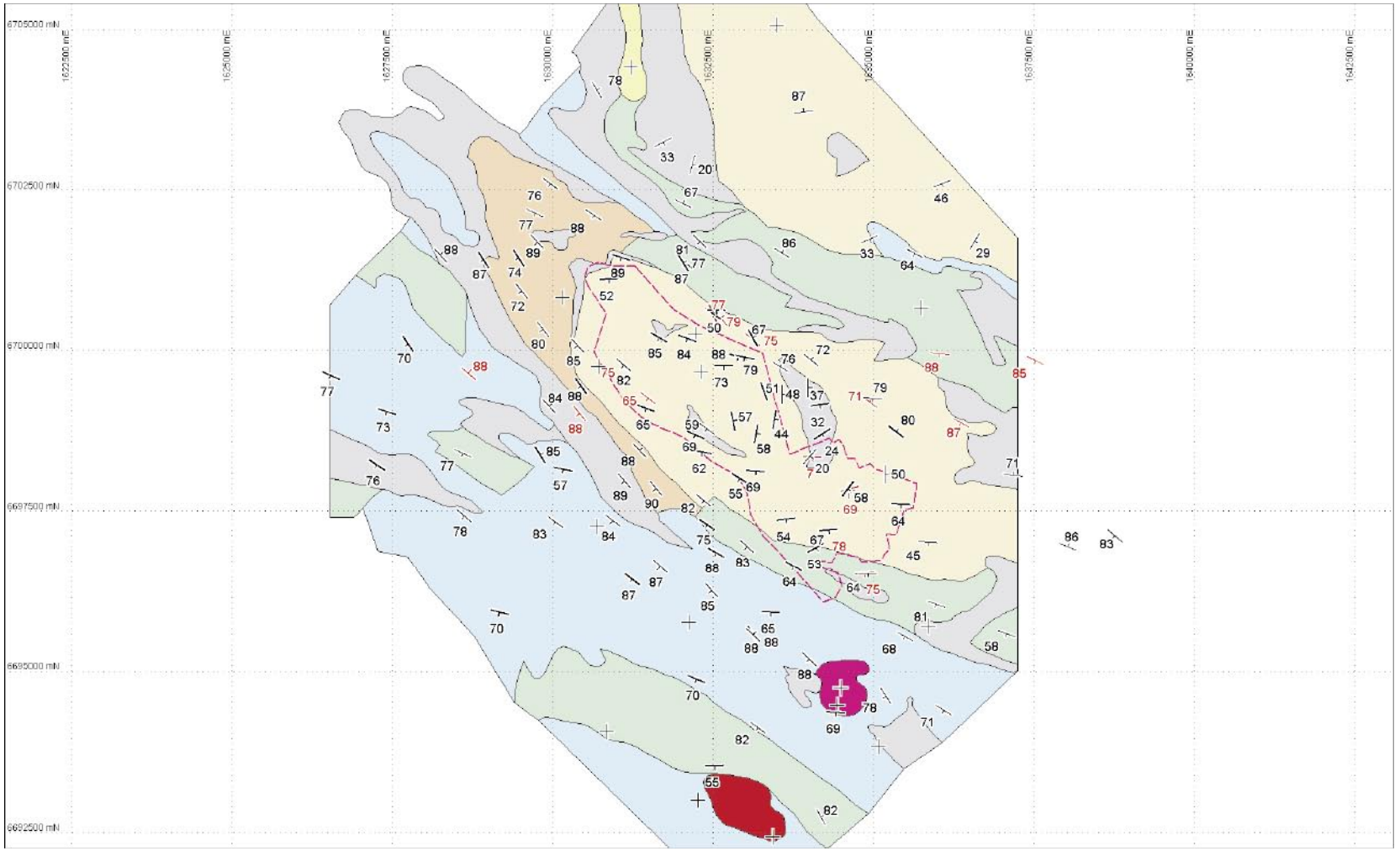

Figure 5-7. *Site mean magnetic foliations (strike and dip) of the rocks in the Forsmark area. See the text for explanation. The background information shows areas with different structural magnetic anomaly patterns (from /26/, Figure 4-5). The Forsmark candidate area is outlined with a dashed magenta line.*

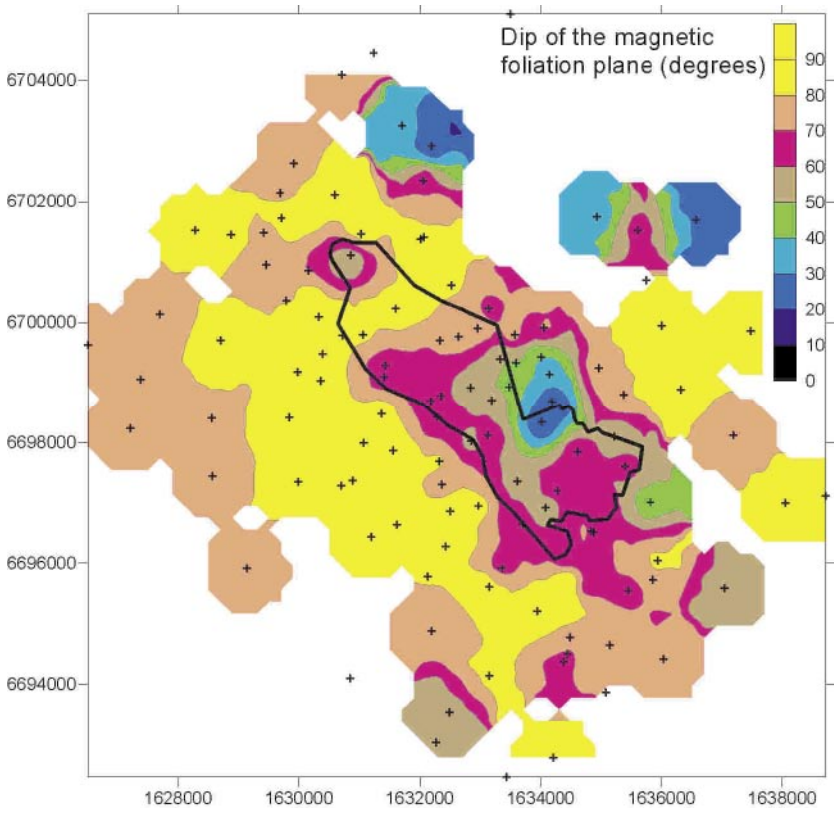

a)

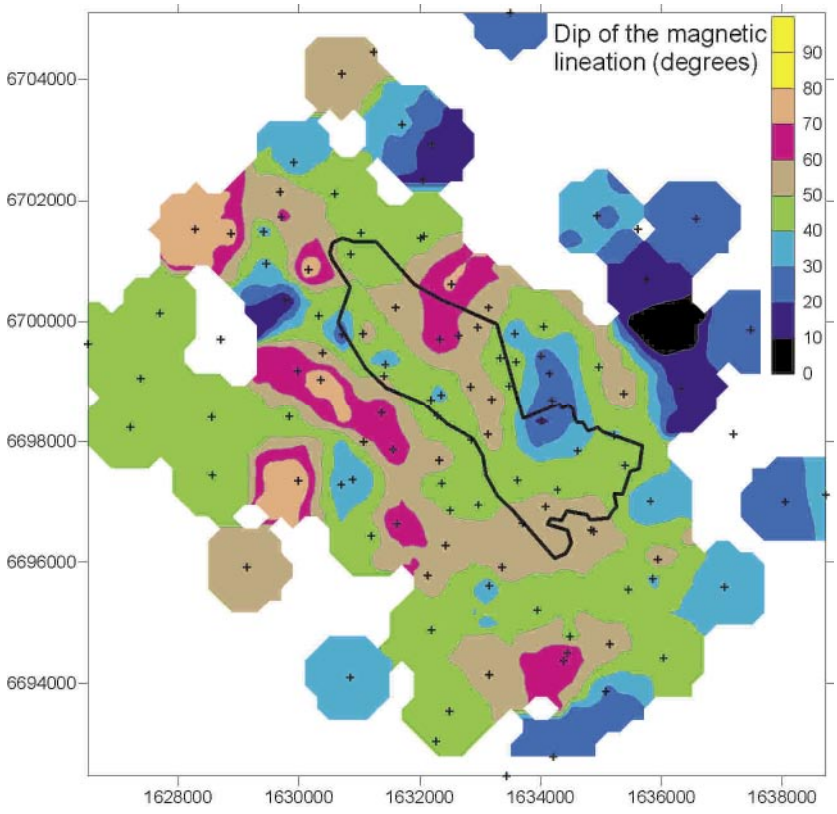

b)

Figure 5-8. *Contour plots of a) dip of the magnetic foliation plane b) dip of the magnetic lineation. The sampling locations are indicated by a black cross and the Forsmark candidate area is outlined with a black line.*

5.4 Conclusions

The following conclusions are drawn based on the AMS study:

- A majority of the investigated rocks have suffered from various degrees of plastic deformation.
- All investigated rock types (groups A, B C and D) seem to have been similarly affected by the plastic deformation, which indicates that the deformation detected by the AMS-method occurred after the emplacement of the youngest investigated rock.
- The highest strained rocks occur along a northwest-southeast trending region located just outside the western boundary of the candidate area. Higher degrees of deformation are also indicated outside the eastern boundary of the candidate area.
- Within the central part of the candidate area the rocks are folded. The fold axis is oriented at Declination = 132° and Inclination = 43°. The magnetic lineation is parallel to the fold axis orientation, which indicates that the maximum strain is parallel to the fold axis.
- Dominant pure shear type of deformation, causing dip-slip movement, appears to have affected the highest strained rocks along the north-western boundary of the candidate area, whereas the deformational movement northeast of the candidate area seems to have been dominated by oblique strike-slip.

6 Electrical properties and porosity

Electric resistivity

The contrast in resistivity (ρ) between silicate minerals and more conducting media like water or sulphides/graphite is extremely high. The bulk resistivity of a rock is therefore virtually independent of the type of silicate minerals that it contains. Electric conduction will be almost purely electrolytic if the rock not contains sulphides or graphite. Archie's law /24/ is frequently used to estimate the conductivity (1/ρ) of sedimentary rocks.

$$\sigma = a \cdot \sigma_w \cdot \varphi^m \cdot s^n$$

where

σ = bulk conductivity (=1/ρ, S/m),

σ_w = pore water conductivity (S/m),

φ = volume fraction of pore space,

s = fraction of pore space that is water saturated,

a, m, n = dimensionless numbers, $m \approx 1.5$ to 2.2, $a \geq 1$.

Archie's law has proved to work well for rocks with a porosity of a few percent or more. Old crystalline rocks usually have a porosity of 0.1 to 2% and sometimes even less. With such low porosity, the interaction between the electrolyte and the solid minerals becomes relevant. Some solids, especially clay minerals, have a capacity to adsorb ions and retain them in an exchangeable state /25/. This property makes clays electrically conductive but the same property can to some degree be found for most minerals. The resulting effect, surface conductivity, can be accounted for by the parameter a in Archie's law. The relative effect of surface conductivity will be greatly reduced if the pore water is salt. The amount of surface conductivity is dependent upon the grain size and texture of the rock. Fine grained and/or chlorite and mica-rich, foliated rocks are expected to have a large relative portion of thin membrane pore spaces that contribute to surface conductivity. The power m in Archie's law accounts for variations in pore space geometry. Rocks with relatively straight pores with small variations in cross-sectional area will show low values of m. High values are typical for rocks with vugs and constrictions in the pore space and with crocked pore paths.

The electric resistivity is in reality not a simple scalar. Most rocks show electric anisotropy and the resistivity is thus a tensor. On a micro-scale the anisotropy is caused by a preferred direction of pore spaces and micro fractures.

Induced polarisation (IP)

The IP effect can be caused by different mechanisms of which two are the most important. When the electric current passes through an interface between electronic and electrolytic conduction there is an accumulation of charges at the interface due to the kinetics of the electrochemical processes involved. Such situations will occur at the surface of sulphide, oxide or graphite grains in a rock matrix with water filled pores. The second mechanism is related to electric conduction through thin membrane pore spaces. In this case an accumulation of charges will occur at the beginning and end of the membrane. The

membrane polarisation is thus closely related to the surface conduction effect mentioned above for electric resistivity. Fine grained and/or mica and chlorite rich, foliated rocks are therefore expected to show membrane polarisation. Also, the membrane polarisation is greatly reduced in salt water in the same way as the effect of surface conductivity.

Since the polarisation is caused by several complicated processes it is not possible to describe the frequency or time dependence of IP with any analytical function. It is however common to model the complex resistivity of a rock material with the empirical Cole-Cole model:

$$\rho(\omega) = \rho_0\left[1 - m\left(1 - \frac{1}{1 + (i\omega\tau)^c}\right)\right]$$

where

ρ_0 = resistivity at zero frequency (Ωm),

ω = angular frequency (rad/s),

m = chargeability,

τ = time constant (s),

c = shape factor,

$i = \sqrt{-1}$.

The complex resistivity is thus described by ρ_0, m, τ and c. High chargeability is expected for rocks containing significant amounts of conductive minerals but also for rocks with clay alteration or considerable membrane pore space. The frequency at which the IP effect is strongest is related to the time constant. IP caused by conductive minerals or clay will in general give IP with long time constants whereas membrane polarisation will cause IP with short time constants that might be just of the order of milliseconds. The time constant is also texture dependent, where coarse grained rocks in general will cause IP with longer time constants than fine grained rocks. Field surveys are usually performed at 0.1 to 10 Hz (or equivalent times if performed in the time domain). They will therefore mainly detect IP sources with long time constants.

Measurement procedure

The sample handling and laboratory procedure has been described in /1/ and is therefore only treated briefly here.

The electric properties were measured on 135 rock samples. Out of the generally four drill cores that were collected for each rock type at each site, one was selected for electric measurements. The measurements were then performed with an in-house, two electrode equipment of Luleå University of Technology, which uses a saw-tooth wave-form at three base frequencies (0.1, 0.6 and 4 Hz). The complex resistivity was measured on the samples in accordance with SKB MD 230.001. The samples were first soaked in tap water and measured and then soaked in salt water (125 g NaCl per 5 kg of water) and measured once more. It should be noted that the 48 hours minimum that the samples were soaked in salt water might not be enough to completely saturate all pore spaces with salt water. However, the resulting accuracy of the measurements is expected to be good enough for the application of the data to bedrock mapping.

The porosity of the samples was calculated by measuring the weight of the samples water saturated, dry and suspended in water. This procedure also gives input for calculation of wet and dry density. Porosity and density measurements were performed on all drill cores of a rock type from each site assembled together.

6.1 Data processing

A correction for drift caused by drying of the sample during measurements is done automatically by the instrumentation software by comparing the harmonics of low frequency measurements with the base frequency result of the next higher frequency.

The resistivity data were compared with the measured porosity in order to make a fit in accordance to Archie's law. It should however be noted that the porosity measurements in this study were performed on all samples of a rock type from a site assembled together, whereas the electric properties were measured on one sample only. This will introduce some uncertainty in the analysis of the relation between resistivity and porosity.

Estimates of the effect of pore space geometry and the contribution of surface conductivity to the overall bulk conductivity of the samples were estimated in the following way. Assuming a reasonable and low value of the parameter a in Archie's law for measurements in salt water and using the measured values of σ, σ_w and φ, an apparent value of the power m was calculated for each sample. This apparent m-value is then used together with the fresh water data to estimate an apparent a-value. High a-values will correspond to a large contribution from surface conductivity to the bulk conductivity and vice versa. The porosity data will be cancelled out in the calculation of the apparent a-values.

The measurements, including harmonics, ranged from 0.1 to 30 Hz. This makes accurate fits of data to the Cole-Cole model possible for samples with a time constant in the interval 5 milliseconds to 1.7 seconds. Since it was obvious that samples with both shorter and longer time constants exist in the study, fits were only performed for a few samples to obtain typical values of the Cole-Cole parameters. The fit was performed with a GeoVista in-house procedure based on Monte-Carlo inversion. A simple estimate of the IP frequency characteristics was however obtained by calculating the ratio of the phase angle at 4 Hz to the phase angle at 0.1 Hz. Large ratios will then, in general, correspond to short time constants and vice versa.

6.2 Results

Porosity

The distribution of measured porosities can be seen in Figure 6-1. The range of porosities is, with a few exceptions, rather narrow. Most samples have porosity between 0.3 and 0.6%. The low number of samples with higher porosity might be due to the fact that mainly fresh rock was sampled in this study. The two samples of group A with very high porosity are from the Fe-mineralizations (PFM000336 and PFM000446) south of the Forsmark candidate area and the two high porosity samples of group B are from altered ultra-mafic rocks (PFM001201 and PFM001205). Although the porosity ranges of the groups overlap, some differences can be noted. Group A has lower porosity than the other groups with a median value of 0.374%. Group B has slightly higher porosity with a median value of 0.413%. Group C and D have even higher median values of 0.484 and 0.509% respectively, but since the number of samples of these rock groups is small, the difference might not be significant.

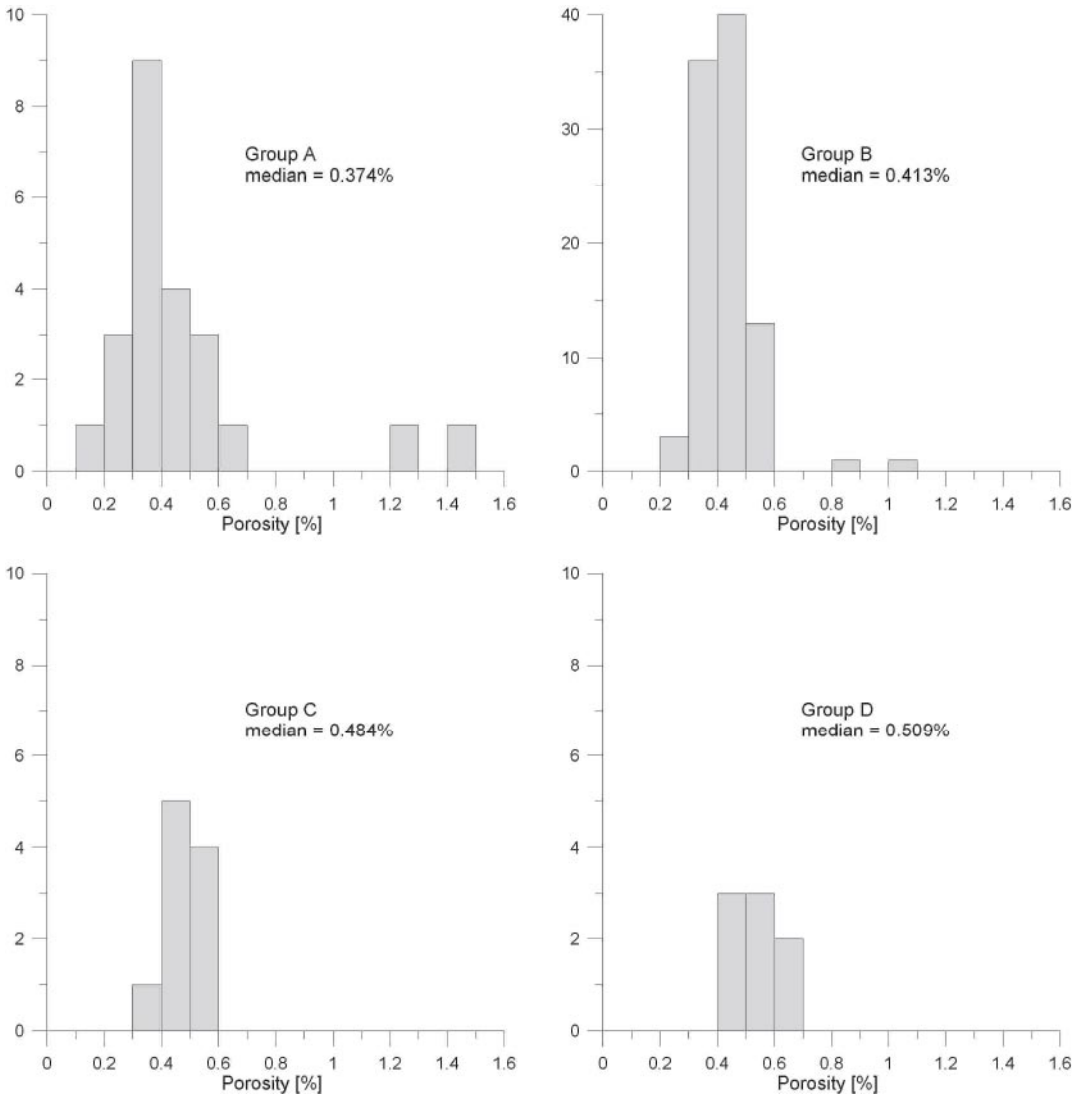

Figure 6-1. *Histograms showing distribution of measured porosities for the rock groups A, B, C and D.*

Within group B there is a weak tendency that the mafic samples have slightly lower porosity than the felsic samples. The median porosity of the B2/B3 group combined is 0.370% whereas the corresponding values for B5/B6 combined and B8/B9 combined is 0.394% and 0.426% respectively. However, these differences are hardly statistically significant.

Figure 6-2 shows the spatial distribution of porosity values. The candidate area is quite uniform with most samples having porosity between 0.4% and 0.52%. A few samples with higher values can be found along the north-eastern border of the candidate area and smaller values can be found north-east of Bolundsfjärden. Samples from the areas south and west of the candidate area have, in general, lower porosity. This is not entirely due to the presence of A type rocks; also the B type rocks have lower porosity here, which might be an effect of the ductile deformation of the rock.

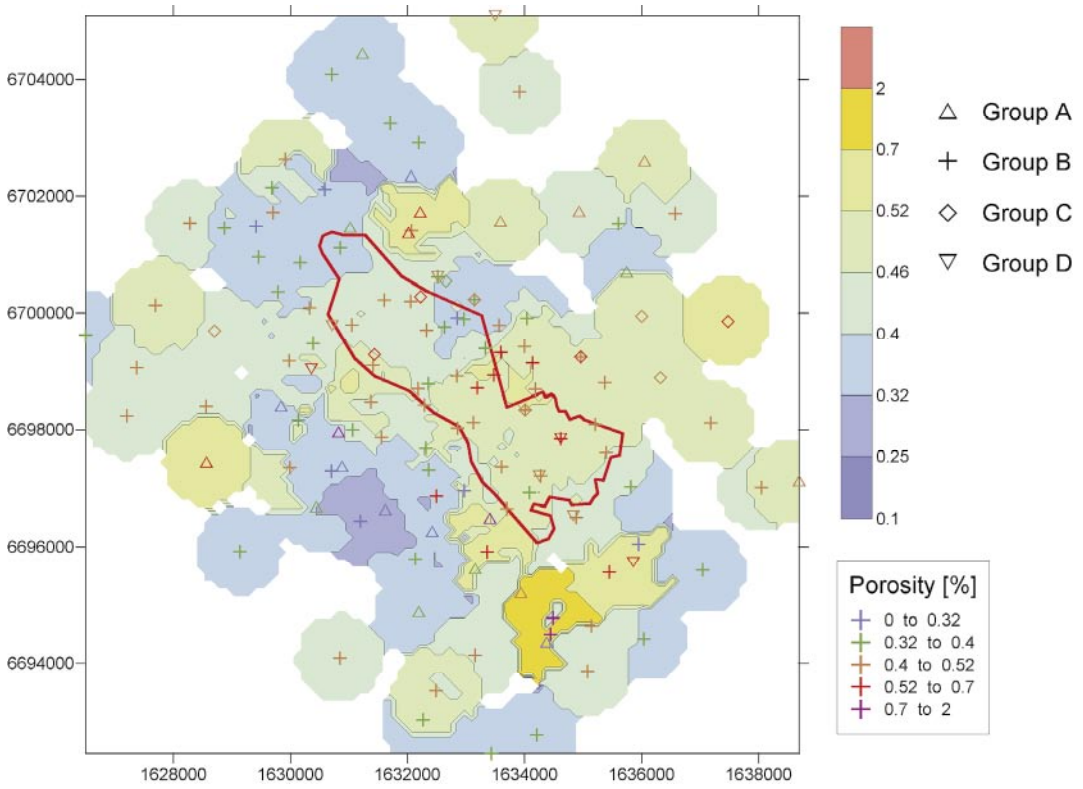

Figure 6-2. *Map showing the measured porosity of the samples. The contour lines have been interpolated by taking the median value of values within a search radius of 800 m. The Forsmark candidate area is shown with a red line. The different rock groups are indicated with different symbols with the measured porosity indicated by the symbol colour.*

Electrical properties

The spatial distribution of electrical properties and the properties of different rock groups have been analyzed.

The IP effect as a function of resistivity in fresh water can be seen in Figure 6-3. With a few exceptions the samples have resistivities ranging from 8,000 to 35,000 Ωm and IP-values (phase angles) ranging from 5 to 18 mrad. Both ranges can be considered to be quite normal for non-mineralized crystalline rocks.

Four samples have significantly different properties compared to the others. They show unusually low resistivity and very high IP values. Two of the samples are from Fe-mineralization at PFM000336 and PFM000446 and the other two are from meta-ultramafic rocks at PFM001201 and PFM001205. High grades of magnetite explain the low resistivity and high IP of these samples. Only a few more samples have IP values above 30 mrad, all belonging to the A and B groups and having densities of more than 2,720 kg/m^3. One non-mineralised sample of the A group (PFM001640) have a rather low resistivity of 1,725 Ωm.

The differences in resistivity between the rock groups are rather small. Group A has the lowest median resistivity (10,900 Ωm) and also the largest spread. Group B has the highest median resistivity (17,600 Ωm). Within the B group, the mafic subgroups have slightly lower resistivity than the felsic ones. B2/B3 combined has a median resistivity of 14,400 Ωm, whereas the corresponding values for B5/B6 combined and B8/B9 combined are 16,100 Ωm and 20,300 Ωm, respectively. The higher value for B8/B9 is significant.

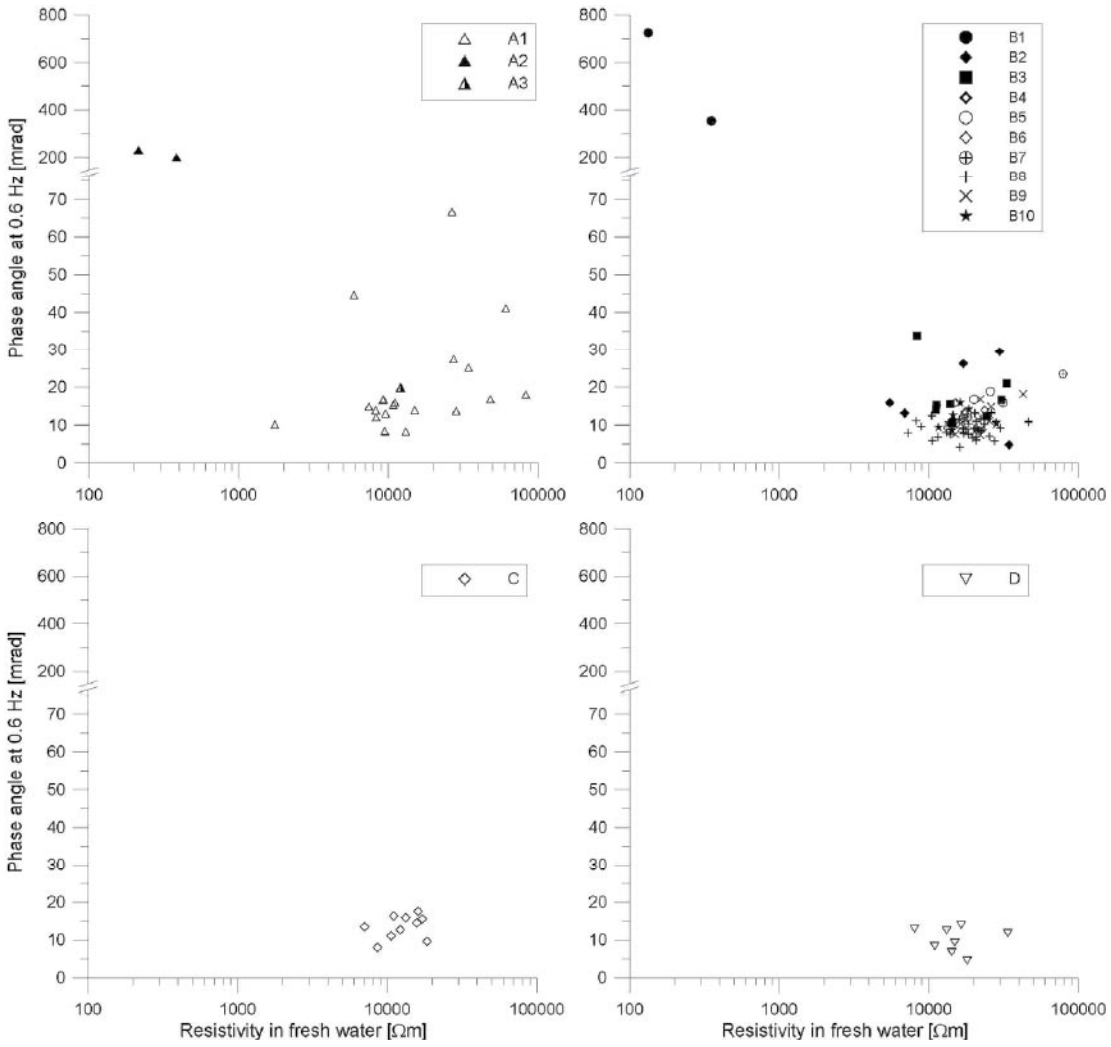

Figure 6-3. *Resistivity and IP-effect (phase angle) for samples soaked in tap water.*

The ranges of IP values for the rock groups overlap but the group A has a higher median value (15.9 mrad) compared to the others (B: 11.0 mrad, C: 14.0 mrad, D: 10.5 mrad). Within the B group there is a difference between the mafic and the felsic rocks where the latter ones have lower IP although the ranges overlap. The median value for the B2/ B3 combined is 15.4 mrad whereas the corresponding value for the B5/B6 combined and the B8/B9 combined are 12.8 and 8.9 mrad respectively.

Maps showing the resistivity and IP values of the samples can be seen in Figure 6-4 and 6-5. Contour lines have been interpolated by taking the median measured value within a search radius of 800 m. The candidate area show fairly uniform resistivity values. Hardly any resistivities above 25,000 Ωm or below 8,000 Ωm have been measured on samples from this area. Resistivities above 25,000 Ωm can be found for some samples along the southern border of the candidate area. The ductile deformed belt south of the candidate area shows more variable resistivities where both high and low resistivity values can be found. The area to the northeast of the candidate area is characterised by fairly low resistivity values.

Almost all samples with IP below 8 mrad can be found within the candidate area. The northern part of the candidate area has slightly higher values. Even higher IP can be found in the ductile deformation belt in the south and also to the north, even though there are several exceptions from this pattern.

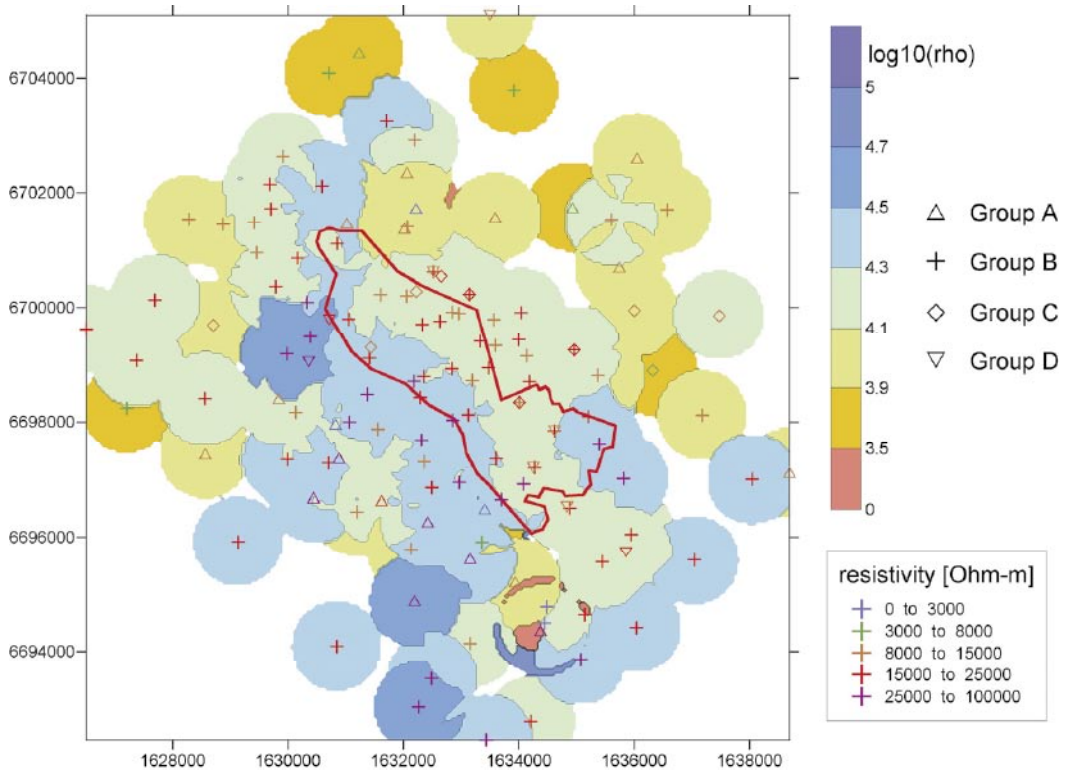

Figure 6-4. *Map showing the resistivity of samples soaked in fresh water. The contour lines have been interpolated by taking the median value of values within a search radius of 800 m. The Forsmark candidate area is shown with a solid red line.*

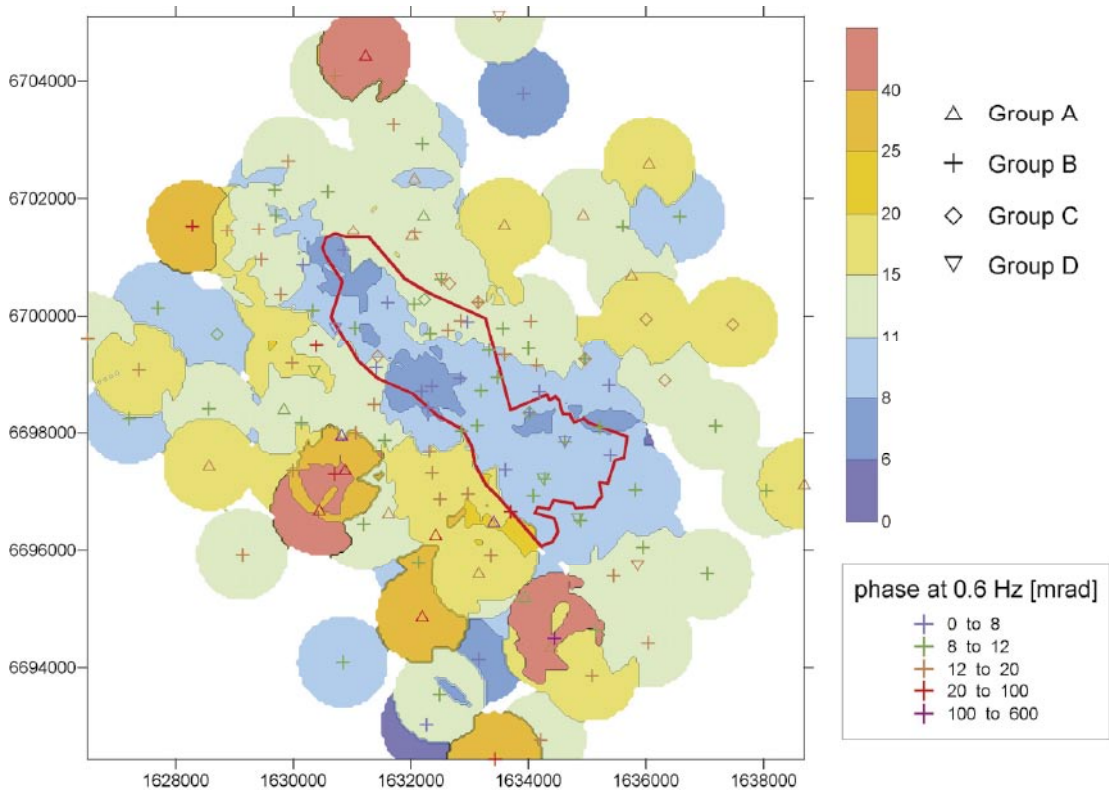

Figure 6-5. *Map showing the IP effect (phase angle) of samples soaked in fresh water. The contour lines have been interpolated by taking the median value of values within a search radius of 800 m. The Forsmark candidate area is shown with a solid red line.*

The measured resistivity as a function of porosity is plotted in Figure 6-6. A negative correlation might be expected since high porosity should correspond to low resistivity and vice versa. This relationship might be modelled with Archie's law according to the discussion in Section 6.1. However, such a correlation is hardly possible to see in Figure 6-6. There are some possible reasons for this. Firstly, the porosity has been measured on all drill cores from a site assembled to one sample in order to get a high accuracy, whereas the resistivity has been measured on one drill core only. This procedure will introduce some scatter in the plot in Figure 6-6. However, it can hardly entirely explain the lack of correlation. A second reason is that samples have different surface conductivity properties. Samples where the porosity to a relatively high degree consists of thin membranes will have a lower resistivity than a sample with the same porosity but wider pore spaces. A third reason for the poor correlation in Figure 6-6 is that the samples might be anisotropic. It has only been possible to measure the resistivity in one direction for each sample. The porosity is a simple scalar and this means that the position of a sample in the plot in Figure 6-6 to some degree might be dependent on the drill core orientation relative rock foliation and rock lineation. Finally it should be noted that the range of porosities in the measured samples is quite narrow. It is likely that a better correlation to the resistivity could be found if samples with higher and lower porosities had been available.

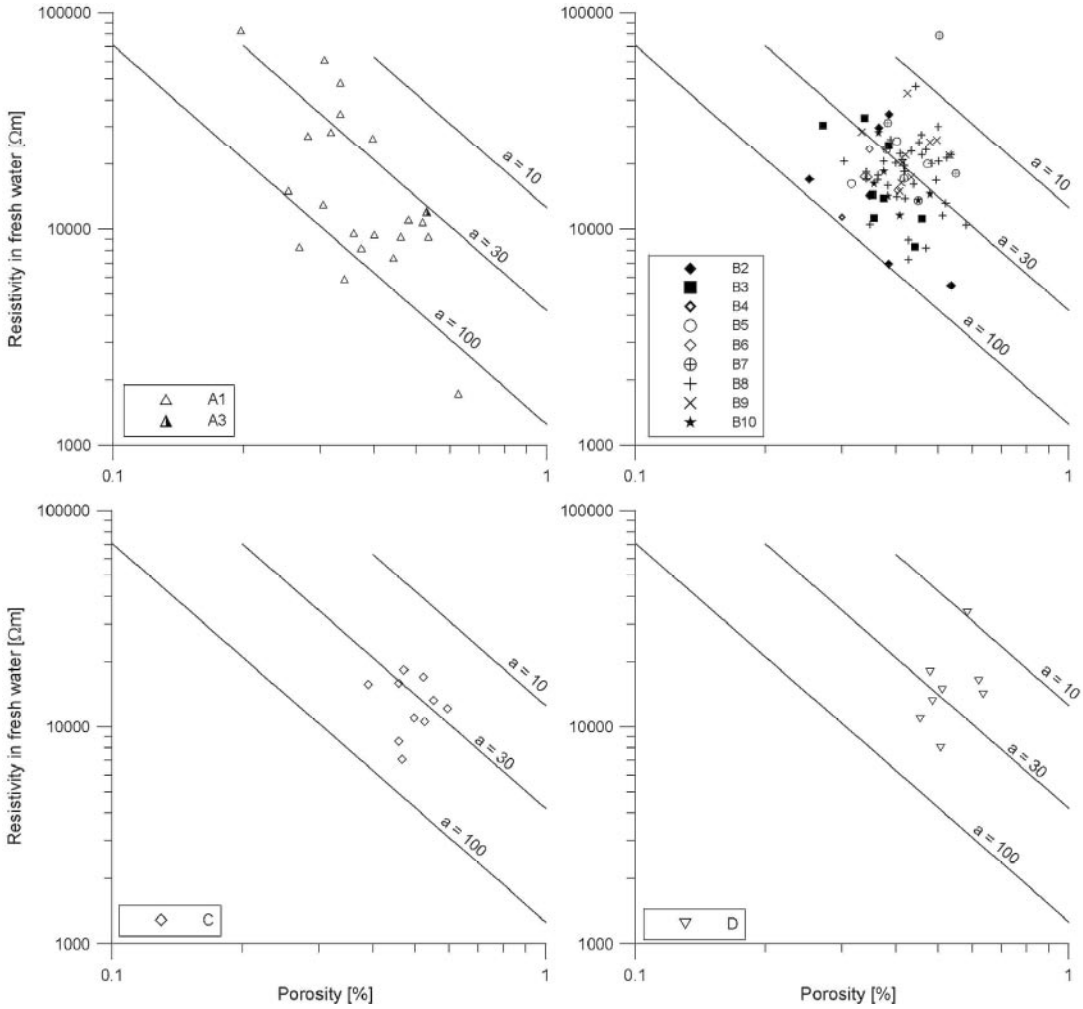

Figure 6-6. *Measured resistivity as a function of porosity for samples soaked in fresh water. The three straight lines represent the resistivity according to Archie's law calculated for m = 1.75 and σ_w = 0.025 S/m. The samples then show different apparent a-values which might correspond to different amounts of surface conductivity. It should however be noted that the apparent a-value can be corrected for pore space geometry (value of m in Archie's law).*

The straight lines in Figure 6-6 corresponding to the resistivity calculated with Archie's law and different values for the factor a indicates that surface conductivity is dominating over pure electrolyte conduction. This means that pore space thickness and geometry will be the most important factors determining the resistivity of the rock and not pore space volume.

The resistivity measured on samples soaked in salt water as a function of porosity can be seen in Figure 6-7. The salt concentration was 125 g NaCl per 5 kg of water. This is not a saturated solution and even if the relative effect of surface conductivity is reduced by the salt, it might not be completely removed. The correlation between porosity and resistivity is rather poor also for this case and no reliable fit to Archie's law can be made. Straight lines corresponding to resistivity calculated with Archie's law and different values of m are also plotted in Figure 6-7. Reasonable values of m range from 1.5 to 2.2 according to literature. The factor a in Archie's law has been assigned a value of 5.0 in order to get reasonable apparent m-values. Assuming that this procedure does not introduce any large errors it can be presumed that pore space geometry varies for the different samples, especially within the A and B rock groups.

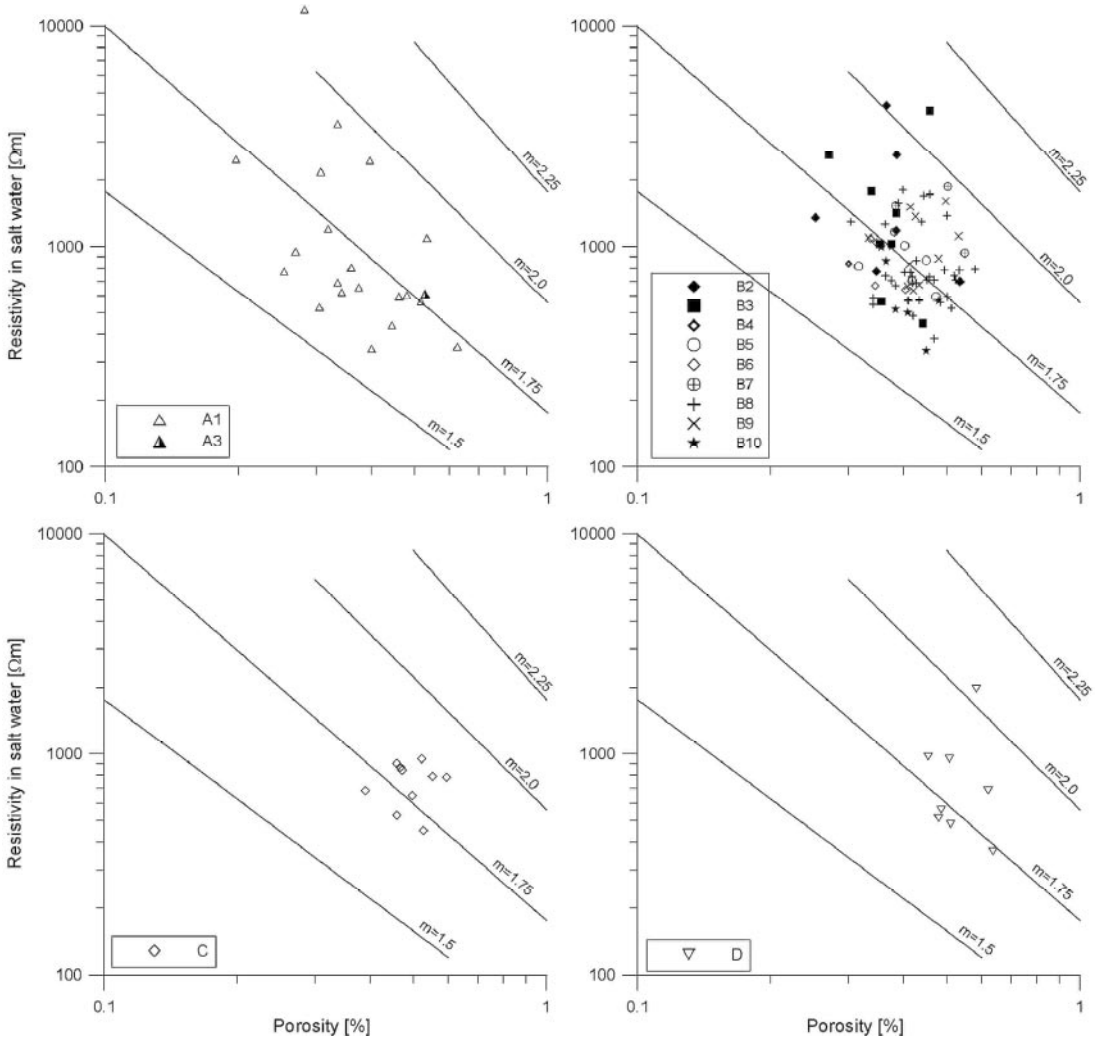

Figure 6-7. *Measured resistivity as a function of porosity for samples soaked in salt water. The straight lines represent the resistivity according to Archie's law calculated for a = 5.0 and* σ_w *= 3.57 S/m.*

Using apparent m-values from Figure 6-7, apparent a-values that indicate the amount of surface conductivity in the samples can be calculated. High values would then correspond to a large contribution of surface conductivity to the bulk conductivity of the samples. These apparent a-values are shown on a map in Figure 6-8. Most samples from the belts of ductile deformation have high values of a as might be expected. However, there are also a number of samples in the northern-central part of the candidate area with high values. This might indicate some kind of pore space textural anomaly possibly related to presence of chlorite or fine-grained mica. This area partly coincides with the area of low porosity in Figure 6-2.

A map showing apparent m-values calculated from salt water measurements can be seen in Figure 6-9. High values would indicate the presence of vugs, constrictions and/or crocked paths in the pore space. High values are found for some samples in the south but also for samples in the central part of the candidate area. It should be noted that these samples were collected in the vicinity of drill site 2 where vuggy granite has been found in the cored drill hole KFM02A.

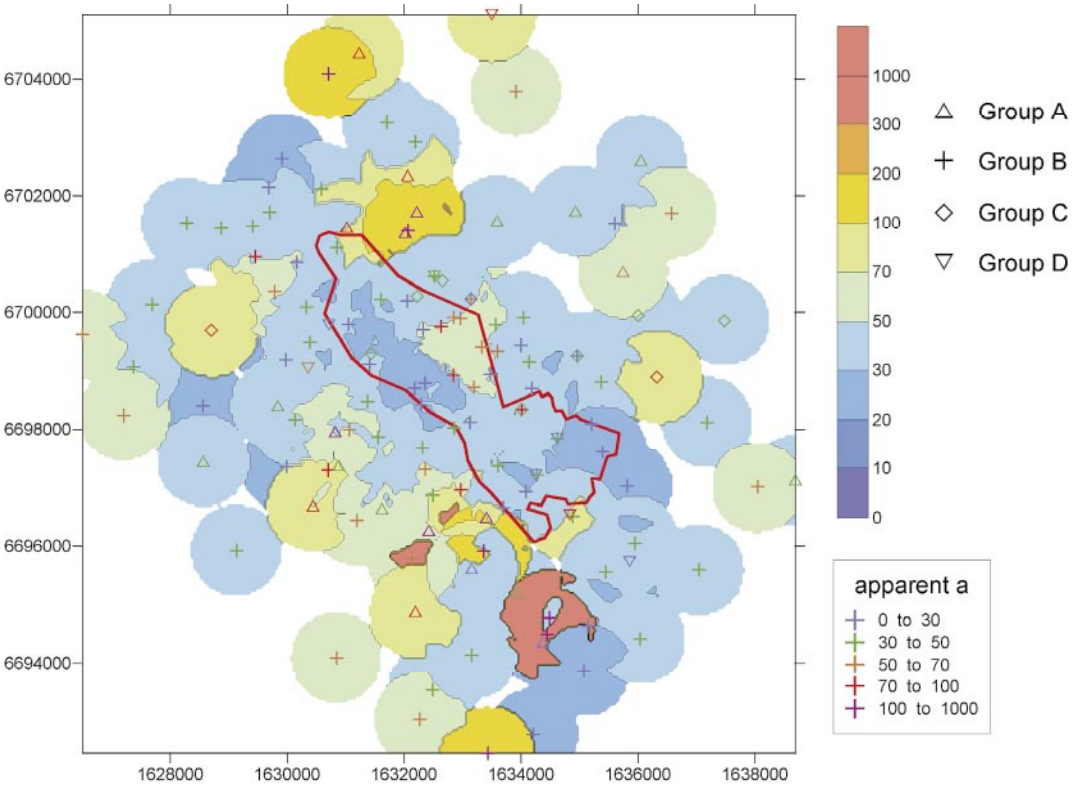

Figure 6-8. *Map showing apparent a-values in fits to Archie's law. High values correspond to large contributions of surface conductivity. The contour lines have been interpolated by taking the median value of values within a search radius of 800 m. The candidate area is shown with a red line.*

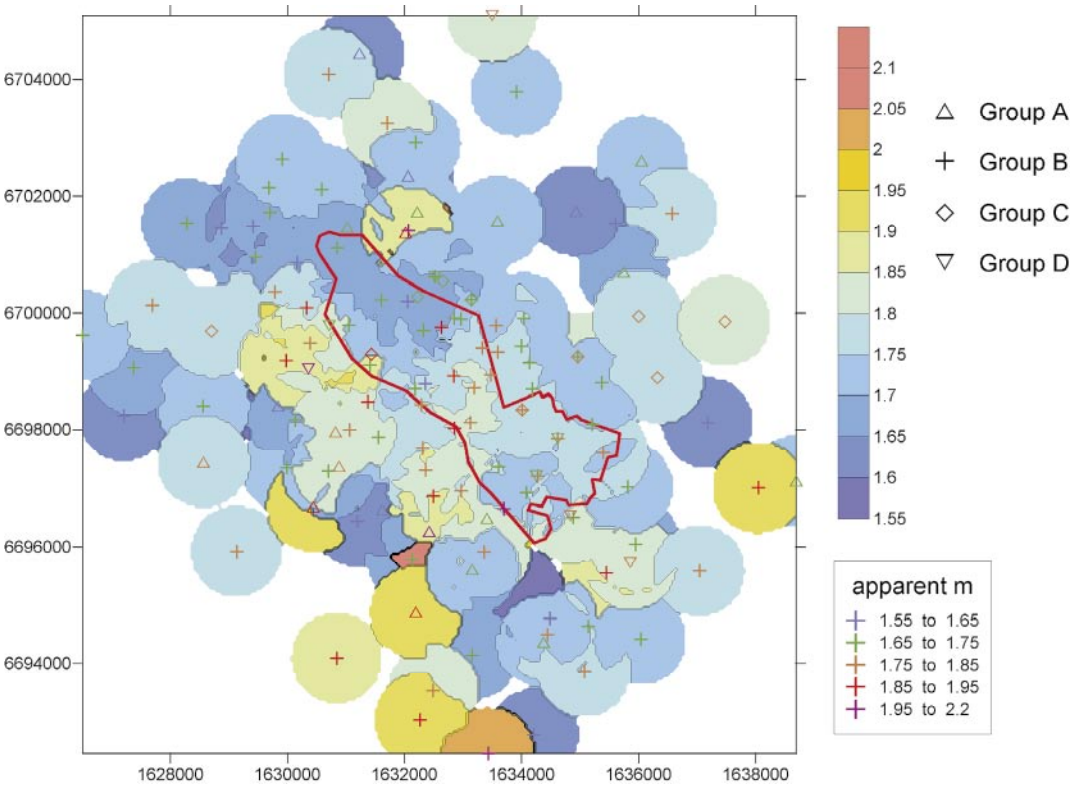

Figure 6-9. *Map showing apparent m-values in Archie's law estimated from measurements of the resistivity of samples soaked in salt water. The contour lines have been interpolated by taking the median value of values within a search radius of 800 m. The candidate area is shown with a red line.*

Another way of investigating the influence of surface conductivity is to compare the resistivity measured in fresh and salt water respectively, Figure 6-10. The contrast in resistivity between the fresh and salt water is in the interval 135 to 180 (fresh water conductivity varied between measurement dates). However, the average ratio in sample resistivity measured in fresh and salt water respectively is only 21. Since the effect of surface conductivity to a large extent is removed in salt water, the ratio of resistivity values can be taken as a measure of the relative contribution of surface conductivity in the fresh water measurements. In Figure 6-10 it can be seen that the four low resistivity samples of the Fe-mineralization and ultramafic rocks plot rather close to the solid line corresponding to equal resistivity for fresh and salt water measurements. This is due to the fact that electronic conduction is dominating over electrolyte conduction in these samples. One high resistivity sample of group A (PFM001885) and one from group B (PFM001235) also plots close to the line. It is possible that these samples have been poorly saturated with salt water but it is also possible that electronic conduction in oxide or sulphide minerals is significant. The PFM001885 sample has a fairly high magnetic susceptibility.

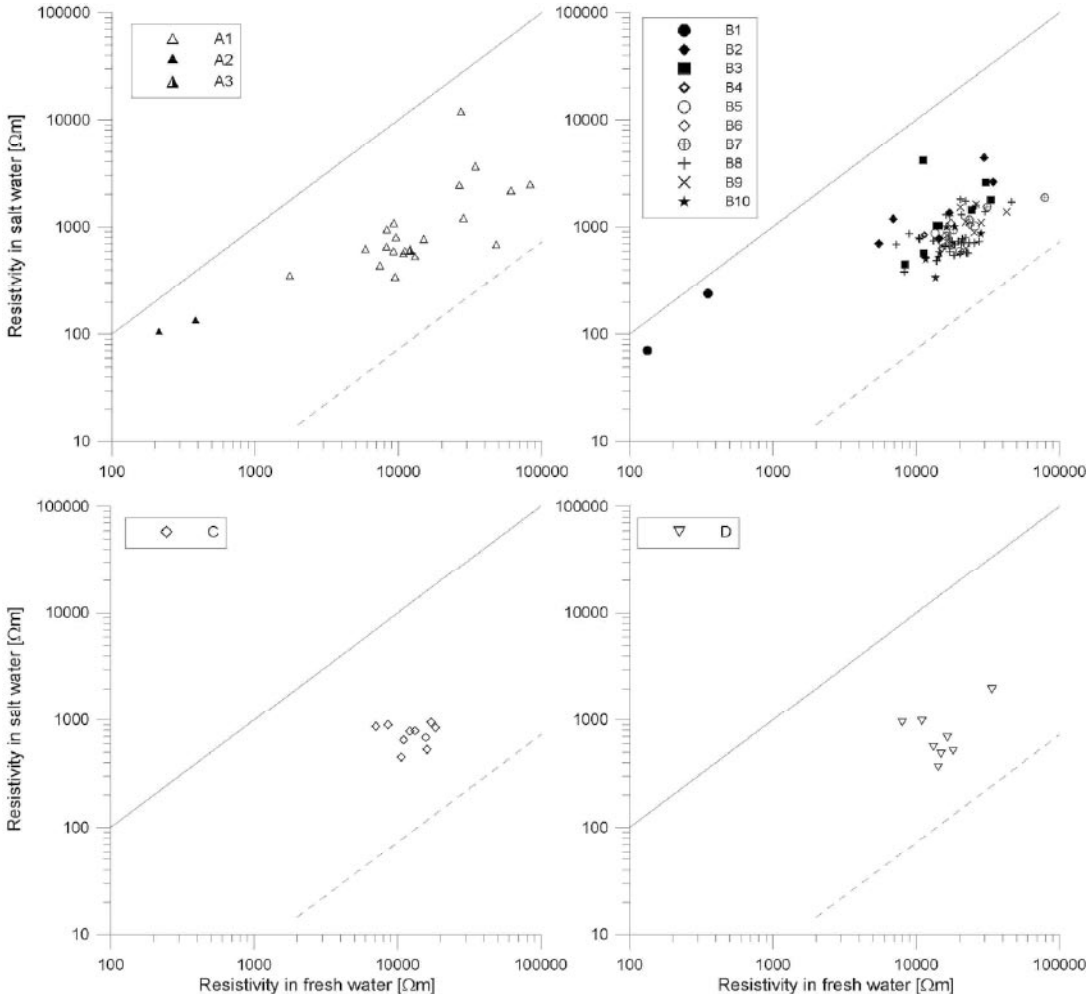

Figure 6-10. *Resistivity measured with the samples soaked in fresh and salt water. The straight line corresponds to equal resistivity for the two cases. The dashed line corresponds roughly to the contrast in resistivity that would be achieved without any surface conductivity or electronic conduction. The contrast in resistivity between the fresh and salt water was between 135 and 180 whereas the contrast in resistivity for most of the samples was just between 15 and 25.*

The relation between IP measured in fresh and salt water can be seen in Figure 6-11. Most samples have very low IP in salt water indicating that the IP in fresh water is due to membrane polarisation. The samples with significant IP effect in salt water are all from the belts with ductile deformation south and north of the candidate area. With a few exceptions these samples have high magnetic susceptibility and the likely explanation for their IP effect is magnetite. However, four low-magnetic samples show some IP in salt water for which the cause is unknown, namely PFM002056, PFM002087, PFM001235 and PFM001156.

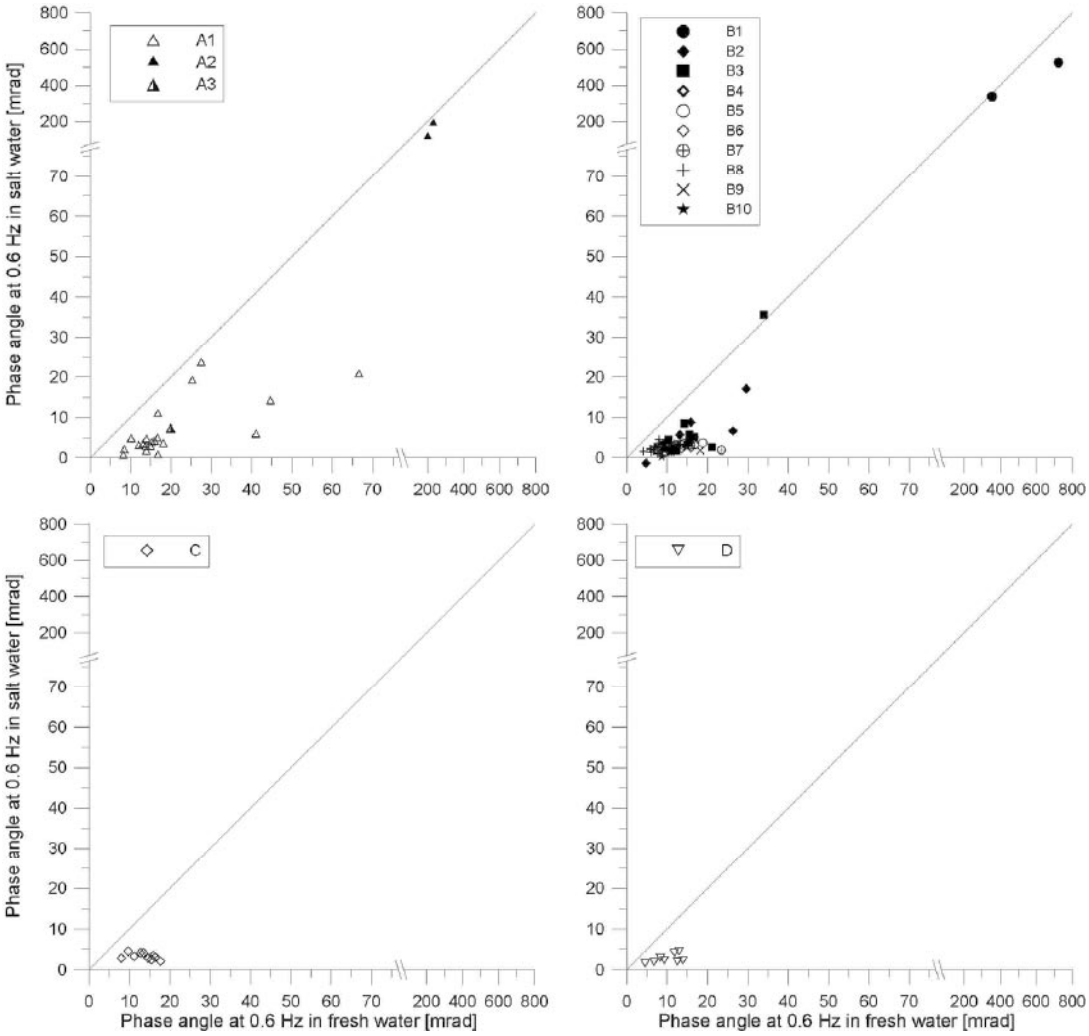

Figure 6-11. *IP-effect measured with the samples soaked in fresh and salt water. The straight line indicates equal IP for the two cases. Most samples show low IP in salt water indicating that membrane polarisation is the dominating IP effect in fresh water. With a few exceptions, the samples with significant IP in salt water have high magnetic susceptibility indicating that magnetite is the cause to this IP-effect*

The IP-effect has been plotted for two different frequencies in Figure 6-12. Stronger IP in the higher frequency compared to the lower frequency indicate IP with a short time constant. Most samples plot close to the straight line indicating equal IP for the two cases. All samples with significantly higher IP in the higher frequency are from the ductile deformation belt south of the candidate area. Most of them also have high magnetic susceptibility and IP in salt water, indicating presence of magnetite. Exceptions are PFM000240, PFM000253 and PFM000259. A few samples have lower IP for the high frequency. Some of these samples have noisy IP-data for the high frequency. However, the ultra-mafic rocks with very high IP at PFM001201 and PFM001205 have higher IP for the low frequency and thus long time constants and so have some samples of the A group with fairly low density sampled north of the candidate area, e.g. PFM000725 and PFM001156. These samples have low magnetic susceptibility and the cause of the anomalous IP properties is not known.

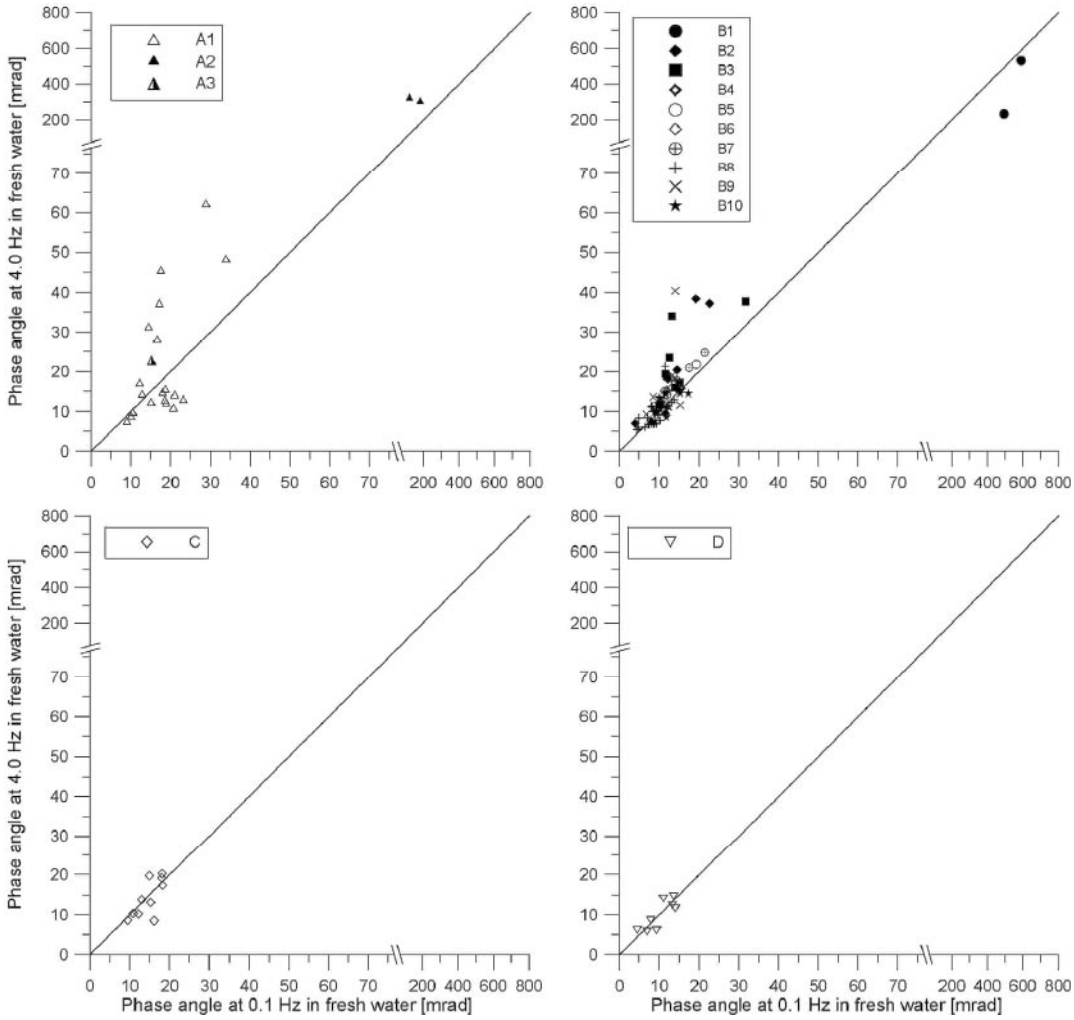

Figure 6-12. *IP-effect as phase angle for two frequencies. Samples that plot above the straight line are expected to have short time constants.*

Cole-Cole parameters have been calculated for a few of the samples to give an idea of what values to expect from different types of rocks. The results are shown in Table 6-1. It should be remembered that fits to the Cole-Cole model are not accurate for very short and very long time constants due to the limited frequency range of the measurements. The sample PFM000695 is of the B9 group from the candidate area and the sample PFM000739 is of the B10 group from just north of the candidate area. These can be seen as samples with fairly typical complex resistivities of granitic rocks in the candidate area. They have low chargeability, medium long time constants and high resistivity. Two samples (PFM000240 and PFM001521) are of the A group from the ductile deformation belt south of the candidate area selected for their fairly strong IP-effect. Both samples have high resistivity, high chargeability and short time constants. One sample (PFM000725) is from the deformation belt north of the candidate area and was selected for having anomalous IP properties. This sample has a very long time constant, low chargeability and moderate resistivity. The last sample (PFM001201) is of the B1 group and it has a very long time constant, high chargeability and low resistivity.

Table 6-1. Estimated Cole-Cole parameters for some selected samples with different electrical properties. Note that the estimates are very rough for samples with time constants shorter than 5 ms or longer than 1.7 s.

Sample	ρ0 (Ωm)	τ (s)	m	c	Rock group
PFM000240	64,640	0.00097	0.617	0.304	A1
PFM001521	31,100	0.013	0.623	0.229	A1
PFM000725	9,495	62.76	0.181	0.257	A1
PFM001201	1,170	44.67	0.913	0.389	B1
PFM000739	17,290	0.371	0.146	0.255	B10
PFM000695	25,980	0.015	0.085	0.22	B9

6.3 Conclusions

The majority of samples in this investigation show values of porosity and electrical properties that can be regarded as quite normal for crystalline rocks. The samples from the candidate area are characterised by having fairly high electric resistivity, low IP-effect and small variations in porosity. Some notes about the results are given below:

- Very low resistivity, high IP and fairly high porosity are found for samples of Fe-mineralisation and altered ultra-mafic rocks from the belt of ductile deformation south of the candidate area.
- Fairly high IP are found for some samples that also show high density and high magnetic susceptibility. The high IP of these samples is probably due to magnetite. All these samples are from outside the candidate area.
- Samples showing membrane polarisation and surface conductivity have been collected in the northern-central part of the candidate area. This might indicate a higher than normal content of chlorite and/or fine-grained mica.
- Some samples from the central part of the candidate are indicated to have pore volumes containing vugs, constrictions and/or crocked pore paths to a larger degree than the rest of the candidate area.
- Metavolcanic rocks to the north of the candidate area in general show a moderate IP effect with long time constant and lower than average electric resistivity.

7 Gamma ray spectrometry on outcrops and bare soil

7.1 Data processing

The in-situ gamma-ray measurements carried out in 2002 and 2003 have been treated statistically. Based on individual measurements, site averages have been calculated and the results are plotted as histograms and as hue-saturation plots. Site locations are presented in Figure 3-1.

7.2 Results

The results regarding the distribution of potassium (K), uranium (U) and thorium (Th) in the bedrock are discussed in conjunction with the histograms and hue-saturation plots in Figure 7-1 and 7-4 as well as the compilations in Appendix 1 and 2. Data from a few measurements on bare soil are presented in Figure 7-2 and 7-4.

The metamorphic, dacite and andesite rocks (group A1) show very scattered potassium content, from 0.4–4.3%, while uranium and thorium show a coherent pattern, Figure 7-1a. The group A1 shows an average content of 2.1% K, 4 ppm U and 11 ppm Th, based on measurements at 19 sites. One additional group A site is a veined gneiss (group A3), which shows a high potassium content, 5.1%, depending on its high K-feldspar content. Magnetite mineralizations (group A2) show low radiogenic content at two observation sites.

The potassium, uranium and thorium contents for ultramafic to mafic rocks are commonly low, which is also the case in Forsmark. Ultramafic rocks (group B1), measured at two sites show 0% K, 0 ppm U and 0 ppm Th. The metagabbro to metadiorite (group B2/B3) show an average content of 0.8% K, 1 ppm U and 2 ppm Th, based on measurements at 14 sites, Figure 7-1b. The metamorphic tonalite-granodiorite, group B5/B6, shows an average content of 1.9% K, 4 ppm U and 9 ppm Th, based on measurements at 20 sites, Figure 7-1c. Of interest is that this result is similar to the corresponding contents in dacites and andesites of group A1.

Granodiorite, metamorphic, group B7 shows a rather coherent distribution with content common for granodiorite, with an average of 1.9% K, 4 ppm U and 9 ppm Th, based on measurements at 5 sites.

Granite-granodiorite, metamorphic, group B8/B9 shows a coherent distribution with content common for granites, with an average of 2.9% K, 5 ppm U and 15 ppm Th, based on measurements at 47 sites, Figure 7-1d and Figure 7-4a. However, a few sites located at the margin of the Forsmark candidate area show depletion in the potassium content, and sites with < 2.2% K are marked in Figure 7-3.

Measurements on the metamorphic aplitic granite, group B10, show a very scattered result with a potassium content ranging from 0.8% to 4.1% and a thorium content ranging from 9 ppm to 28 ppm, Figure 7-1e. The uranium content is normal for granite rocks, 5 ppm in average on 9 sites. In general, the aplitic metagranite is more Th-dominant than typical granite, Figure 7-3b.

The metamorphic granodiorite, tonalite and granite, fine- to medium-grained, group C, indicates three radiogenic populations, Figure 7-1f. One site with diorite composition show typically low radiogenic content. One population is based on 8 sites, and show low potassium, 1.7%, and moderate uranium and thorium contents, 4 and 12 ppm respectively. Another population based on 6 sites show potassium and uranium contents normal for granite rocks, 2.4% and 4 ppm respectively. However, the thorium contents are anomalous, 20–30 ppm, average 25 ppm, Figure 7-4e. The latter two populations are both of tonalite-granodiorite-granite composition, thus indicating that the group C rocks possibly can be divided into two different subgroups independent from rock type. The geographical distribution of these two populations is scattered.

The radiogenic distribution for pegmatitic granite and pegmatite indicate three populations independent from the geological code, Figure 7-1h–i and Figure 7-4c–d. One population (33 individual measurements on 13 sites) is uranium-dominant and shows a high natural exposure rate, contents; 3.5% K, 23 ppm U and 18 ppm Th. Another population (25 individual measurements on 8 sites) is thorium and potassium dominant and shows only slightly higher natural exposure rate compared to the metagranite, contents; 4.8% K, 4 ppm U and 28 ppm Th. The third population (20 individual measurements on 10 sites) is potassium dominant, containing 5.3% K, 3 ppm U and 8 ppm Th. The geographical distribution of the different populations, Figure 7-5, shows that the Th-K dominated sites predominantly occur within the Forsmark candidate area and close to Storskäret, in the south-eastern part of the candidate area. The U dominated population mainly occurs southwest, west and north of the candidate area. Most of the K dominated population also occurs within the Forsmark candidate area mainly in conjunction with the Th-K dominant population.

Interpretation of airborne geophysics indicated a Th-U dominated radiogenic pattern and high natural exposure rate in the northwest part of the candidate area /26/. No explanation of the source for this anomaly pattern has been found in the in-situ measurements carried out.

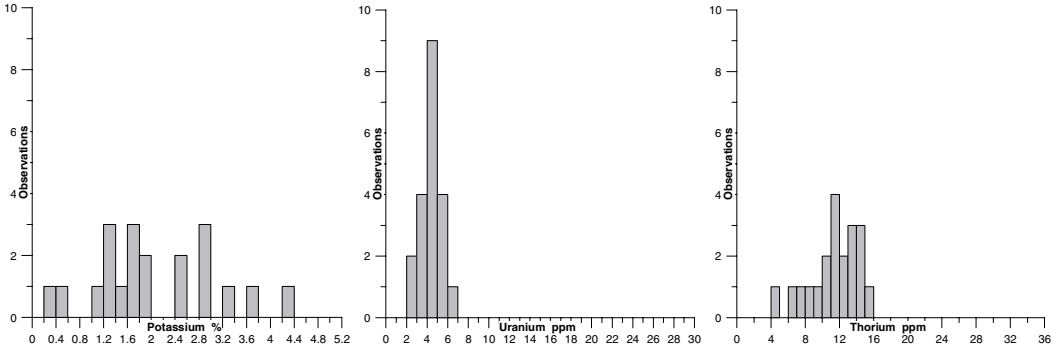

a) Dacit and andesite, metamorphic (Group A1), Site average on 20 sites (8 sites 2003).

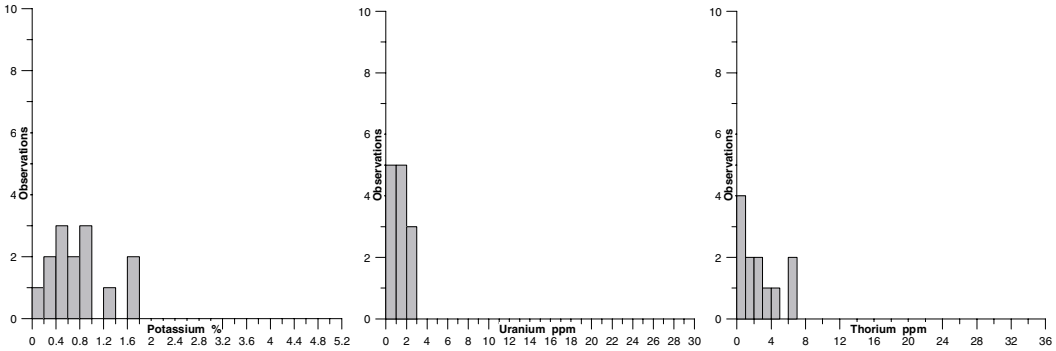

b) Diorite, quartz diorite and gabbro, metamorphic (Group B2/B3), Site average on 13 sites (2 sites 2003).

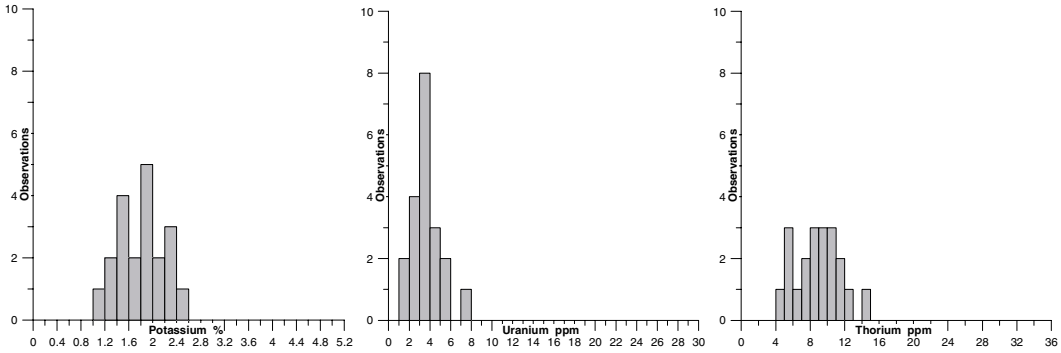

c) Tonalite granodiorite, metamorphic (Group B5/B6), Site average on 20 sites (6 sites 2003).

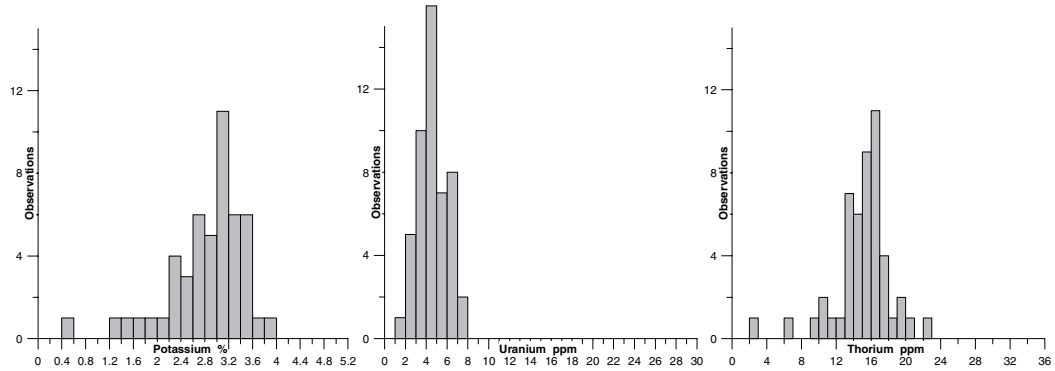

d) Granodiorite–granite, metamorphic, medium-grained (Group B8/B9), Site average on 47 sites (16 sites 2003). Note the different scaling of the vertical axis.

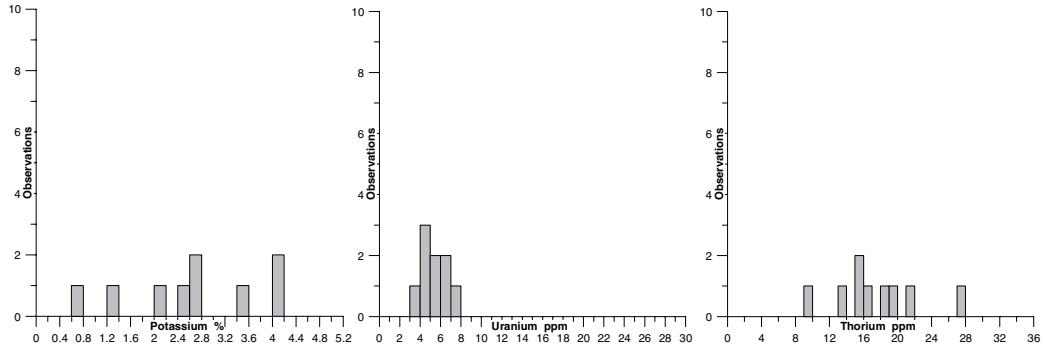

e). Granite, metamorphic, aplitic (Group B10), Site average on 9 sites (3 sites 2003).

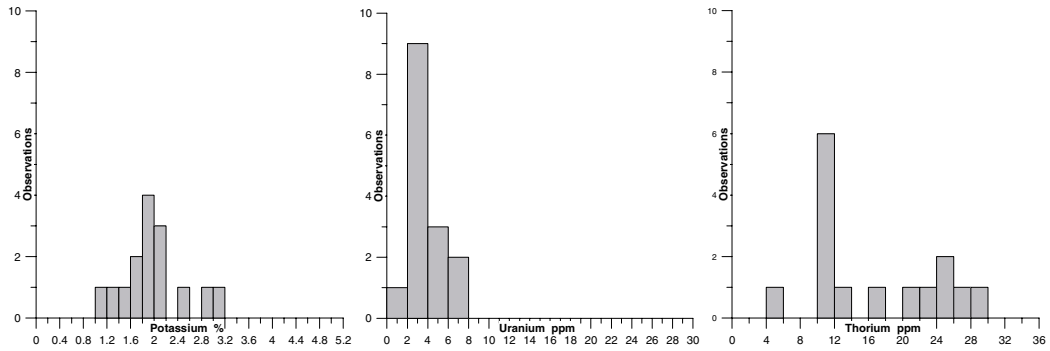

f). Granodiorite, tonalite and granite, metamorphic, fine- to medium-grained (Group C), Site average on 15 sites (9 sites 2003).

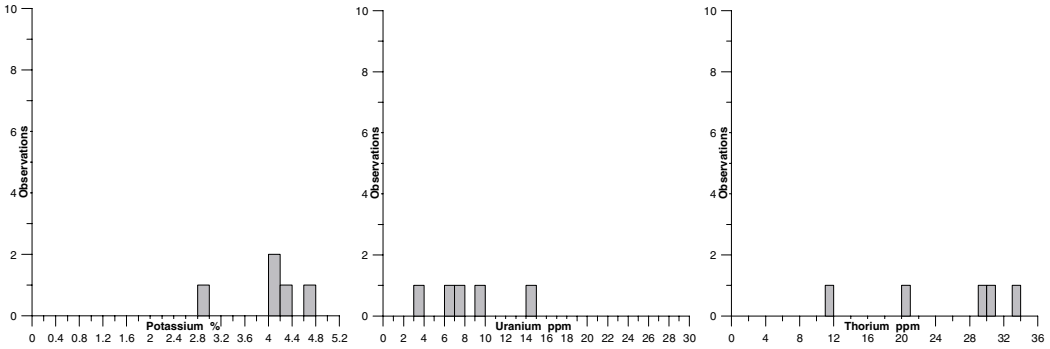

g) Granite, fine- to medium-grained (Group D1), Site average on 5 sites (2 sites 2003).

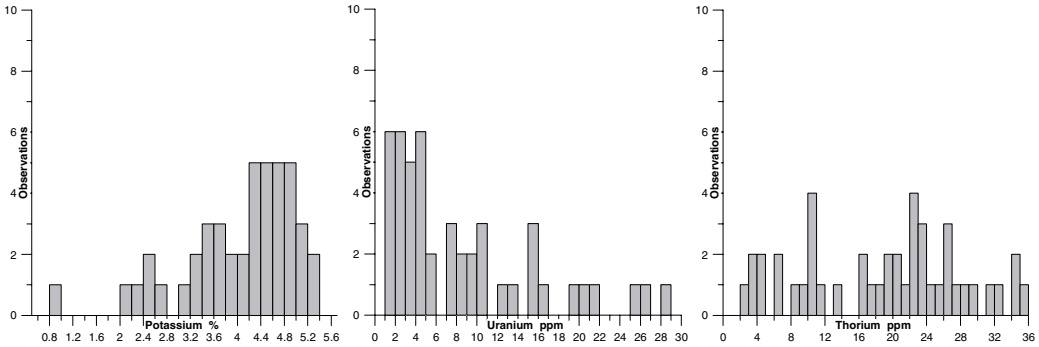

h). Pegmatitic granite (Group D2), 47 individual measurements at 11 sites (18 measurements at 3 sites 2003).

Figure 7-1 a–i. *Histogram showing the potassium (%), uranium (ppm) and thorium (ppm) content for the in-situ, gamma ray spectrometry measurements. The results are presented for each of the different rock groups with more than 5 occurrences.*

Gamma-ray spectrometry measurements were also carried out on bare soil on the Storskäret farmland in the southeast part of the candidate area, Figure 7-2, 7-4f and 7-5. The purpose was to investigate the radiogenic distribution and the possible source of the Th-K dominated, high intensity pattern identified from the helicopter borne gamma-ray spectrometry survey /26, Figure 4-21/, which characterizes the area around Storskäret.

The investigation shows that the soil surface is Th-K dominated with contents; 2.6% K, 2 ppm U and 10 ppm Th. The natural exposure rate is rather low; 8.2 microR/h. However, the flat and open farmland surface would typically give a contribution of considerable proportions.

Despite these results it is important to note that the exposed rock types, surrounding the farmland also shows similar characteristics, that is; pegmatite granites (D2/D3) and to some extent also metamorphic, granodiorite-granite (B8/B9). This implies that both soil and bedrock contribute to the Th-K dominated anomaly pattern in the Storskäret area.

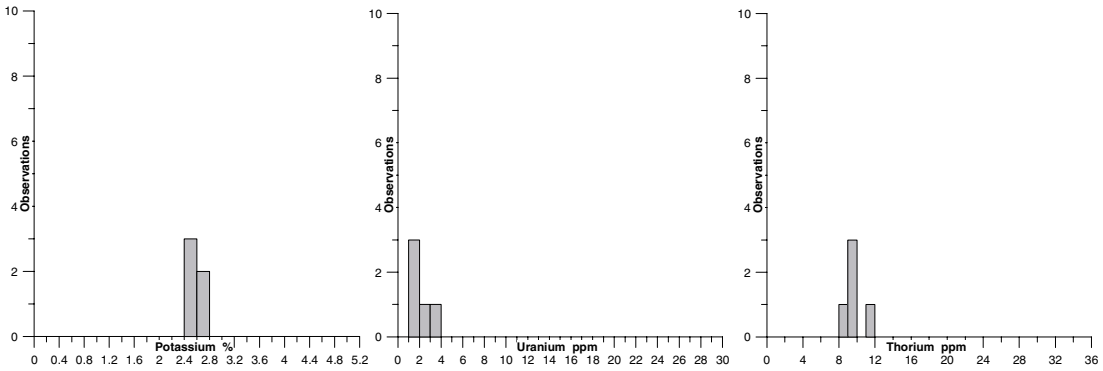

Figure 7-2. *Histogram showing the potassium (%), uranium (ppm) and thorium (ppm) content for the in-situ, gamma ray spectrometry measurements on bare soil at Storskäret farmland. Site average on 5 sites (0 sites reported 2002).*

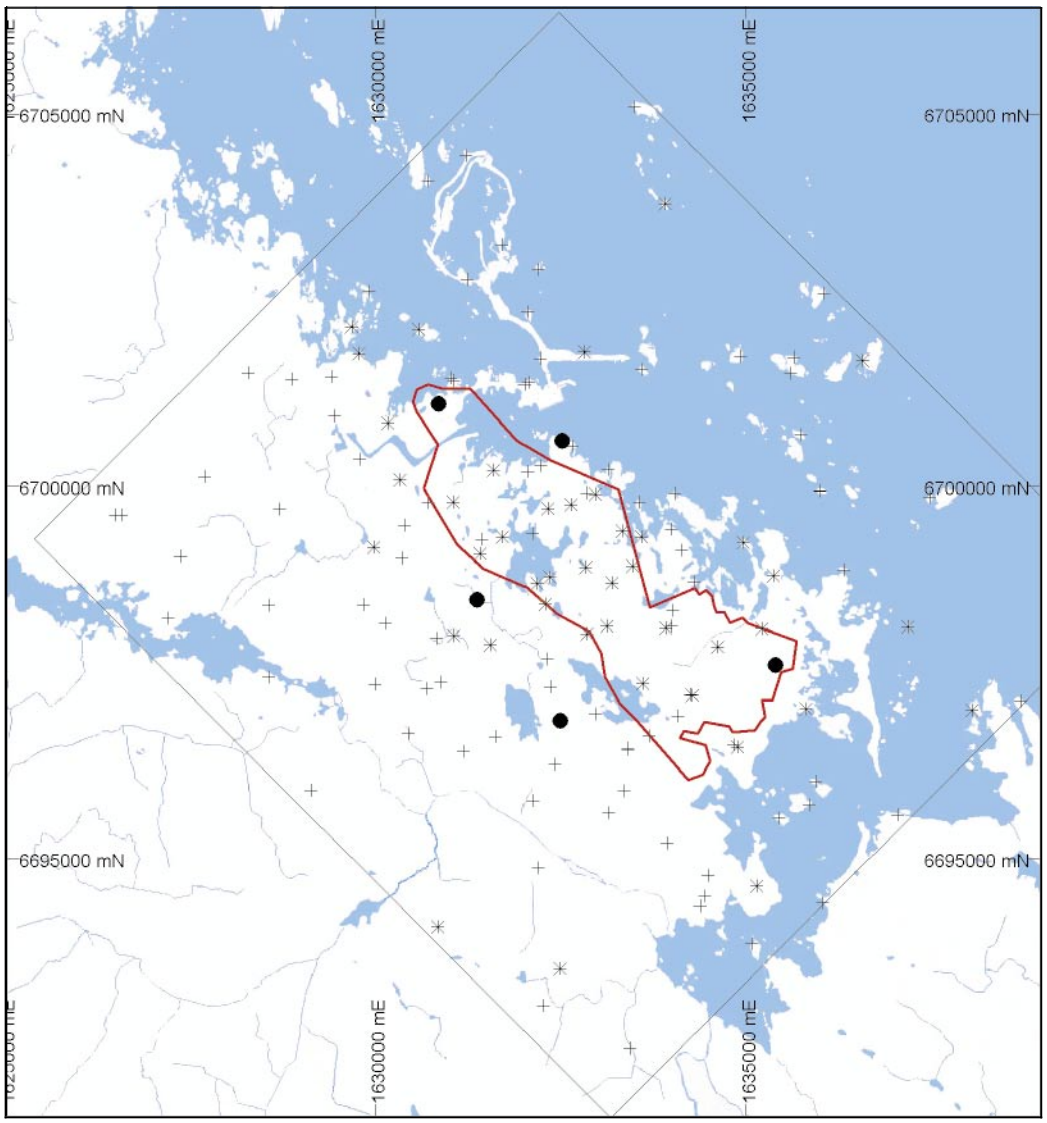

Figure 7-3. *In-situ, gamma ray spectrometry, site locations;*

✳ *Granodiorite-granite, metamorphic*
● *Granodiorite-granite, metamorphic with low potassium content (< 2.2% K)*
\+ *Other site location*

The Forsmark candidate area is outlined with a solid red line.

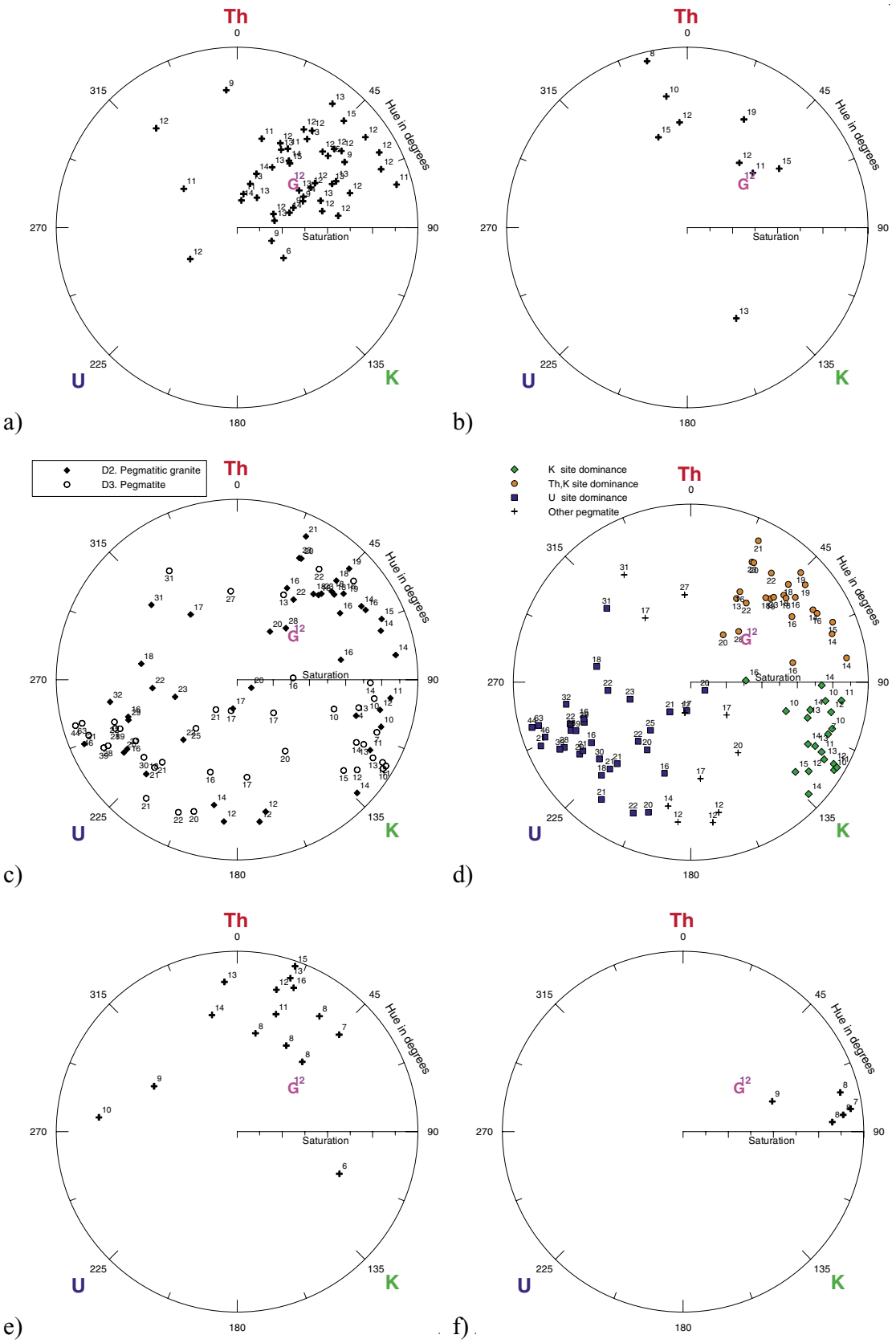

Figure 7-4. *Hue-Saturation plot of in-situ, gamma ray spectrometry measurements. The presentation shows the relative distribution in uranium equivalent units (Ur), between potassium, uranium and thorium. The letter* **G** *marks the position for a normal granite distribution (3% K, 5 ppm U, 15 ppm Th). Digits show the natural exposure in microR/h.*

a) Granodiorite to granite, metamorphic, medium-grained (Group B8/B9)
b) Granite, metamorphic, aplitic (Group B10)
c) Pegmatitic granite, pegmatite (Group D2 and D3)
d) Pegmatitic granite, pegmatite (Group D2 and D3), classified in K, Th-K and U dominance
e) Granodiorite, tonalite and granite, metamorphic, fine- to medium-grained (Group C)
f) Bare soil, Storskäret farmland

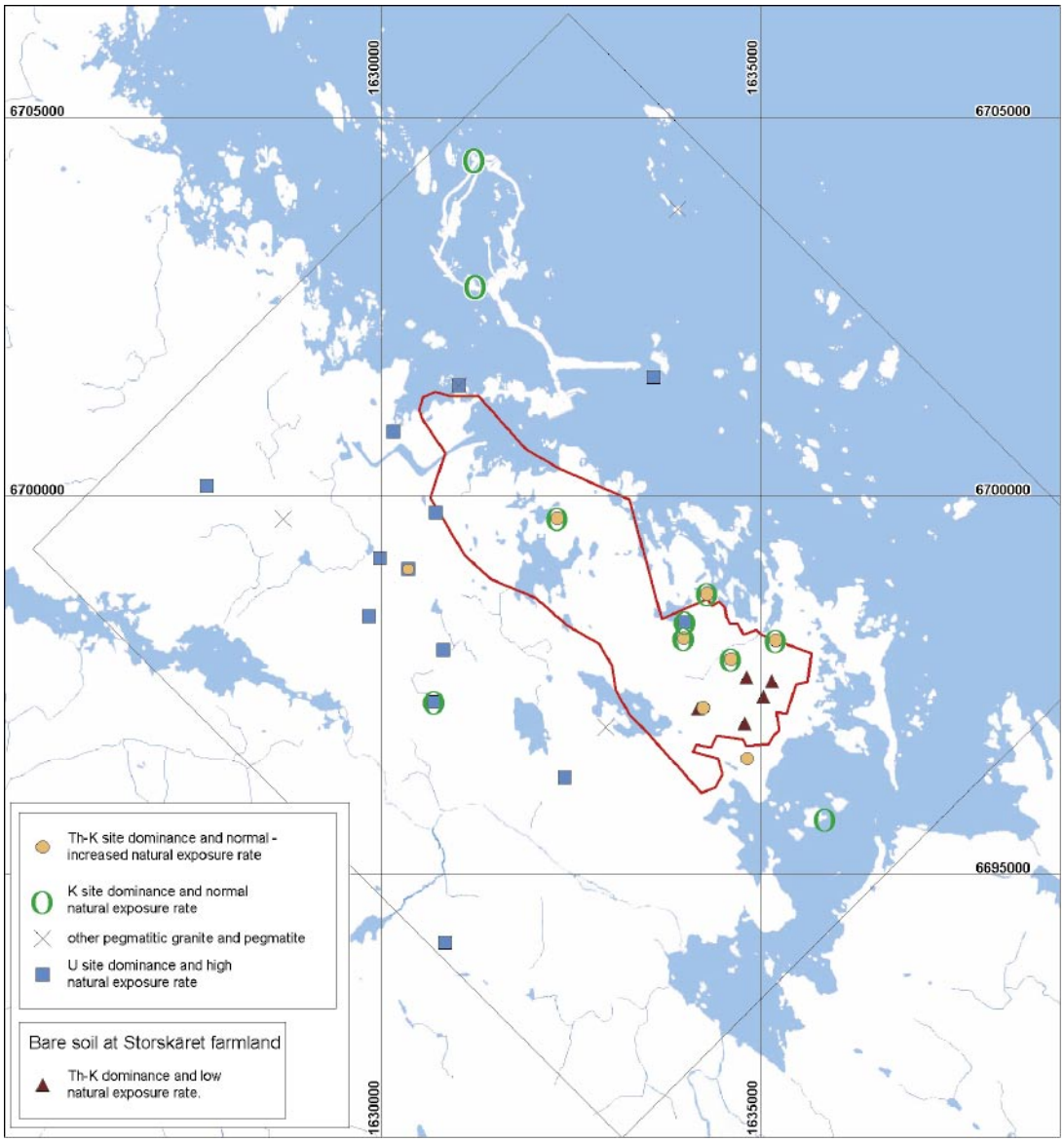

Figure 7-5. *In-situ, gamma ray spectrometry, pegmatitic granite – pegmatite site locations. (One location can show overlapping character). The Forsmark candidate area is outlined with a solid red line.*

7.3 Conclusions

The most common rock type within the Forsmark candidate area, the granite-granodiorite, metamorphic, group B8/B9 shows a coherent distribution with content common for granites; average of 2.9% K, 5 ppm U and 15 ppm Th. A few sites located at the margin of the candidate area show depletion in the potassium content.

The presence of two radiogenic populations, both of tonalite-granodiorite-granite composition, indicates that the group C rocks possibly can be divided into two different subgroups independent from rock type; one population with low radiogenic content and another with distinct Th dominance.

The radiogenic distribution for pegmatitic granite and pegmatite indicates three populations independent from the geological code. One population is U dominant and shows a high natural exposure rate. Another population is Th-K dominant, with moderate natural exposure rate. The third population is K dominant, with normal natural exposure rate. The geographical distribution of the different populations shows that the Th-K dominated sites predominantly occur close to Storskäret, in the southeastern part of the Forsmark candidate area. The U dominated population mainly occurs, southwest, west and north of the candidate area. Most of the K dominated population also occurs within the Forsmark candidate area, mainly in conjunction with the Th-K dominant population.

Gamma-ray spectrometry measurements carried out on bare soil on the Storskäret farmland in the southeast part of the candidate area, shows that the soil surface is Th-K dominated with rather low natural exposure rate. However, the flat and open farmland surface would typically give a contribution of considerable proportions. The surrounding exposed rock types also show similar characteristics, which implies that both soil and bedrock contribute to the characteristic Th-K dominated gamma-ray spectrometry pattern in the Storskäret area.

Interpretation of airborne geophysics indicated a Th-U dominated radiogenic pattern and high natural exposure rate in the northwest part of the candidate area /26/. No explanation of the source for this anomaly pattern has been found in the in-situ measurements carried out.

8 Compilation of petrophysical parameters for different sampling sites and rock types

A listing and compilation of the petrophysical properties for the different sampling sites and rock types in the petrophysical sampling campaigns in 2002 and 2003 is presented in Appendix 1. Appendix 1 also includes a few gamma-ray spectrometry measurements on bare soil. A statistical compilation of the different petrophysical and bare soil properties is presented in Appendix 2. A brief summary of selected petrophysical parameters (averages) for the rock groups that have sufficient amount of data (> 10 samples) to form the basis of a statistical conclusion, is presented in Table 8-1. Rock code, code and number of observations are presented in the left column. Rock groups with between 5–9 samples are also presented with a note (*) of few samples. The rock units in Table 8-1 correspond to the rock type classification presented in Table 3-1. The gamma-ray spectrometry results for bare soil at Storskäret farmland is presented in Table 8-2.

Table 8-1. Summary of petrophysical parameters for different rock groups. Each parameter value given is based on different number of observations. A more detailed compilation can be found in Appendix 2a. (* Only a few samples/measurements (5–9)).

Rock group code observations	Volume susceptibility	Q-value	Density	Porosity	Resistivity	IP	K	U	Th	Natural exposure
	SI	*SI*	*kg/m³*	*%*	*ohmm*	*mrad*	*%*	*ppm*	*ppm*	*microR/h*
A1 103076 19	0.00235	0.21	2,732	0.37	14,374	20.9	2.1	4.3	11.3	9.4
B2/B3 101033 14	0.00293	0.10	2,934	0.37	15,315	17.2	0.8	1.2	1.7	2.3
B5/B6 101054 20	0.00201	0.12	2,735	0.40	15,348	12.3	1.9	3.7	8.8	7.8
B7 * 101056 5	0.00963	0.22	2,689	0.45	27,810	15.0	1.9	4.0	9.1	8.2
B8/B9 101057 45–47	0.00408	0.16	2,658	0.43	18,642	9.5	2.9	4.7	15.3	12.1
B10 * 101058 7–9	0.00657	0.14	2,635	0.40	15,876	11.7	2.7	5.3	17.6	12.8
C 101051 10–15	0.00118	0.08	2,711	0.49	12,314	13.5	2.0	3.9	16.6	10.6
D1 * 111058 5							4.1	8.4	25.0	19.2
D2/D3 * 101061 6–8	0.00281	0.38	2,626	0.55	16,754	9.1				
D2/D3 101061 25							4.1	14.6	20.0	21.5

Table 8-2. Summary of gamma-ray spectrometry for bare soil at Storskäret farmland. A more detailed compilation can be found in Appendix 2b.

Soil group observations	Volume susceptibility	Q-value	Density	Porosity	Resistivity	IP	K	U	Th	Natural exposure
	SI	*SI*	*kg/m³*	*%*	*ohmm*	*mrad*	*%*	*ppm*	*ppm*	*microR/h*
Bare soil							2.6	2.2	9.6	8.2
5							(–)	(–)	(–)	(–)

9 Magnetic susceptibility measurements on outcrops

As part of the bedrock mapping programme /3, 4/, data from in situ measurements of the magnetic susceptibility have been recorded for the most important rock types identified on each mapped site (outcrop).

Out of 2,119 mapped sites, the magnetic susceptibility has been recorded at 1,832 sites. At these sites, 3,254 individual rock objects have been measured and a total of 24,248 individual measurements have been recorded. Corresponding figures for 2003 were 1,065 observed sites, 979 measured sites, 1,652 individual rock objects and 12,556 individual measurements, respectively /2/.

9.1 Data processing

Normally, 8 measurements have been recorded for each rock type at each mapped site. The data have been treated statistically and the geometric mean, the standard deviation, minimum, maximum and the number of measurements for each measured site and rock type have been calculated. A geographical database containing this information and connected geological information has been created.

A map showing the surface distribution of magnetic susceptibility is presented in Figure 9-1. The map is based on the most common rock type for each outcrop and, hence, this map also indicates the spatial distribution of the magnetite content in the common rocks.

9.2 Results

Figure 9-1 gives a general view of the geographical susceptibility distribution. Within the candidate area, the susceptibilities of the most common rock, metamorphic granite-granodiorite (group B8/B9) are in general in the range of $200–800\times10^{-5}$ SI, with an average around 400×10^{-5} SI. Minor parts show lower susceptibility, see also Figure 9-2h. The metamorphic, tonalite-granodiorite rock (B5/B6) at Lillfjärden shows a very low susceptibility, $0–100\times10^{-5}$ SI. The metamorphic, granite-granodiorite (B8/B9), immediately northwest of the candidate area and Forsmarksverket shows a higher and more evenly distributed susceptibility from $500–1{,}200\times10^{-5}$ SI. The susceptibility pattern southwest of the candidate area and northeast of Forsmarksån is more scattered with both low and high susceptibilities.

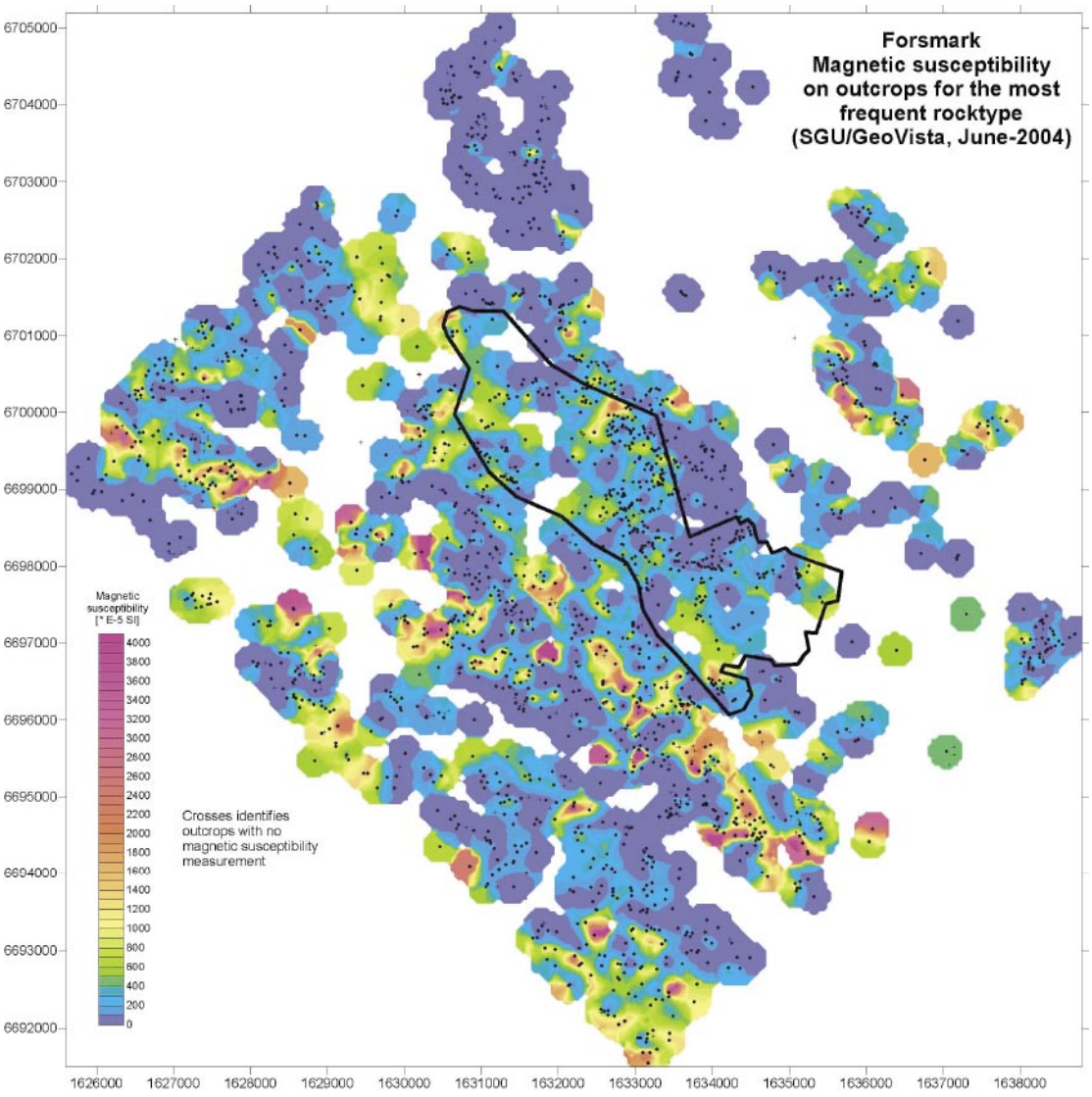

Figure 9-1. *Site average of magnetic susceptibility on outcrops for the most frequent rock type. Crosses identify outcrops with no magnetic susceptibility measurement. The Forsmark candidate area is outlined with a solid black line.*

The results are discussed in more detail in conjunction with the histograms in Figure 9-2a–m and Table 9-1. In some cases bimodal (or more) distributions of the data within a group indicates that the calculation of the geometric average can be less suitable. Hence, alternative peak values based on the histograms in Figure 9-2a–m are given in brackets. The latter figures can be necessary to consider e.g. for local geophysical modelling, while the former figure can be used to represent the rock group as a whole.

The metamorphic dacite and andesite rocks (group A1) indicate three different populations, low (< 80×10^{-5}SI), moderate (80–800×10^{-5} SI) and high (800–$11{,}000\times10^{-5}$ SI), Figure 9-2a. The three different groups constitute 58%, 16% and 26% of the total population, respectively. The two low susceptibility populations are geographically scattered over the mapped area. In contrary, the outcrops with high magnetic susceptibility have mostly been observed in the area between Forsmarksån and the candidate area and on a few of the islands northeast of the candidate area. These areas also coincide with the spotted appearance of higher susceptibilities shown in Figure 9-1.

Table 9-1. Compilation of magnetic susceptibility measurements on outcrops, calculated as site averages for different rock groups. Susceptibility values in 10^{-5} SI. Histogram peak values alternative to the geometric average is indicated in brackets.

Rock Group (SGU)	Code (SKB)	Geometric average	Geometric standard deviation above average	Geometric standard deviation below average	Min	Max	No of susceptibility site observations	Total No of site observations
A1	103076	76 (5, 30, 200, 3,500)	1,038	71	0	11,115	311	429
A1	106000				25	10,000	4	5
A2	109014	41,450	40,547	20,497	20,000	80,000	5	9
A4	108019	702	24,904	682	93	60,000	4	7
A5	109010				20	80	1	1
B1	101004	508 (50, 1,000)	2,108	409	21	8,786	49	73
B2/B3	101033	106 (50)	319	80	4	11,447	294	414
B4	102017	84 (50)	179	57	6	8,438	286	921
B5/B6	101054	157 (30,630)	823	132	0	8,881	445	584
B7	101056	302 (15,800)	1,390	248	3	3,956	138	170
B8/B9	101057	252 (25,500)	863	195	0	3,464	630	764
B10	101058	188 (10,400)	754	150	2	3,128	157	241
C	101051	112 (20, 1,000)	781	98	0	5,477	199	271
C or D1		199	1,151	169	0	5,768	101	199
D1	111058	190 (400)	870	156	0	3,464	79	247
D2	101098	43 (5,100)	232	37	0	1,536	168	248
D3	101061	16	108	14	0	10,681	310	1,352
D2/D3 together		23	151	20	0	10,681	478	1,600
	111051	68	540	61	0	1,689	27	47

In spite of the fact that the number of sites is fairly limited, the ultramafic rocks (group B1), indicate two populations; one population with low susceptibility (20–100×10^{-5} SI), and one with moderate – high susceptibility (200–9,000×10^{-5} SI), Figure 9-2b. No characteristic geographical pattern has been identified for the two populations. Mostly, the group B1 rocks occur southwest of the candidate area.

The metamorphic diorites, quartz-diorites and gabbros (group B2/B3) possibly indicate three magnetic susceptibility populations, Figure 9-2c. A low susceptibility group vary from 5–250×10^{-5} SI, with a very distinct concentration on levels around 40–100×10^{-5} SI, which is similar to the amphibolites in group B4. Moderate susceptibilities vary between 250–1,600×10^{-5} SI and a small group with high magnetic susceptibility vary between 1,600–12,000×10^{-5} SI. No characteristic geographical pattern has been identified. Most of the group B2/B3 rocks occur outside the candidate area.

The amphibolites, Figure 9-2d, are dominated by a very distinct grouping of magnetic susceptibilities at 20–100×10^{-5} SI and constitutes about 70% of the population. In addition to that, the distribution is widespread and varies from very low to high. Of interest is that no amphibolites with magnetic susceptibility > 250×10^{-5} SI is identified within the Forsmark candidate area.

The metamorphic, tonalite to granodiorite group (B5/B6), Figure 9-2e, also indicates three populations; a low susceptibility group with values varying from 10–200×10^{-5} SI, moderate-high susceptibilities varying between 200–9,000×10^{-5} SI and a small group with very low magnetic susceptibilities varying between 0–10×10^{-5} SI. The three different groups constitute 50%, 47% and 3% of the total population, respectively. The metatonalite-metagranodiorite, rock unit occurring at Lillfjärden, shows a uniform and low – very low magnetic susceptibility. Low susceptibility values follow a low magnetic band parallel to Forsmarksån. Apart from this, no characteristic geographical pattern has been identified.

The metamorphic granodiorite group (B7) shows a similar distribution as the metagranodiorite-metagranite group (B8/B9), see the following paragraph and Figure 9-2f.

The metamorphic granodiorite-granite group of rocks (B8/B9) have moderate – high susceptibilities, 100–3,500×10^{-5} SI, with an individual peak at 500×10^{-5} SI, Figure 9-2g. There is also a group of lower magnetic susceptibilities, 0–100×10^{-5} SI, without any characteristic maxima. The latter group constitute approximately 20% of the total contribution. When analyzing all the individual magnetic susceptibility measurements performed, a similar pattern is found for the outcrop site averages.

A special histogram for group B8/B9 within the candidate area is presented in Figure 9-2h. This shows the same distribution as for all metamorphic granodiorite-granite rocks, Figure 9-2g. However, the low susceptibility group is more distinct between 0–80×10^{-5} SI. This group constitute about 15% of the total number of B8/B9-sites in the candidate area. This also corresponds with the visual geographical susceptibility distribution within the candidate area in Figure 9-1. The location of the low susceptibility group is presented in Figure 9-3.

The aplitic metamorphic granite (B10) shows a distinct group of susceptibilities varying from 60–3,000×10^{-5} SI, with a peak at 400×10^{-5} SI. There is also a small group with very low magnetic susceptibility, from 0–60×10^{-5} SI, Figure 9-2i. The latter group constitute approximately 30% of the total contribution.

The metamorphic, fine- to medium-grained, granodiorite, tonalite and granite rocks (group C) show a clear bimodal distribution with approximately equal contribution, Figure 9-2j. The rocks that certainly belong to this group show a wide grouping ranging from moderate to high susceptibility, 100–5,500×10^{-5} SI, and a more distinct group with low to very low susceptibility, 0–100×10^{-5} SI. Individual peaks occur at 1,000 and 20×10^{-5} SI, respectively.

Rocks with uncertain provenance, belonging either to granitoids in group C or to granites, group D1 are analyzed together and shows a similar distribution as for group C rocks. Typically the rocks with moderate – high susceptibility are more common, Figure 9-2k.

The statistics for granite, fine- to medium-grained (D1) is based on a limited number of observations. A distribution from 10–3,500×10^{-5} SI is indicated, with an individual peak around 400×10^{-5} SI. Medium – high susceptibilities appear more common, Figure 9-2l.

Pegmatite granite (D2) generally shows very low to moderate magnetic susceptibility with peaks at 5×10^{-5} SI and 100×10^{-5} SI. Typically low susceptibilities are more common, Figure 9-2m.

Pegmatite (D3) shows a similar pattern as for pegmatite granite with a scattered susceptibility distribution, Figure 9-2n. Some pegmatite outcrops give very high and uniform magnetic susceptibility readings, which are often related to dissemination of coarse magnetite grains. Also very low magnetic susceptibility is common.

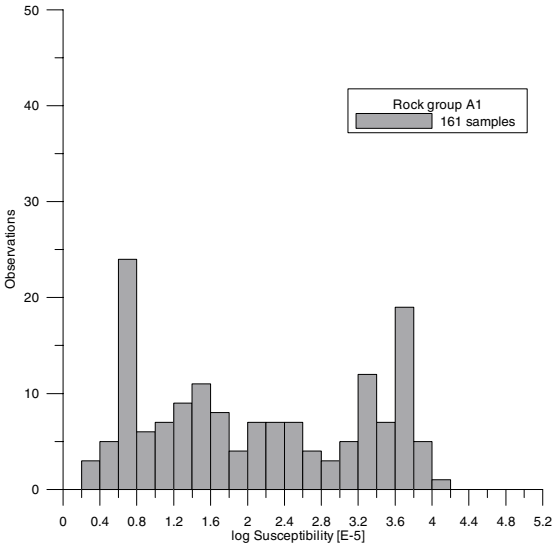

a) Dacite and andesite, metamorphic (Group A1), 311 outcrop observations (150 obs., 2003)

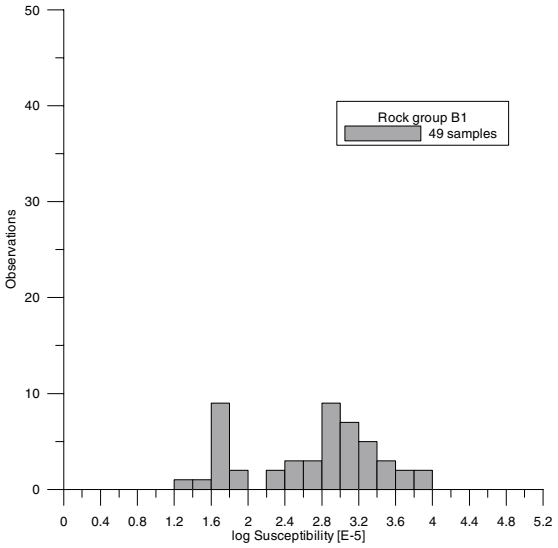

b) Ultramafic rocks (B1), 49 outcrop observations (29 obs., 2003)

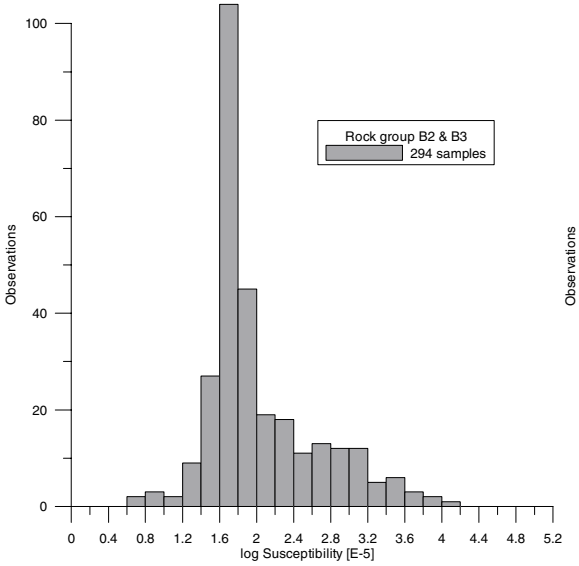

c) Diorite, quartz-diorite and gabbro, metamorphic (B2/B3), 294 outcrop observations (130 obs., 2003)

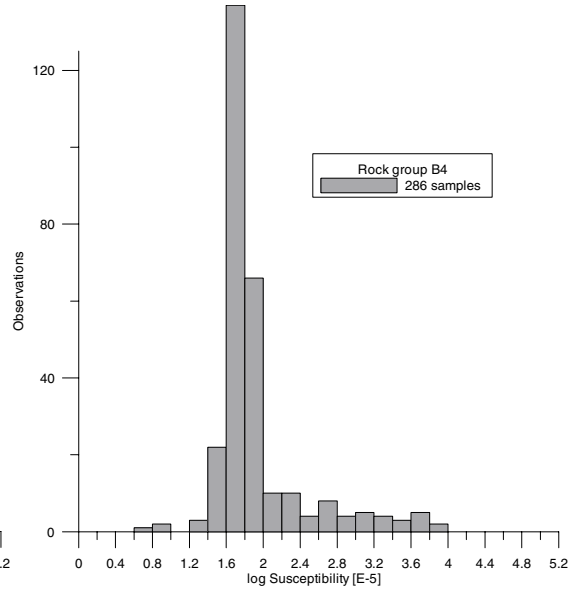

d) Amphibolite (B4), 286 outcrop observations (125 obs., 2003)

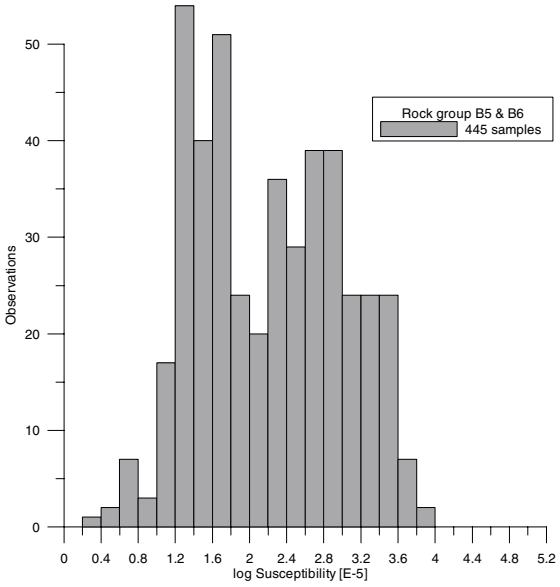

e) Tonalite and granodiorite, metamorphic (B5/B6), 445 outcrop observations (228 obs., 2003)

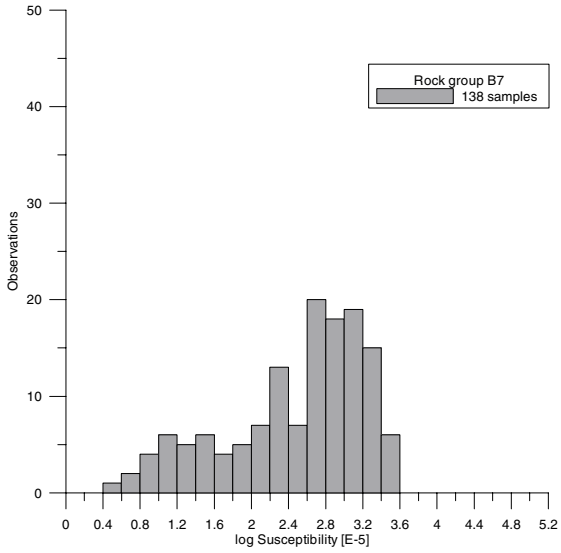

f) Granodiorite, metamorphic (B7), 138 outcrop observations (75 obs., 2003)

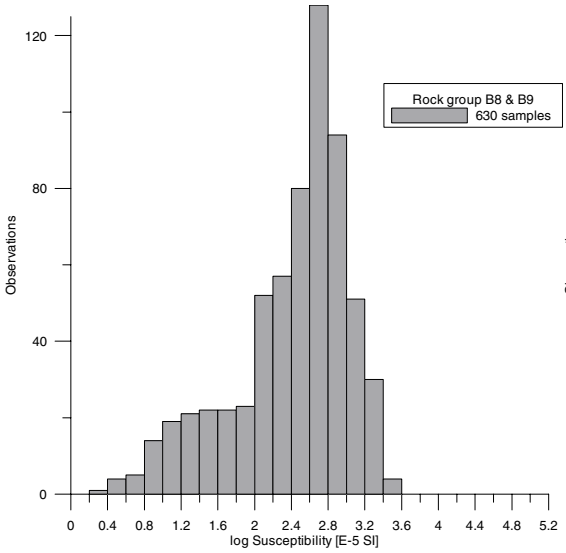

g) Granodiorite and granite, metamorphic (B8/B9), 630 outcrop observations (344 obs., 2003)

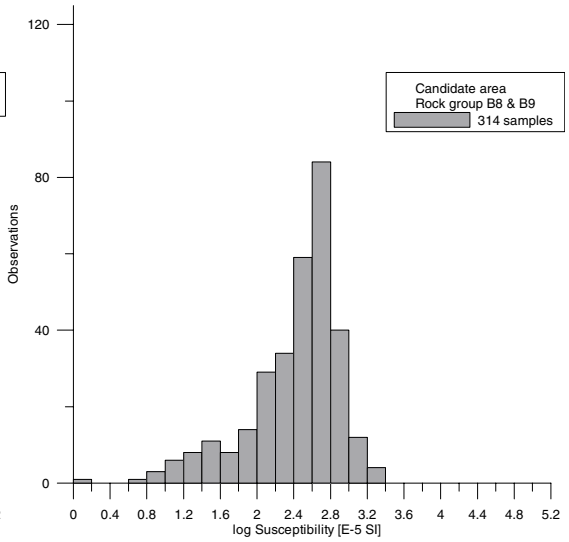

h) Granodiorite and granite, metamorphic (B8/B9), 314 outcrop observations within the Forsmark candidate area

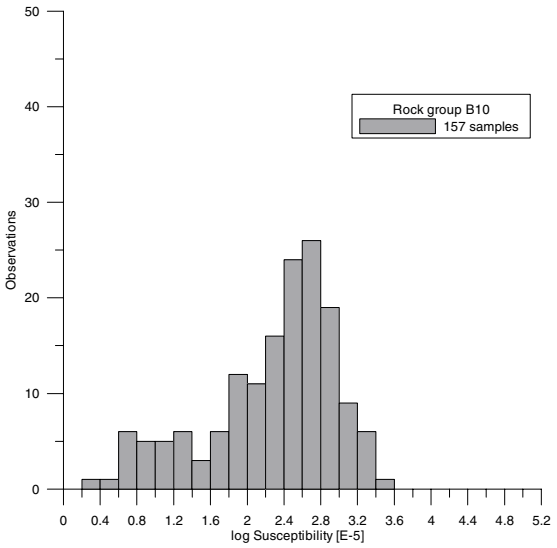

i) Granite,metamorphic, aplitic (B10), 157 outcrop observations (71 obs., 2003)

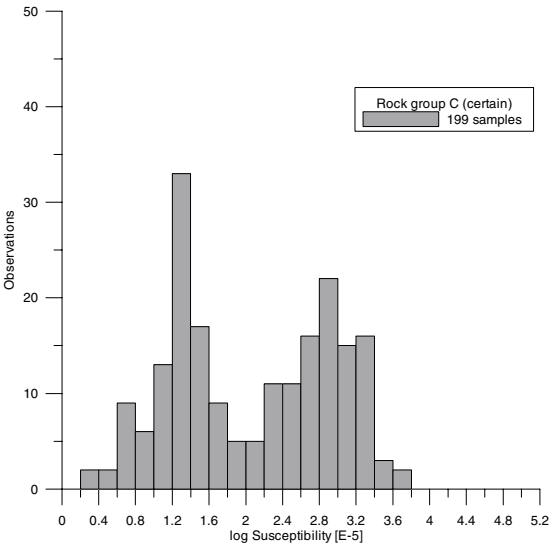

j) Granodiorite, tonalite and granite, metamorphic, fine- to medium-grained (C), 199 outcrop observations (129 obs., 2003)

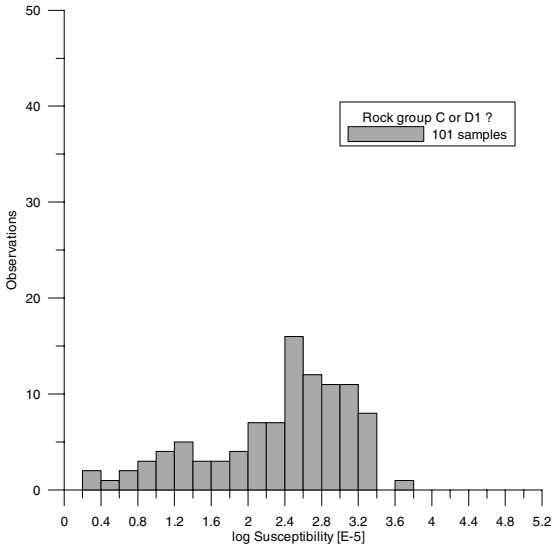

k) Granite (C or D1), uncertain provenance, 101 outcrop observations (0 obs., 2003)

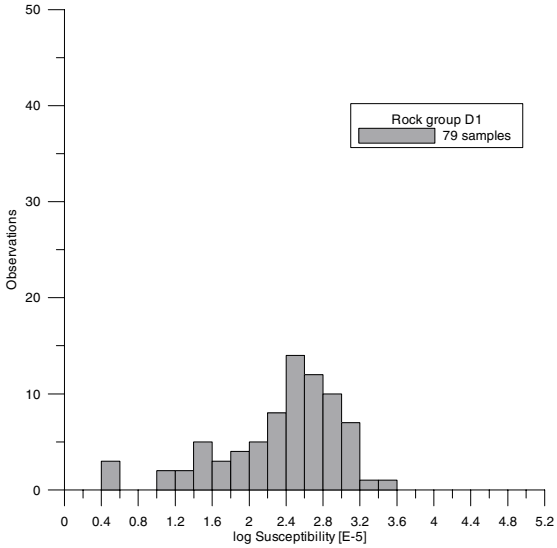

l) Granite, fine- to medium-grained (D1), 79 outcrop observations (79 obs.,m 2003)

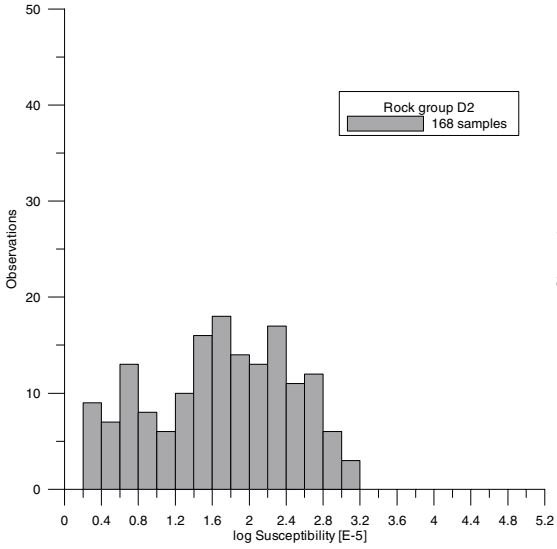

m) Pegmatitic granite (D2), 168 outcrop observations (68 obs., 2003)

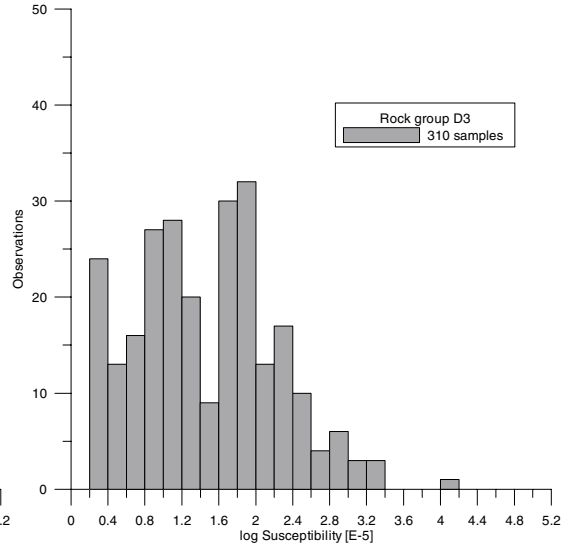

n) Pegmatite (D3), 310 outcrop observations (215 obs., 2003)

Figure 9-2, a–n. *Histogram of the magnetic susceptibility (logarithm of site average) measured on outcrops. The results are presented for each of the different rock groups. Note that the scaling of the vertical axis is different for c) B2/B3, d) B4, g) B8/B9 and h) B8/B9 candidate area. Number of observations during 2003 is presented in brackets.*

9.3 Conclusions

The site averages of the magnetic susceptibility in many cases indicate bimodal (or more) distributions of the data within a rock group. The calculation of the geometric average provides an estimate of the rock group characteristics. However, it can be less suitable for geophysical modelling or to delineate geological structures.

The bimodal appearance is clear and of similar character for the rocks in group B5/B6, B7, B8/B9 and B10 as well as for group C. However, the proportion between the lower and higher susceptibility distribution varies. For group B5/B6 and group C, the contribution from lower susceptibilities is more common. The dacite and andesite, metamorphic rocks, group A1, show a large variation in susceptibility with probably three populations.

In the Forsmark area, the metamorphic granodiorite-granite group of rocks (B8/B9) have moderate – high susceptibilities, 100–3,500×10^{-5} SI, with an individual peak value at 500×10^{-5} SI. There is also a group of lower magnetic susceptibilities, 0–100×10^{-5} SI, which constitutes approximately 20% of the total contribution.

Within the candidate area, the metamorphic granodiorite-granite rocks, group B8/B9, show the same distribution as for the whole area. However, the low susceptibility group between 0–80×10^{-5} SI is more distinct and constitute about 15% of the total number of B8/B9-sites in the candidate area. The geographical distribution of the two susceptibility groups within the candidate area is presented in Figure 9-3. The metamorphic granite-granodiorite immediately northwest of the candidate area and Forsmarksverket shows a higher and more evenly distributed susceptibility from 500–1,200×10^{-5} SI. The susceptibilities of the metamorphic, tonalite-granodiorite rock (B5/B6) at Lillfjärden is very low, 0–100×10^{-5} SI.

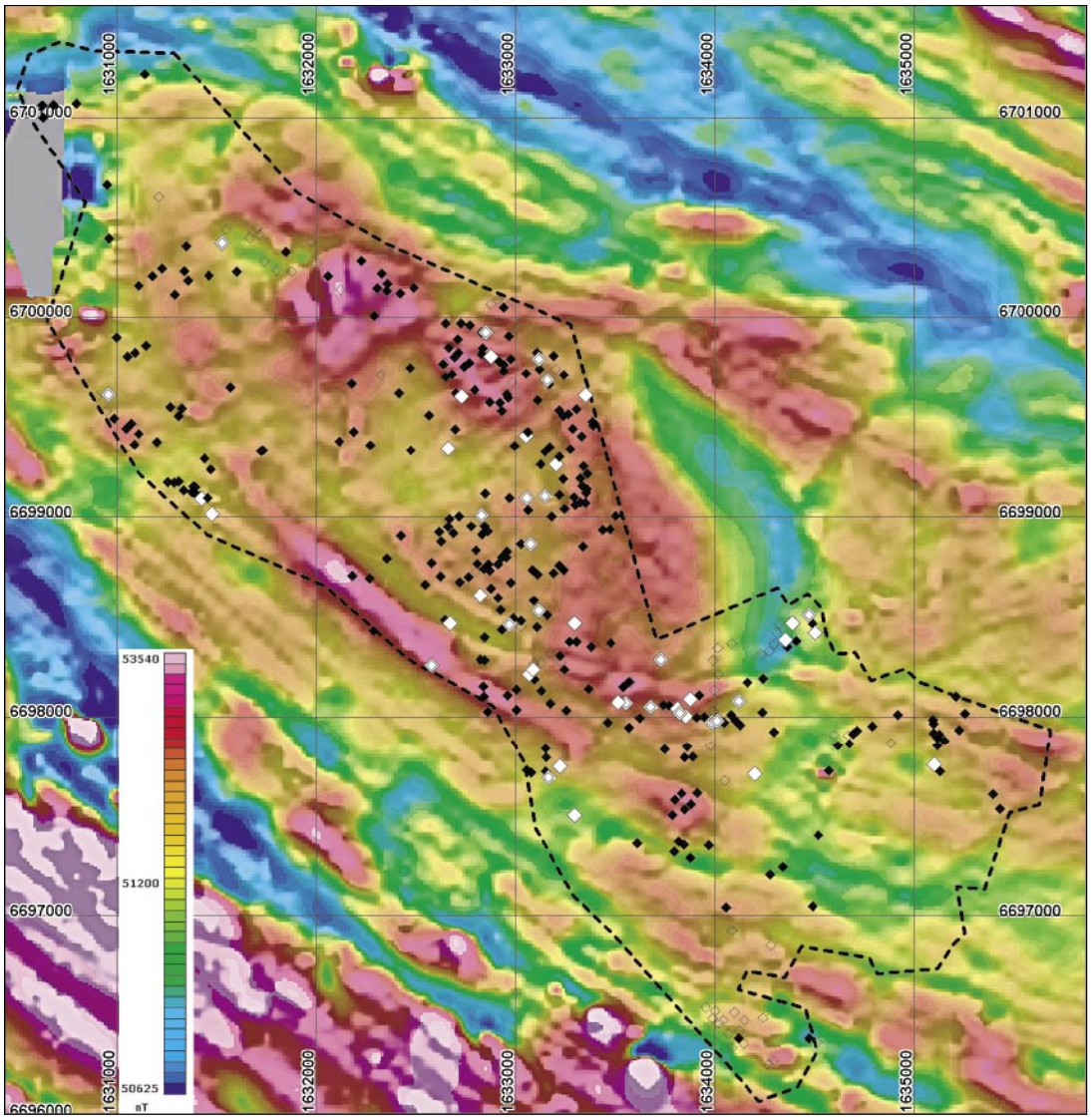

Figure 9-3. *Site averages of magnetic susceptibility on outcrops in the Forsmark candidate area, presented on an airborne magnetic map. Filled black squares show the location of higher susceptibility, granodiorite and granite, metamorphic rocks (B8/B9), while white squares show the location of the low susceptibility group. The Forsmark candidate area is outlined with a dashed black line. Magnetic total field is superimposed with the 2:nd vertical derivative to enhance bedrock structures. Magnetic lows in blue colours and highs in magenta colours.*

10 Data delivery

The processed data and interpretation results have been delivered to SKB as described below. The SICADA field note number is Forsmark 30 (samples from 2002) and 32 (samples from 2003). All data have been documented according to "SICADA – Inleverans av data", SKB SD–080 and "GIS – Inleverans av data", SKB SD–081 (SKB internal controlling document).

Data have been delivered in four data formats for storage in the GIS-database and SICADA. Grid-file that shows post-processed data of magnefic susceptibility on outcrops have been delivered and also used in the creation of a figure in the report. Information that has resulted in some kind of interpreted vector; point, line or polygon information has been stored in Shape format. Petrophysical data from laboratory analysis and spectrometry field measurements as well as site average calculations have been delivered in Excel format for storage in SICADA. A listing of delivered products is shown in Appendix 3.

11 References

/1/ **Mattsson H, Isaksson H, Thunehed H, 2003.** Petrophysical rock sampling, measurements of petrophysical rock parameters and in situ gamma ray spectrometry measurements on outcrops carried out 2002. SKB P-03-26. Svensk Kärnbränslehantering AB.

/2/ **Isaksson H, Mattsson H, Thunehed H, Keisu M, 2003.** Interpretation of petrophysical surface data. Stage 1 (2002). SKB P-03-102. Svensk Kärnbränslehantering AB.

/3/ **Stephens M B, Bergman T, Andersson J, Hermansson T, Wahlgren C-H, Albrecht L, Mikko H, 2003. F**orsmark Bedrock mapping. Stage 1 (2002) – Outcrop data including fracture data. SKB P-03-09. Svensk Kärnbränslehantering AB.

/4/ **Bergman T, Andersson J, Hermansson T, Zetterström Evins L, Albrecht, L, Stephens M B, Petersson J, Nordman, C, 2004.** Forsmark site investigation. Bedrock mapping. Stage 2 (2003) – bedrock data from outcrops and the basal parts of trenches and shallow boreholes through the Quaternary cover. SKB P-04-91. Svensk Kärnbränslehantering AB.

/5/ **Rönning H J S, Kihle O, Mogaard J O, Walker P, Shomali H, Hagthorpe P, Byström S, Lindberg H, Thunehed H, 2003.** Forsmark site investigation. Helicopter borne geophysics at Forsmark, Östhammar, Sweden. SKB P-03-41. Svensk Kärnbränslehantering AB.

/6/ **SKB, 2004.** Preliminary site description. Forsmark area – version 1.1. SKB R-04-15. Svensk Kärnbränslehantering AB.

/7/ **Henkel H, 1991.** Petrophysical properties – density and magnetization of rock from the northern part of the Baltic Shield. Tectonophysics 192, page1–19.

/8/ **Collinson D W, 1983.** Methods in rock magnetism and paleomagnetism, Chapman and Hall, London, United Kingdom. 503 pp.

/9/ **Parasnis D S, 1997.** Principles of applied geophysics. Chapman and Hall, London, 429 pp.

/10/ **Puranen R, 1989.** Susceptibilities, iron and magnetite content of Precambrian rocks in Finland. Geological survey of Finland, Report of investigations 90, 45 pp.

/11/ **Tarling D. H, Hrouda F, 1993.** The magnetic anisotropy of rocks, Chapman and Hall, London, United Kingdom. 217 pp.

/12/ **O'Reilly W, 1984.** Rock and mineral magnetism, Chapman and Hall, New York, USA. 220 pp.

/13/ **Janak F, 1965.** Determination of anisotropy of magnetic susceptibility of rocks, Studia geoph. et geod. 9, p. 290–300.

/14/ **Bouchez J. L, Gleizes G, 1995.** Two-stage deformation of the Mont-Louis-Andorra granite pluton (Variscan Pyrenees) inferred from magnetic susceptibility anisotropy. Journal of Geological Society, London 152, 669–679.

/15/ **Knight M D, Walker G P L, 1988.** Magma Flow Directions in Dikes of the Koolau Complex, Oahu, Determined From Magnetic Fabric Studies, Journal of Geophysical Research, vol. 93, NO. B5, p. 4301–4319.

/16/ **Bates M P, Mushayandebvu M F, 1995.** Magnetic fabric in the Umvimeela Dyke, satellite of the Great Dyke, Zimbabwe. Tectonophysics 242, 241–254.

/17/ **Raposo M. I. B, 1997.** Magnetic fabric and its significance in the Florianópolis dyke swarm, southern Brazil. Geophys. J. Int. 131, 159–170.

/18/ **Bouillin J-P, Bouchez J-L, Lespinasse P, Pêcher A, 1993.** Granite emplacement in an extensional setting: an AMS study of the magmatic structures of Monte Capanne (Elba, Italy). Earth and Planetary Science Letters, v.118, p. 263–279.

/19/ **Bouchez J L, Gleizes G, Djouadi T, Rochette P, 1990.** Microstructure and magnetic susceptibility applied to emplacement kinematics of granites: the example of the Foix pluton (French Pyrenees). Tectonophysics 184, 157–171.

/20/ **Mattsson H J, Elming S-Å, 2001.** Magnetic fabrics and paleomagnetism of the Storsjön-Edsbyn deformation zone, central Sweden. Precambrian Research 107, 265–281.

/21/ **Borradaile G J, Henry B, 1997.** Tectonic applications of magnetic susceptibility and its anisotropy. Earth-Science Reviews 42, 49–93.

/22/ **Hirt A M, Lowrie W, Clendenen W S, Kligfield R, 1993.** Correlation of strain and the anisotropy of magnetic susceptibility in the Onaping formation: evidence for a near circular origin of the Sudbury Basin. Tectonophysics, v. 225, p. 231–254. Svensk Kärnbränslehantering AB.

/23/ **Borradaile G J, Alford C, 1988.** Experimental shear zones and magnetic fabrics, Journal of structural geology 10, No 8, 895–904.

/24/ **Archie G E, 1942.** The electrical resistivity log as an aid in determining some reservoir characteristics: Trans. Am. Inst. Min, Metallurg, Petr.Eng, 146, 54–62.

/25/ **Keller G V, Frischknecht F C, 1966.** Electrical methods in geophysical prospecting. Pergamon Press.

/26/ **Isaksson H, Thunehed H, Keisu M, 2004.** Interpretation of airborne geophysics and integration with topography. Stage 1 (2002). SKB P-04-29. Svensk Kärnbränslehantering AB.

A compilation of petrophysical properties for different sites and rock groups (Results marked in yellow are from 2003)

Group A. Supracrustal rocks.

Group and PFM-number	Coordinates		Geological map. Rock unit	Rock unit, order number	*Geological map. 1=BLS or SL, 2=LS*	*Geological model. Rock domain*	Magnetic properties					Density	Porosity	Electrical properties		Gamma-ray spectrometry properties			
	Northing	Easting					Remanence_declination (deg)	Remanence_inclination (deg)	Remanence_intensity (A/m)	Volume_susceptibility (SI)	Q-value (SI)	Wet_density (kg/m3)	Porosity (%)	Electric resistivity (in fresh water, Ωm)	Induced polarization (phase at 0.6 Hz in fresh water, mrad)	K (%)	U (ppm)	Th (ppm)	Natural Exposure (microR/h)
A1. 103076. Dacit and andesite, metamorphic																			
PFM000240	6697370	1630884	3076	1			115,7	73,2	0,7955	0,00453	0,44	2722,6	0,31	58657	41,1	1,1	4,1	11,3	7,7
PFM000351	6696640	1631621	3076	1			86,2	81,3	0,3136	0,02996	0,13	2725,1	0,25	14851	14,0	1,7	4,1	10,2	8,2
PFM000526	6694879	1632191	3076	1			134,1	13,1	3,7850	0,07152	1,20	2779,2	0,33	33765	25,3	2,6	3,0	7,6	8,2
PFM000531	6696468	1633409	3076	1												2,0	4,6	13,8	10,3
PFM000725	6701464	1631021	3076	1			15,9	21,8	0,0018	0,00020	0,20	2695,4	0,37	8097	13,9	1,8	5,7	13,5	10,4
PFM001156	6701371	1632016	3076	1			7,0	41,8	0,0005	0,00006	0,16	2686,5	0,53	9059	16,8	0,4	3,1	11,0	6,0
PFM001200	6694369	1634380	3076	1			269,6	75,9	0,0231	0,00053	1,74	2716,5	0,20	81878	18,1	1,7	4,3	6,3	7,1
PFM001221	6695616	1633153	3076	1			354,2	87,2	0,0007	0,00035	0,05	2733,3	0,32	27650	13,8	2,0	3,2	8,5	7,6
PFM001221	6695616	1633153	3076	5			1,4	77,6	0,3816	0,03170	0,22	2822,3	0,33	47582	16,8				
PFM001521	6696685	1630440	3076	1			113,2	80,4	2,3030	0,24000	0,24	2946,4	0,40	24942	66,6	2,9	4,7	11,9	11,1
PFM001524	6698414	1629838	3076	1			3,5	79,0	0,0502	0,01986	0,20	2699,7	0,30	12932	8,3	1,6	4,2	11,1	8,4
PFM001885	6696272	1632419	3076	1			316,6	68,2	0,1400	0,03525	0,21	2882,0	0,28	26701	27,5	1,4	2,5	4,8	5,2
PFM002248	6695208	1633937	3076	1			247,9	75,8	0,0002	0,00009	0,09	2647,8	0,40	9330	8,4	3,7	3,7	12,6	11,8
PFM001640	6701718	1632225	3086	2			349,4	54,3	0,00017	0,00009	0,05	2685,5	0,62	1725	10,1	2,9	6,8	14,3	13,0
PFM001654	6704448	1631228	3086	1			104,3	83,3	2,17100	0,08472	0,53	2768,3	0,34	5640	44,7	2,5	4,4	11,8	10,1
PFM001728	6697121	1638712	3086	1			347,4	33,8	0,00063	0,00006	0,25	2680,6	0,52	10560	15,3	0,5	4,1	13,0	7,4
PFM001729	6701743	1634929	3086	1			102,6	67,6	0,00015	0,00007	0,06	2650,0	0,44	7271	14,9	4,3	3,9	14,7	13,4
PFM001904	6702348	1632059	3086	1			342,9	65,0	0,04525	0,02167	0,14	2730,3	0,27	8215	12,1	1,4	4,1	9,0	7,4
PFM005204	6701571	1633591	3086	2			295,2	34,8	0,00191	0,00030	0,54	2658,4	0,46	9087	16,7	2,9	5,7	15,0	12,6
PFM005252	6700698	1635746	3086	1			318,2	53,9	0,04836	0,00569	0,15	2668,7	0,36	9465	13,1	3,2	5,5	14,7	12,9
A1. 106001. Sedimentary rock, metamorphic, veined to migmatitic																			
PFM001094	6702598	1636051	8017	2			143,0	64,8	0,00049	0,00270	0,06	2690,8	0,48	10888	15,9	1,3	5,3	12,8	9,2
A2. 109014. Magnetite mineralization associated with calc-silicate rock (skarn)																			
PFM000336	6696490	1633408	9014	1			110,2	53,8	75,9300	0,12400	14,90	4224,7	1,24	168	232,0	1,0	5,2	5,9	6,6
PFM000336	6696490	1633408	9014	1			141,4	15,8	6,7170										
PFM000446	6697966	1630821	9014	1			71,0	3,8	79,7000	0,12220	15,90	4130,2	1,47	324	200,8	0,8	6,2	5,5	6,7
A3. No SKB code. Veined gneiss																			
PFM001606	6697443	1628563	8011	1			130,6	62,4	0,5328	0,04876	0,41	2700,9	0,53	11875	20,0	5,1	4,1	12,8	14,3
A4. 108019. Calc-silicate rock (skarn)																			
A5. 109010. Sulphide mineralization																			

Group B. Ultramafic, mafic, intermediate and quartz-rich felsic (granitoid) meta-intrusive rocks.

Group and PFM-number	Coordinates		Geological map. Rock unit	Rock unit, order number	*Geological map. 1=BLS or SL, 2=LS*	*Geological model. Rock domain*	Magnetic properties					Density	Porosity	Electrical properties		Gamma-ray spectrometry properties			
	Northing	Easting					Remanence_declination (deg)	Remanence_inclination (deg)	Remanence_intensity (A/m)	Volume_susceptibility (SI)	Q-value (SI)	Wet_density (kg/m3)	Porosity (%)	Electric resistivity (in fresh water, Ωm)	Induced polarization (phase at 0.6 Hz in fresh water, mrad)	K (%)	U (ppm)	Th (ppm)	Natural Exposure (microR/h)
B1. 101004. Ultramafic rock, metamorphic																			
PFM001201	6694496	1634445	1004	1			100,5	77,6	9,1800	0,10853	1,70	2785,8	0,88	228	353,7	0,0	0,1	0,0	0,1
PFM001205	6694774	1634487	1004	1			30,7	61,2	4,6750	0,04572	2,26	3044,5	1,04	52	724,8	0,0	0,0	0,0	0,0
B2/B3. 101033. Diorite, quartz diorite and gabbro, metamorphic																			
PFM000229	6697308	1632363	1033	1			6,9	67,6	0,0009	0,00053	0,05	2879,1	0,37	13734	15,5	1,0	1,7	2,7	3,4
PFM000233	6696951	1632971	1038	1			348,6	73,9	0,0404	0,01079	0,15	2738,4	0,27	29994	16,7	1,8	2,2	6,3	6,0
PFM000243	6698165	1630133	1022	2			352,8	24,8	22,3900	0,01625	25,50	3074,7	0,35	14228	11,4	0,4	0,1	0,0	0,7
PFM000253	6699484	1630390	1033	1			135,1	81,2	0,4956	0,01504	1,01	2871,1	0,34	32410	21,1	1,0	1,5	3,3	3,5
PFM000518	6692462	1633431	1022	1			346,0	81,8	0,6565	0,05543	0,33	3119,8	0,36	29015	29,6	0,5	0,3	0,7	1,2
PFM000522	6693032	1632267	1022	1			222,6	53,4	0,0015	0,00036	0,14	2882,4	0,39	34227	4,8	0,1	0,0	0,0	0,2
PFM000780	6701446	1628872	1030	1			152,1	86,9	0,0011	0,00067	0,04	2928,2	0,36	11123	15,4	0,9	1,4	2,1	2,8
PFM000850	6701527	1628282	1033	1			173,9	75,4	0,2186	0,03696	0,10	2941,4	0,44	8016	33,9	0,8	1,2	1,6	2,5
PFM001235	6701402	1632065	1033	1			19,3	66,1	0,0003	0,00092	0,01	3023,4	0,46	10998	14,2	0,6	0,9	1,0	1,7
PFM001515	6697287	1630699	1022	1			110,0	72,5	0,2557	0,05592	0,16	3017,8	0,25	16583	26,3	0,4	1,1	0,1	1,4
PFM002087	6695918	1633360	1022	1			89,5	75,3	0,0003	0,00071	0,01	2951,8	0,54	5412	15,9	0,8	0,7	1,3	2,1
PFM005223	6704095	1630709	1022	1			28,9	60,2	0,00075	0,00053	0,03	2926,6	0,38	6824	13,1	0,5	0,2	0,7	1,0
PFM005215	6703247	1631707	1033	1			341,7	60,8	0,00020	0,00052	0,01	2872,7	0,38	24139	12,3	1,3	2,1	4,6	4,8
PFM005206	6702911	1632195	1038	1			335,1	75,3	0,00112	0,00048	0,05	2843,2	0,35	14283	10,3	1,7	2,8	6,7	6,4
B4. 102017. Amphibolite																			
PFM001169	6699917	1632851	2017	2			16,2	52,9	0,0001	0,00071	0,00	2928,3	0,30	11211	15,3	1,3	1,1	2,6	3,4
B5/B6. 101054. Tonalite to granodiorite, metamorphic																			
PFM000380	6696440	1631192	1053	1			303,6	56,1	0,0005	0,00033	0,04	2753,0	0,32	12081	11,3	1,9	4,0	9,2	8,2
PFM000527	6695922	1629134	1053	1			161,1	69,2	0,1004	0,02043	0,10	2697,1	0,39	22923	13,1	2,0	3,4	9,1	8,0
PFM000774	6701476	1629415	1053	1			169,7	72,7	0,2119	0,01087	0,36	2758,0	0,31	14609	12,5	1,5	4,3	8,7	7,7
PFM000777	6700365	1629786	1053	1			310,3	80,4	0,1563	0,00425	0,71	2794,4	0,38	19221	15,6	1,6	3,3	6,0	6,3
PFM000804	6698235	1627207	1053	1			30,2	75,2	0,0013	0,00029	0,09	2743,3	0,42	6659	9,9	2,0	2,8	8,6	7,5
PFM000808	6699624	1626501	1054	1			144,3	67,9	0,8301	0,03507	0,38	2720,2	0,34	17276	13,1	1,1	3,5	7,2	6,1
PFM000891	6699062	1627374	1054	1			254,1	64,8	0,0673	0,01521	0,12	2700,7	0,40	14883	16,0	2,3	2,7	10,2	8,4
PFM001162	6698339	1634013	1053	1			13,9	43,8	0,0013	0,00039	0,09	2780,1	0,44	13124	7,0	2,0	2,8	7,5	7,1
PFM001217	6700952	1629455	1053	1			187,5	56,3	0,2949	0,00472	0,66	2831,4	0,33	10235	13,2	1,7	4,9	8,4	8,2
PFM001510	6695787	1632130	1053	1			8,1	75,5	0,0004	0,00031	0,03	2746,2	0,37	9168	9,3	2,5	3,6	11,2	9,5
PFM001858	6698716	1634302	1053	1												2,2	4,9	10,3	9,6
PFM001859	6698693	1634187	1053	1			54,9	51,3	0,0003	0,00022	0,04	2704,0	0,49	17508	7,9				
PFM001860	6699145	1634136	1053	1			31,4	69,5	0,0002	0,00020	0,02	2703,1	0,53	13850	13,3	1,9	7,4	11,1	10,9
PFM001861	6699427	1634000	1053	1			265,3	35,6	0,0012	0,00030	0,14	2721,9	0,47	19500	11,1	2,4	5,4	12,4	10,7
PFM002056	6700134	1627695	1053	1			2,1	48,2	0,0041	0,00074	0,11	2796,4	0,51	15843	10,9	1,4	2,5	6,3	5,6
PFM000433	6697347	1629993	1053	1			215,6	64,0	0,11550	0,02753	0,12	2673,8	0,47	19734	16,9	1,7	3,0	4,9	6,0
PFM001022	6696045	1635946	1053	1			27,3	62,4	0,00404	0,00066	0,14	2687,1	0,32	16109	10,0	2,4	3,6	10,3	9,0
PFM001025	6693864	1635078	1053	1			160,6	76,8	0,18440	0,02386	0,19	2717,6	0,40	25249	18,8	1,4	1,6	5,3	4,7
PFM001898	6699793	1633567	1053	1			68,7	52,2	0,00051	0,00032	0,03	2743,4	0,45	13397	9,3	2,1	3,4	9,3	8,2
PFM000557	6692780	1634208	1054	1			112,6	68,9	0,07266	0,00508	0,37	2742,5	0,34	17168	13,6				
PFM001109	6694416	1636040	1054	1			66,3	-8,3	0,00040	0,00574	0,04	2682,9	0,35	23206	14,0	1,5	5,2	14,4	9,9
PFM001258	6698126	1633997	1054	2												1,6	1,8	5,2	5,1

Group B. Ultramafic, mafic, intermediate and quartz-rich felsic (granitoid) meta-intrusive rocks, continuation.

Group and PFM-number	Coordinates		Geological map. Rock unit	Rock unit, order number	*Geological map. 1=BLS or SL, 2=LS*	*Geological model. Rock domain*	Magnetic properties					Density	Porosity	Electrical properties		Gamma-ray spectrometry properties			
	Northing	Easting					Remanence_declination (deg)	Remanence_inclination (deg)	Remanence_intensity (A/m)	Volume_susceptibility (SI)	Q-value (SI)	Wet_density (kg/m3)	Porosity (%)	Electric resistivity (in fresh water, Ωm)	Induced polarization (phase at 0.6 Hz in fresh water, mrad)	K (%)	U (ppm)	Th (ppm)	Natural Exposure (microR/h)
B7. 101056. Granodiorite, metamorphic																			
PFM000692	6696651	1633697	1056	1			140,8	73,4	0,1442	0,00673	0,37	2703,9	0,50	76646	23,5	1,7	3,3	8,3	7,2
PFM001601	6698409	1628561	1056	1			180,2	72,6	0,05621	0,00687	0,13	2689,1	0,42	16962	11,9	2,2	3,6	10,2	8,7
PFM001616	6695552	1635448	1056	1			217,5	79,9	0,08696	0,01101	0,21	2661,3	0,55	17906	12,1	2,3	3,6	9,8	8,7
PFM001687	6695590	1637041	1056	1			261,7	47,1	0,05840	0,01042	0,16	2685,8	0,38	23122	11,3	2,5	5,1	8,7	9,6
PFM002057	6697686	1632313	1056	1			107,7	83,5	0,23760	0,01563	0,29	2706,3	0,38	30905	16,0	1,0	4,4	8,3	6,9
B10. 101058. Granite, metamorphic, aplitic																			
PFM000687	6696919	1634082	1058	1			97,3	53,6	0,0158	0,00584	0,09	2620,4	0,36	27915	10,5	4,1	6,4	27,9	18,9
PFM000706	6700202	1632056	1058	2			90,4	64,4	0,0622	0,01722	0,10	2646,0	0,45	13447	10,5	2,8	4,9	15,5	12,1
PFM000713	6700615	1632520	1058	1			91,3	77,0	0,0194	0,00179	0,31	2632,7	0,41	11467	9,4	1,4	4,1	16,4	9,7
PFM000724	6701426	1631057	1058	2												2,6	7,6	21,6	15,4
PFM000739	6700227	1633143	1058	1			62,5	83,6	0,0195	0,00491	0,45	2642,6	0,36	15961	15,9	0,8	3,3	16,0	8,3
PFM001156	6701371	1632016	1058	6												3,6	6,8	9,4	12,6
PFM001623	6699909	1634042	1058	1			77,4	54,0	0,04940	0,01217	0,12	2640,2	0,37	18269	14,2	2,6	4,2	13,6	10,8
PFM001636	6702627	1629913	1058	1			249,3	34,6	0,01772	0,00689	0,09	2636,3	0,48	14403	12,6	2,0	5,2	18,5	12,1
PFM001682	6701523	1635604	1058	1			71,5	57,4	0,03716	0,00710	0,08	2629,6	0,38	14064	8,6	4,0	5,1	19,8	15,4

Group B. Ultramafic, mafic, intermediate and quartz-rich felsic (granitoid) meta-intrusive rocks, continuation.

Group and PFM-number	Coordinates		Geological map. Rock unit	Rock unit, order number	*Geological map. 1=BLS or SL, 2=LS*	*Geological model. Rock domain*	Magnetic properties					Density	Porosity	Electrical properties		Gamma-ray spectrometry properties			
	Northing	Easting					Remanence_declination (deg)	Remanence_inclination (deg)	Remanence_intensity (A/m)	Volume_susceptibility (SI)	Q-value (SI)	Wet_density (kg/m3)	Porosity (%)	Electric resistivity (in fresh water, Ωm)	Induced polarization (phase at 0.6 Hz in fresh water, mrad)	K (%)	U (ppm)	Th (ppm)	Natural Exposure (microR/h)
B8/B9. 101057. Granite to granodiorite, metamorphic, medium-grained																			
PFM000168	6699705	1632323	1058	1			16,8	32,2	0,0611	0,00922	0,17	2656,1	0,41	22234	8,4	3,1	4,5	14,9	12,1
PFM000173	6699400	1633329	1058	1			88,0	49,7	0,0502	0,01062	0,16	2648,3	0,36	16797	8,1	3,1	5,1	15,0	12,5
PFM000197	6697201	1634276	1058	1			189,0	61,7	0,0285	0,00515	0,24	2646,4	0,49	16694	9,3	3,8	4,8	19,7	14,8
PFM000203	6697357	1633609	1058	1			122,2	73,1	0,0984	0,01974	0,22	2654,5	0,42	19566	6,6	2,8	5,1	16,9	12,6
PFM000206	6698933	1633474	1058	1			289,4	71,8	0,0128	0,00363	0,07	2652,1	0,52	21287	8,8	3,2	2,5	16,4	11,6
PFM000216	6698919	1632840	1058	1			56,9	47,6	0,0378	0,00675	0,14	2648,0	0,44	16115	4,1	3,4	4,4	15,7	12,8
PFM000259	6699183	1629977	1057	1			62,4	81,3	0,0362	0,01938	0,65	2675,5	0,42	42221	18,2	2,3	3,8	10,6	9,1
PFM000271	6697873	1631554	1058	1			15,7	71,9	0,0201	0,00982	0,13	2656,8	0,40	14080	8,7	2,4	5,6	13,2	11,2
PFM000276	6697997	1631059	1058	1			318,6	78,3	0,0027	0,00017	0,35	2663,6	0,39	25859	13,3	3,1	4,7	14,8	12,2
PFM000513	6694094	1630846	1057	1			190,0	62,4	0,0003	0,00199	0,05	2680,7	0,41	20119	8,3	3,1	4,6	13,1	11,6
PFM000515	6693531	1632489	1057	1			117,5	48,4	0,0277	0,00191	0,14	2678,9	0,48	25135	11,1	2,5	2,7	12,2	9,2
PFM000658	6699102	1631413	1057	1			129,7	84,9	0,0361	0,00626	0,13	2642,2	0,42	22026	7,4	3,5	6,4	15,9	14,2
PFM000680	6697848	1634617	1058	2			163,1	59,6	0,0145	0,00420	0,09	2649,3	0,53	21964	8,4	3,6	2,5	16,9	12,2
PFM000683	6697604	1635393	1058	1			149,4	50,4	0,0451	0,00721	0,11	2648,0	0,46	27415	5,8	2,0	6,6	13,6	11,3
PFM000685	6698095	1635210	1058	1			157,5	45,3	0,0758	0,01277	0,16	2654,7	0,48	20049	9,1	3,2	3,5	16,4	12,1
PFM000694	6698425	1632287	1056	1			298,5	73,8	0,0376	0,00506	0,17	2654,5	0,50	20526	6,0	3,3	3,8	14,1	11,7
PFM000695	6698702	1632180	1058	1			113,3	34,8	0,1158	0,02148	0,11	2646,0	0,45	25212	7,0	3,5	6,1	19,3	15,0
PFM000698	6699798	1631052	1058	1			157,4	73,3	0,0984	0,00790	0,17	2651,1	0,43	22813	8,7	2,3	4,7	15,9	11,3
PFM000701	6700223	1631601	1058	1			118,5	65,6	0,0569	0,00771	0,13	2643,8	0,42	13785	7,6	2,9	4,0	17,5	12,2
PFM000713	6700615	1632520	1058	2			20,2	42,0	0,0020	0,00007	0,55	2656,1	0,38	15736	11,6	1,3	3,5	16,1	9,1
PFM000722	6701111	1630850	1058	1			343,2	61,8	0,0007	0,00017	0,10	2654,5	0,37	20518	6,9	1,5	6,7	16,7	11,7
PFM000770	6701719	1629704	1058	1			156,3	84,4	0,0880	0,00817	0,25	2648,8	0,41	20787	9,4				
PFM000772	6701787	1629778	1058	1												3,5	5,7	16,4	13,8
PFM000890	6698713	1633190	1058	1			44,4	78,0	0,0329	0,00425	0,21	2649,0	0,52	13055	8,1	3,4	2,2	13,4	10,7
PFM001159	6699761	1632635	1058	1			26,8	77,9	0,0488	0,00465	0,24	2655,9	0,40	20022	13,2	3,4	4,5	13,5	12,0
PFM001173	6699900	1632964	1058	1			162,3	77,3	0,1338	0,01450	0,25	2648,9	0,35	10454	5,9	2,7	4,9	16,9	12,3
PFM001180	6698125	1633127	1058	1			221,5	77,9	0,0310	0,00336	0,18	2645,3	0,47	23206	10,3	3,2	5,6	17,9	13,8
PFM001183	6698025	1632858	1058	1			150,1	39,5	0,0099	0,00756	0,04	2648,9	0,50	29889	9,2	2,8	6,3	15,8	13,1
PFM001213	6700856	1630163	1058	1			129,6	76,8	0,0053	0,00135	0,11	2654,7	0,34	18277	7,6	3,0	6,5	17,4	14,0
PFM001251	6700093	1630330	1058	1			339,7	80,5	0,0062	0,00340	0,09	2679,1	0,44	45746	10,9	2,8	6,1	14,5	12,6
PFM001864	6698802	1635370	1058	1			334,2	17,9	0,0975	0,00521	0,18	2647,5	0,51	11498	6,9	2,9	5,7	16,5	13,0
PFM001879	6696859	1632494	1057	1			320,1	73,6	0,2117	0,02546	0,21	2666,8	0,53	21764	16,9	2,2	3,9	10,1	8,9
PFM000293	6698480	1631372	1057	1			132,9	80,1	0,10860	0,00510	0,33	2722,3	0,50	25740	14,9	1,7	3,1	6,0	6,3
PFM000580	6694140	1633155	1057	1			145,7	56,0	0,00762	0,00215	0,14	2720,1	0,41	14817	7,6				
PFM001867	6697015	1635815	1057	1			75,8	-1,3	0,00269	0,00323	0,39	2661,6	0,33	28174	10,3	2,8	4,1	17,4	12,2
PFM001870	6696507	1634882	1057	1			15,5	29,4	0,00075	0,00018	0,09	2691,2	0,41	16220	10,4	2,3	4,6	9,4	9,2
PFM002221	6694642	1635144	1057	1			319,1	49,5	0,04780	0,00863	0,11	2654,7	0,43	17233	11,5	2,8	5,5	13,0	11,7
PFM000214	6699329	1633594	1058	1			98,4	69,1	0,07959	0,01021	0,18	2654,3	0,58	10312	12,5	3,1	4,1	16,7	12,4
PFM000666	6698103	1633921	1058	1												3,2	3,2	21,0	13,4
PFM001043	6702115	1630585	1058	1			154,9	69,0	0,11290	0,01431	0,16	2646,7	0,30	20478	11,1	3,0	7,1	16,1	13,9
PFM001081	6701811	1632822	1058	1												3,9	3,7	22,3	15,0
PFM001635	6702146	1629682	1058	1			95,1	76,3	0,05744	0,00921	0,14	2650,5	0,36	17660	8,9	3,0	6,0	13,7	12,5
PFM001666	6701696	1636576	1058	1			165,7	45,6	0,08078	0,01704	0,12	2654,2	0,43	8857	9,7	3,4	4,2	15,8	12,7
PFM001958	6703795	1633914	1058	2			31,6	71,5	0,00180	0,00019	0,27	2648,1	0,43	7212	8,0	2,4	7,6	11,3	11,9
PFM005193	6699251	1634961	1058	1			130,8	41,4	0,10520	0,01410	0,23	2655,6	0,42	18338	10,4	3,1	4,6	18,5	13,4
PFM005226	6698116	1637182	1058	1			348,3	57,9	0,01127	0,00311	0,08	2652,8	0,47	8142	11,1	3,0	3,6	15,9	11,7
PFM005288	6697002	1638048	1058	1			163,6	46,1	0,04303	0,00770	0,11	2649,5	0,46	21936	11,8	3,5	2,6	15,3	11,6
PFM005599	6699324	1631720	1058	1												3,3	4,9	14,8	12,7
PFM005602	6698786	1632353	1058	1			69,3	54,9	0,00054	0,00017	0,10	2659,5	0,34	16933	7,7	2,5	4,4	15,1	11,2

Group C. 101051. Granite, granodiorite and tonalite, metamorphic, fine- to medium-grained.

Group and PFM-number	Coordinates		Geological map. Rock unit	Rock unit, order number	*Geological map. 1=BLS or SL, 2=LS*	*Geological model. Rock domain*	Magnetic properties					Density	Porosity	Electrical properties		Gamma-ray spectrometry properties			
	Northing	Easting					Remanence_declination (deg)	Remanence_inclination (deg)	Remanence_intensity (A/m)	Volume_susceptibility (SI)	Q-value (SI)	Wet_density (kg/m3)	Porosity (%)	Electric resistivity (in fresh water, Ωm)	Induced polarization (phase at 0.6 Hz in fresh water, mrad)	K (%)	U (ppm)	Th (ppm)	Natural Exposure (microR/h)
PFM000168	6699705	1632323	1058	2												2,2	6,5	22,5	14,3
PFM000698	6699798	1631052	1051	5						0,00014									
PFM000703	6700277	1632226	1051	2			30,6	55,3	0,0221	0,00348	0,09	2712,4	0,53	10461	11,1	1,9	3,0	10,4	8,0
PFM000718	6700543	1632654	1051	3			335,3	74,5	0,0025	0,00040	0,09	2693,7	0,39	15558	14,6	1,4	5,8	11,5	9,3
PFM000739	6700227	1633143	1051	2			345,9	58,4	0,0824	0,01921	0,12	2704,9	0,46	15740	17,6	1,2	7,5	11,3	10,0
PFM000822	6699696	1628705	1057	1			117,2	68,1	0,0432	0,00171	0,42	2655,0	0,46	8529	8,0	3,1	4,2	26,7	15,6
PFM001162	6698339	1634013	1051	2			14,7	27,1	0,0005	0,00024	0,05	2737,6	0,47	18252	9,7	1,8	1,9	10,1	7,1
PFM001102	6701738	1635649	1030	2												2,0	2,4	5,4	6,1
PFM005193	6699251	1634961	1054	2			321,7	21,0	0,00037	0,00027	0,04	2713,0	0,52	16887	15,5	2,2	3,5	20,2	11,7
PFM005196	6699859	1637475	1054	1			350,3	31,9	0,05840	0,01619	0,09	2742,6	0,55	13102	15,9	1,5	3,2	11,6	7,9
PFM001094	6702598	1636051	1056	1												1,7	4,9	25,1	13,4
PFM001102	6701738	1635649	1056	1												2,9	3,3	29,2	15,4
PFM001888	6698886	1636321	1056	1			271,6	62,0	0,00053	0,00025	0,05	2731,1	0,47	6959	13,5	2,2	3,8	16,8	10,8
PFM005237	6699944	1636000	1056	1			338,0	70,9	0,10710	0,02539	0,09	2735,6	0,50	10860	16,4	2,0	2,3	12,7	8,3
PFM000196	6699289	1631437	1058	1			89,2	82,9	0,00017	0,00015	0,03	2682,6	0,59	12025	12,7	2,6	3,4	24,3	13,5
PFM005345	6699372	1632115	1058	1												1,8	3,2	11,3	8,2

Group D. Granite, pegmatitic granite, pegmatite. Occurs as dykes and minor intrusive bodies within rocks belonging to Groups A and B. Pegmatites display variable time relationships to Group C.

Group and PFM-number	Coordinates		Geological map. Rock unit	Rock unit, order number	*Geological map. 1=BLS or SL, 2=LS*	*Geological model. Rock domain*	Magnetic properties					Density	Porosity	Electrical properties		Gamma-ray spectrometry properties			
	Northing	Easting					Remanence_declination (deg)	Remanence_inclination (deg)	Remanence_intensity (A/m)	Volume_susceptibility (SI)	Q-value (SI)	Wet_density (kg/m3)	Porosity (%)	Electric resistivity (in fresh water, Ωm)	Induced polarization (phase at 0.6 Hz in fresh water, mrad)	K (%)	U (ppm)	Th (ppm)	Natural Exposure (microR/h)
D1. 111058. Granite, fine- to medium-grained																			
PFM000685	6698095	1635210	1058	4												4,2	6,3	29,9	19,5
PFM000713	6700615	1632520	1058	4			102,9	75,4	0,0534	0,00204	0,22	2631,5	0,48	13017	12,5	4,3	9,5	33,8	22,9
PFM000722	6701111	1630850	1059	3						0,00010									
PFM000807	6699624	1626575	1058	7												4,2	14,9	20,3	22,0
PFM001022	6696045	1635946	1059	2	D1											4,8	3,4	30,1	18,7
PFM005245	6705094	1633496	1058	1	D1		347,5	82,7	0,00490	0,00042	0,29	2644,8	0,51	7897	13,0	3,0	7,7	11,1	12,7
D2. 101061. Pegmatitic granite																			
PFM000198	6697205	1634253	1098	2			189,9	68,9	0,0130	0,00349	0,49	2622,2	0,51	14814	9,3	4,4	3,8	24,1	16,4
PFM000245	6699041	1630358	1098	1			321,0	80,4	0,0196	0,00033	0,44	2630,4	0,58	33483	11,8	4,2	17,5	25,7	25,2
PFM000446	6697966	1630821	1098	2						0,00498						2,1	18,8	10,8	18,2
PFM000680	6697848	1634617	1098	1			87,7	71,4	0,2542	0,00498	0,33	2626,7	0,64	14129	6,8	4,7	2,9	22,2	15,7
PFM000726	6699787	1630715	1098	1			356,3	68,8	0,1167	0,02028	0,20	2631,2	0,48	17936	4,6	2,9	16,0	14,7	18,9
PFM001515	6697287	1630699	1098	2												5,8	10,3	10,2	18,2
PFM001869	6696530	1634832	1098	1			256,6	62,0	0,0179	0,00452	0,40	2620,6	0,45	10865	8,4	4,4	4,8	26,6	18,0
PFM002056	6700134	1627695	1098	2												3,5	17,7	33,6	26,7
PFM001258	6698126	1633997	1098	1	D2											5,0	4,5	28,0	19,0
PFM001618	6695726	1635857	1098	1	D2		16,5	46,1	0,00813	0,00267	0,52	2622,0	0,62	16192	13,9	4,7	2,3	9,6	11,5
PFM001958	6703795	1633914	1098	1	D2											3,7	8,7	4,5	12,4
D3. 101061. Pegmatite																			
PFM000168	6699705	1632323	1061	3												3,9	3,8	17,0	13,5
PFM000233	6696951	1632971	1061	3												4,4	8,3	15,4	16,6
PFM000259	6699183	1629977	1061	2												4,9	14,5	20,6	22,9
PFM000513	6694094	1630846	1061	2												5,0	27,4	18,0	30,2
PFM000680	6697848	1634617	1061	5						0,00057						5,3	7,0	17,2	17,6
PFM000685	6698095	1635210	1061	3												4,7	2,3	20,4	14,9
PFM000725	6701464	1631021	1098	2												3,5	25,8	18,8	27,2
PFM000726	6699787	1630715	1061	3												3,0	61,7	36,4	54,3
PFM000822	6699696	1628705	1061	3												3,1	17,2	51,6	31,5
PFM001162	6698339	1634013	1061	3												5,1	14,7	6,9	19,0
PFM001213	6700856	1630163	1061	2												2,3	17,7	13,6	18,8
PFM001524	6698414	1629838	1061	3												3,2	36,1	19,7	33,4
PFM001858	6698716	1634302	1061	2												4,4	4,0	23,2	16,3
PFM001885	6696272	1632419	1061	2												4,0	17,8	12,7	21,0
PFM001051	6702783	1631243	1061	1	D3											5,6	1,1	2,6	9,9
PFM001654	6704448	1631228	1061	2	D3											5,5	4,4	9,4	13,9
PFM005204	6701571	1633591	1061	1	D3											3,9	14,9	11,7	18,8

Appendix 1b

Gamma-ray spectrometry measurements on bare soil at Storskäret (Results marked in yellow are from 2003)

Bare soil

Group and PFM-number	Coordinates		Geological map. Rock unit												Gamma-ray spectrometry properties			
	Northing	Easting													K (%)	U (ppm)	Th (ppm)	Natural Exposure (microR/h)
Bare soil, Storskäret farmland																		
PFM002648	6697350	1635050	Soil												2,5	1,7	9,7	7,8
PFM002649	6697200	1634180	Soil												2,5	3,5	11,2	9,5
PFM002650	6697559	1635156	Soil												2,5	1,5	8,8	7,5
PFM002651	6697000	1634800	Soil												2,7	2,2	9,3	8,3
PFM002652	6697611	1634822	Soil												2,7	1,8	9,1	8,0

Appendix 2a

A compilation of petrophysical properties for different rock groups

Group A. Supracrustal rocks (23 samples and 23 gamma spectrometry measurements).

	A1. (103076) Dacit and andesite, metamorphic	(Unit)	Arithmetic mean (α95 for remanence directions)	Arithmetic standard deviation (α95 for remanence directions)	Geometric mean	Geometric standard deviation above average	Geometric standard deviation below average	Min	Max	No
Magnetic properties	**Remanence_ declination**	deg.	357.5	14.8						19
	Remanence_ inclination	deg.	76.0	14.8						19
	Remanence_ intensity	A/m			0.0194	0.6326	0.0188	0.0002	3.7850	19
	Volume_ susceptibility	SI			0.00235	0.04163	0.00222	0.00006	0.24000	19
	Q-value	SI			0.21	0.35	0.13	0.05	1.74	19
Density	**Wet_density**	kg/m^3	2,732	79				2,648	2,946	19
Porosity	**Porosity**	%	0.37	0.11				0.20	0.62	19
Electrical properties	**Electric resistivity (in fresh water)**	ohmm			14,374	22,146	8,716	1,725	81,878	19
	Induced polarization (phase at 0.6 Hz in fresh water)	mrad	20.9	14.8				8.3	66.6	19
Gamma-ray spectrometry	**K**	%	2.1	1.0				0.4	4.3	19
	U	ppm	4.3	1.0				2.5	6.8	19
	Th	ppm	11.3	3.0				4.8	15	19
	Natural Exposure	microR/h	9.4	2.5				5.2	13.4	19

Group A. Supracrustal rocks (23 samples and 23 gamma spectrometry measurements).

A2. 109014. Magnetite mineralization associated with calc-silicate rock (skarn)		(Unit)	Arithmetic mean (α95 for remanence directions)	Arithmetic standard deviation (α95 for remanence directions)	Geometric mean	Geometric standard deviation above average	Geometric standard deviation below average	Min	Max	No
Magnetic properties	Remanence_ declination	deg.	106.7	75.0						2
	Remanence_ inclination	deg.	27.6	75.0						2
	Remanence_ intensity	A/m			77.7922	2.7117	2.6204	75.9300	79.7000	2
	Volume_ susceptibility	SI			0.12310	0.00128	0.00127	0.12220	0.12400	2
	Q-value	SI			15.39	0.72	0.69	14.90	15.90	2
Density	Wet_density	kg/m^3	4,177	67				4,130	4,225	2
Porosity	Porosity	%	1.36	0.16				1.24	1.47	2
Electrical properties	Electric resistivity (in fresh water)	ohmm			233	138	87	168	324	2
	Induced polarization (phase at 0.6 Hz in fresh water)	mrad	216.4	22.1				200.8	232.0	2
Gamma-ray spectrometry	K	%	0.9	0.1				0.8	1.0	2
	U	ppm	5.7	0.7				5.2	6.2	2
	Th	ppm	5.7	0.3				5.5	5.9	2
	Natural Exposure	microR/h	6.7	0.1				6.5	6.7	2

Group B. Ultramafic, mafic, intermediate and quartz-rich felsic (granitoid) meta-intrusive rocks (94 samples and 98 gamma spectrometry measurements).

B2/B3. 101033. Diorite, quartz diorite and gabbro, metamorphic		(Unit)	Arithmetic mean (α95 for remanence directions)	Arithmetic standard deviation (α95 for remanence directions)	Geometric mean	Geometric standard deviation above average	Geometric standard deviation below average	Min	Max	No
Magnetic properties	Remanence_ declination	deg.	6.3	12.7						14
	Remanence_ inclination	deg.	79.8	12.7						14
	Remanence_ intensity	A/m			0.0112	0.4413	0.0109	0.0002	22.3900	14
	Volume_ susceptibility	SI			0.00293	0.01914	0.00254	0.00036	0.05592	14
	Q-value	SI			0.10	0.70	0.09	0.01	25.50	14
Density	Wet_density	kg/m^3	2,934	100				2,738	3,120	14
Porosity	Porosity	%	0.37	0.07				0.25	0.54	14
Electrical properties	Electric resistivity (in fresh water)	ohmm			15,315	12,575	6,905	5,412	34,227	14
	Induced polarization (phase at 0.6 Hz in fresh water)	mrad	17.2	8.0				4.8	33.9	14
Gamma-ray spectrometry	K	%	0.8	0.5				0.8	1.8	14
	U	ppm	1.2	0.9				0.0	2.8	14
	Th	ppm	1.7	1.9				0.0	6.7	14
	Natural Exposure	microR/h	2.3	1.6				0.2	6.4	14

Group B. Ultramafic, mafic, intermediate and quartz-rich felsic (granitoid) meta-intrusive rocks (94 samples and 98 gamma spectrometry measurements).

	B5/B6. 101054. Tonalite to granodiorite, metamorphic	(Unit)	Arithmetic mean (α95 for remanence directions)	Arithmetic standard deviation (α95 for remanence directions)	Geometric mean	Geometric standard deviation above average	Geometric standard deviation below average	Min	Max	No
Magnetic properties	Remanence_ declination	deg.	59.5	14.1						20
	Remanence_ inclination	deg.	80.6	14.1						20
	Remanence_ intensity	A/m			0.0087	0.1446	0.0082	0.0002	0.8301	20
	Volume_ susceptibility	SI			0.00201	0.01153	0.00171	0.00020	0.03507	20
	Q-value	SI			0.12	0.21	0.07	0.02	0.71	20
Density	Wet_density	kg/m^3	2,735	42				2,674	2,831	20
Porosity	Porosity	%	0.40	0.07				0.31	0.53	20
Electrical properties	Electric resistivity (in fresh water)	ohmm			15,348	5,949	4,287	6,659	25,249	20
	Induced polarization (phase at 0.6 Hz in fresh water)	mrad	12.3	3.1				7.0	18.8	20
Gamma-ray spectrometry	K	%	1.9	0.4				1.1	2.5	20
	U	ppm	3.7	1.4				1.6	7.4	20
	Th	ppm	8.8	2.5				4.9	14.4	20
	Natural Exposure	microR/h	7.8	2.5				4.7	10.9	20

Group B. Ultramafic, mafic, intermediate and quartz-rich felsic (granitoid) meta-intrusive rocks (94 samples and 98 spectrometry measurements).

	B7. 101056. Grano-diorite, metamor-phic	(Unit)	Arithmetic mean (α95 for remanence directions)	Arithmetic standard deviation (α95 for remanence directions)	Geometric mean	Geometric standard deviation above average	Geometric standard deviation below average	Min	Max	No
Magnetic properties	Remanence_ declination	deg.	211.9	21.1						5
	Remanence_ inclination	deg.	78.6	21.1						5
	Remanence_ intensity	A/m			0.0996	0.0850	0.0459	0.0562	0.2376	5
	Volume_ susceptibility	SI			0.00963	0.00409	0.00287	0.00673	0.01563	5
	Q-value	SI			0.22	0.11	0.07	0.13	0.37	5
Density	Wet_density	kg/m^3	2,689	18				2,661	2,706	5
Porosity	Porosity	%	0.45	0.08				0.38	0.55	5
Electrical properties	Electric resistivity (in fresh water)	ohmm			27,810	23,612	12,770	16,962	76,646	5
	Induced polarization (phase at 0.6 Hz in fresh water)	mrad	15.0	5.1				11.3	23.5	5
Gamma-ray spectrometry	K	%	1.9	0.6				1.0	2.5	5
	U	ppm	4.0	0.7				3.3	5.1	5
	Th	ppm	9.1	0.9				8.3	10.2	5
	Natural Expo-sure	microR/h	8.2	1.1				6.9	9.6	5

Group B. Ultramafic, mafic, intermediate and quartz-rich felsic (granitoid) meta-intrusive rocks (94 samples and 98 gamma spectrometry measurements).

B8/B9. 101057. Granite to granodiorite, metamorphic, medium-grained, metamorphic		(Unit)	Arithmetic mean (α95 for remanence directions)	Arithmetic standard deviation (α95 for remanence directions)	Geometric mean	Geometric standard deviation above average	Geometric standard deviation below average	Min	Max	No
Magnetic properties	Remanence_ declination	deg.	95.8	9.4						45
	Remanence_ inclination	deg.	78.6	9.4						45
	Remanence_ intensity	A/m			0.0220	0.0944	0.0179	0.0003	0.2117	45
	Volume_ susceptibility	SI			0.00408	0.01368	0.00314	0.00007	0.02546	45
	Q-value	SI			0.16	0.12	0.07	0.04	0.65	45
Density	Wet_density	kg/m^3	2,658	17				2,642	2,722	45
Porosity	Porosity	%	0.43	0.06				0.30	0.58	45
Electrical properties	Electric resistivity (in fresh water)	ohmm			18,642	8,517	5,846	7,212	45,746	45
	Induced polarization (phase at 0.6 Hz in fresh water)	mrad	9.5	2.8				4.1	18.2	45
Gamma-ray spectrometry	K	%	2.9	0.6				1.3	3.9	47
	U	ppm	4.7	1.3				2.2	7.6	47
	Th	ppm	15.3	2.9				6.0	22.3	47
	Natural Exposure	microR/h	12.1	1.7				6.3	15.0	47

Group B. Ultramafic, mafic, intermediate and quartz-rich felsic (granitoid) meta-intrusive rocks (94 samples and 98 gamma spectrometry measurements).

B10. 101058. Granite, metamorphic, aplitic		(Unit)	Arithmetic mean (α95 for remanence directions)	Arithmetic standard deviation (α95 for remanence directions)	Geometric mean	Geometric standard deviation above average	Geometric standard deviation below average	Min	Max	No
Magnetic properties	Remanence_ declination	deg.	90.8	24.9						7
	Remanence_ inclination	deg.	74.3	24.9						7
	Remanence_ intensity	A/m			0.0276	0.0204	0.0117	0.0158	0.0622	7
	Volume_ susceptibility	SI			0.00657	0.00691	0.00337	0.00179	0.01722	7
	Q-value	SI			0.14	0.14	0.07	0.08	0.45	7
Density	Wet_density	kg/m^3	2,635	9				2,620	2,646	7
Porosity	Porosity	%	0.40	0.05				0.36	0.48	7
Electrical properties	Electric resistivity (in fresh water)	ohmm			15,876	5,288	3,967	11,467	27,915	7
	Induced polarization (phase at 0.6 Hz in fresh water)	mrad	11.7	2.7				8.6	15.9	7
Gamma-ray spectrometry	K	%	2.7	1.1				0.8	4.1	9
	U	ppm	5.3	1.4				3.3	7.6	9
	Th	ppm	17.6	5.2				9.4	27.9	9
	Natural Exposure	microR/h	12.8	3.3				8.3	18.9	9

Group C. Quartz-rich felsic (granitoid) meta-intrusive rock, fine- to medium-grained. Occurs as dykes and lenses within rocks belonging to Groups A and B (11 samples and 15 gamma spectrometry measurements).

Group C. 101051. Granite, granodiorite and tonalite, meta-morphic, fine- to medium-grained		(Unit)	Arithmetic mean (α95 for remanence directions)	Arithmetic standard deviation (α95 for remanence directions)	Geometric mean	Geometric standard deviation above average	Geometric standard deviation below average	Min	Max	No
Magnetic properties	Remanence_ declination	deg.	351.3	20.3						10
	Remanence_ inclination	deg.	63.4	20.3						10
	Remanence_ intensity	A/m			0.0054	0.0645	0.0050	0.0002	0.1071	10
	Volume_ susceptibility	SI			0.00118	0.00811	0.00103	0.00014	0.02539	11
	Q-value	SI			0.08	0.09	0.04	0.03	0.42	10
Density	Wet_density	kg/m^3	2,711	28				2,655	2,743	10
Porosity	Porosity	%	0.49	0.06				0.39	0.59	10
Electrical properties	Electric resistivity (in fresh water)	ohmm			12,314	4,511	3,302	6,959	18,252	10
	Induced polarization (phase at 0.6 Hz in fresh water)	mrad	13.5	3.1				8.0	17.6	10
Gamma-ray spectrometry	K	%	2.0	0.5				1.2	3.1	15
	U	ppm	3.9	1.6				1.9	7.5	15
	Th	ppm	16.6	7.4				5.4	29.2	15
	Natural Exposure	microR/h	10.6	3.1				6.1	15.6	15

Group D. Granite, pegmatitic granite, pegmatite. Occurs as dykes and minor intrusive bodies within rocks belonging to Groups A and B. Pegmatites display variable time relationships to Group C (11 samples and 30 gamma spectrometry measurements).

D1. 111058. Granite, fine- to medium-grained		(Unit)	Arithmetic mean (α95 for remanence directions)	Arithmetic standard deviation (α95 for remanence directions)	Geometric mean	Geometric standard deviation above average	Geometric standard deviation below average	Min	Max	No
Magnetic properties	Remanence_ declination	deg.						102.9	347.5	2
	Remanence_ inclination	deg.						75.4	82.7	2
	Remanence_ intensity	A/m						0.0049	0.0534	2
	Volume_ susceptibility	SI			0.00045	0.00154	0.00035	0.00010	0.00204	3
	Q-value	SI						0.22	0.29	2
Density	Wet_density	kg/m^3						2,631	2,645	2
Porosity	Porosity	%						0.48	0.51	2
Electrical properties	Electric resistivity (in fresh water)	ohmm						7,897	13,017	2
	Induced polarization (phase at 0.6 Hz in fresh water)	mrad						12.5	13.0	2
Gamma-ray spectrometry	K	%	4.1	0.7				3.0	4.8	5
	U	ppm	8.4	4.3				3.4	14.9	5
	Th	ppm	25.0	9.3				11.1	33.8	5
	Natural Exposure	microR/h	19.2	4.0				12.7	22.9	5

Group D. Granite, pegmatitic granite, pegmatite. Occurs as dykes and minor intrusive bodies within rocks belonging to Groups A and B. Pegmatites display variable time relationships to Group C (11 samples and 30 gamma spectrometry measurements).

D2/D3. (101061) Pegmatitic granite and Pegmatite		(Unit)	Arithmetic mean (α95 for remanence directions)	Arithmetic standard deviation (α95 for remanence directions)	Geometric mean	Geometric standard deviation above average	Geometric standard deviation below average	Min	Max	No
Magnetic properties	Remanence_ declination	deg.	349.5	23.5						6
	Remanence_ inclination	deg.	82.4	23.5						6
	Remanence_ intensity	A/m			0.0322	0.0929	0.0239	0.0081	0.2542	6
	Volume_ susceptibility	SI			0.00281	0.00761	0.00205	0.00033	0.02028	8
	Q-value	SI			0.38	0.16	0.11	0.20	0.52	6
Density	Wet_density	kg/m^3	2,626	5				2,621	2,631	6
Porosity	Porosity	%	0.55	0.08				0.45	0.64	6
Electrical properties	Electric resistivity (in fresh water)	ohmm			16,754	7,713	5,281	10,865	33,483	6
	Induced polarization (phase at 0.6 Hz in fresh water)	mrad	9.1	3.4				4.6	13.9	6
Gamma-ray spectrometry	K	%	4.1	1.0				2.1	5.8	25
	U	ppm	14.6	13.2				2.3	61.7	25
	Th	ppm	20.0	10.2				4.5	51.6	25
	Natural Exposure	microR/h	21.5	9.0				11.5	54.3	25

Group A, B and D. Rock groups with only one observation.

Group	No	Magnetic properties					Density	Porosity	Electrical properties		Gamma-ray spectrometry properties			
		Remanence_ declination (deg)	Remanence_ inclination (deg)	Remanence_ intensity (A/m)	Volume_ suscepti-bility (SI)	Q-value (SI)	Wet_ density (kg/m^3)	Porosity (%)	Electric resistivity (in fresh water, Ωm)	Induced polarization (phase at 0.6 Hz in fresh water, mrad)	K (%)	U (ppm)	Th (ppm)	Natural Exposure (microR/h)
Group A. Supracrustal rocks														
A1. 106001. Sedimentary rock, metamorphic, veined to migmatitic	1	143.0	64.8	0.0005	0.00270	0.06	2,690.8	0.48	10,888	15.9	1.3	5.3	12.8	9.2
A3. No SKB code. Veined gneiss	1	130.6	62.4	0.5328	0.04876	0.413	2,700.9	0.53	11,875	20.0	5.1	4.1	12.8	14.3
A4. 108019. Calc-silicate rock (skarn)	0													
A5. 109010. Sulphide mineralisation	0													
Group B. Ultramafic, mafic, intermediate and quartz-rich felsic (granitoid) meta-intrusive rocks														
B1. 101004. Ultramafic rock, metamorphic	1	30.7	61.2	4.6750	0.04572	2.260	3,044.5	1.04	52	724.8	0.0	0.0	0.0	0.0
B1. 101004. Ultramafic rock, metamorphic, serpentinized	1	100.5	77.6	9.1800	0.10853	1.70	2,785.8	0.88	228	353.7	0.0	0.1	0.0	0.1
B4. 102017. Amphibolite	1	16.2	52.9	0.0001	0.00071	0.004	2,928.3	0.30	11,211	15.3	1.3	1.1	2.6	3.4

Appendix 2b

Gamma-ray spectrometry properties for bare soil at Storskäret

Bare soil, Storskäret farmland (5 gamma spectrometry measurements).

Bare soil, Storskäret farmland		(Unit)	Arithmetic mean	Arithmetic standard deviation	Geometric mean	Geometric standard deviation above average	Geometric standard deviation below average	Min	Max	No
Gamma-ray spectrometry	K	%	2.6	0.12				2.5	2.7	5
	U	ppm	2.2	0.85				1.5	3.5	5
	Th	ppm	9.6	0.98				9.1	11.2	5
	Natural Exposure	microR/h	8.2	0.79				7.5	9.5	5

Delivered data

Appendix 3

Shape-files

Filename	File type	Content
FM_hallsusc_2002-2003	Shp	Site average on susceptibility, standard deviation, maximum and minimum calculated for each outcrop and rock type. Supplementary data from SGU bedrock database.

Tiff-files

Filename	File type	Content
FM_outcrop_magnetic_susceptibility_site-mean_2002_2003_PFM_1_map	Tiff	Site average on susceptibility, calculated for each outcrop and most frequent rock type (rockno = 1).

Grid- and xls-files

Filename	File type	Content
FM_insitu_gammaspektrometri_2003_rock	xls	K, U and Th for each outcrop and rock type
FM_insitu_gammaspektrometri_2003_soil	xls	K, U and Th for each bare soil location
Gammaspek_site-mean_2003_rock	xls	Site average for K, U and Th calculated for each outcrop and rock type
Gammaspek_site-mean_2003_soil	xls	Site average for K, U and Th calculated for each soil sample
FM_prover_ytpetrofysik_2003	xls	Resistivity/induced polarisation, remanence/Q-value, porosity, density and AMS
FM_prover_ytpetrofysik_2003_AMS_sitemean	xls	Site average AMS (magnetic susceptibility anisotropy)
FM_outcrop_magnetic_susceptibility_sitemean_2002_2003	xls	Site average on susceptibility, standard deviation, maximum and minimum calculated for each outcrop and rock type
FM_outcrop_magnetic_susceptibility_sitemean_2002_2003_PFM_1_grid	grid	Site average on susceptibility, calculated for each outcrop and most frequent rock type (rockno = 1).

Appendix 4

Storage of petrophysical samples 2003

The samples are presently stored at GeoVista but will in due time be transferred to the SKB core handling facility at Forsmark.

This appendix constitutes a description on sample identification and a photographic documentation of the core samples from 2003. The corresponding description and documentation of the core samples from 2002 are available in /1/.

The petrophysical samples are stored in small core boxes. A box contains of 5 rows in which a sample location fills one row. The diameter of a sample is 25 mm. The samples are stored in order after when the samples were taken (scode).

All boxes are marked with labels, showing information on:

- Lokal. Locality, internal petrophysical identity (C…)
- Löpnr. Internal petrophysical sample numbers (scode)
- ID code. Identity for geological observation (PFM…)
- Rock No Link to observed rock type

See also examples, below:

SKB FORSMARK Petrofysik 2003

Parameterprover AP PF 400-02-11

GeoVista AB / 2004-02-05

Lokal	**Löpnr 1**	**:**	**Löpnr 2**
IDcode	**:**	**Rockno**	

C4:5	**1**	**:**	**4**
PFM000168	**:**	**1**	

The following pages show photos of the core boxes and give a view of the rock type for each sample location. The caption specifies the idcode and rock_no for each sample location, in order from the top of the photo to the bottom, see example below. The geological reference specimens are marked with tape.

Legend:

Top of photo Bottom of photo

PFM001043 Rock_no: 1 **PFM001635** Rock_no: 1 **PFM001636** Rock_no: 1 **PFM005204** Rock_no: 2 **PFM005245** Rock_no: 3

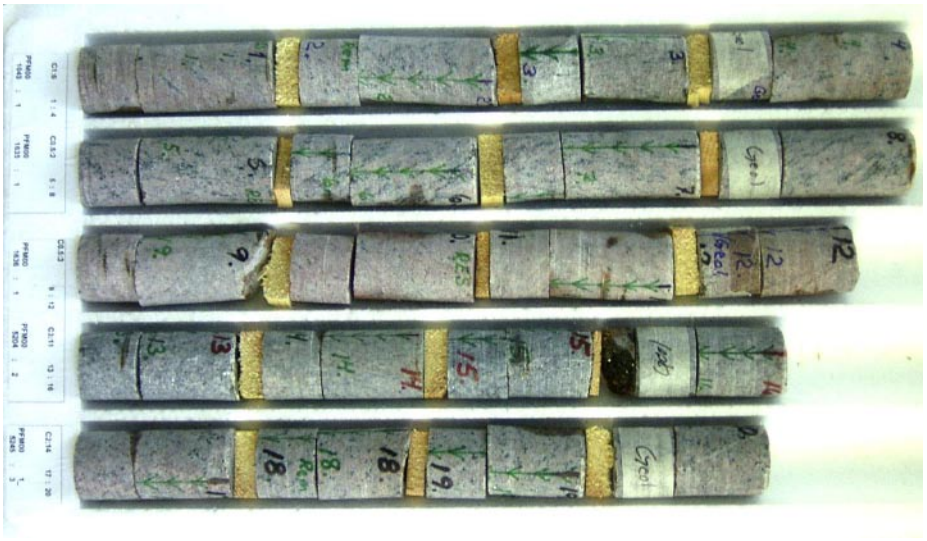

PFM001043 Rock_no: 1 **PFM001635** Rock_no: 1 **PFM001636** Rock_no: 1 **PFM005204** Rock_no: 2 **PFM005245** Rock_no: 1_3

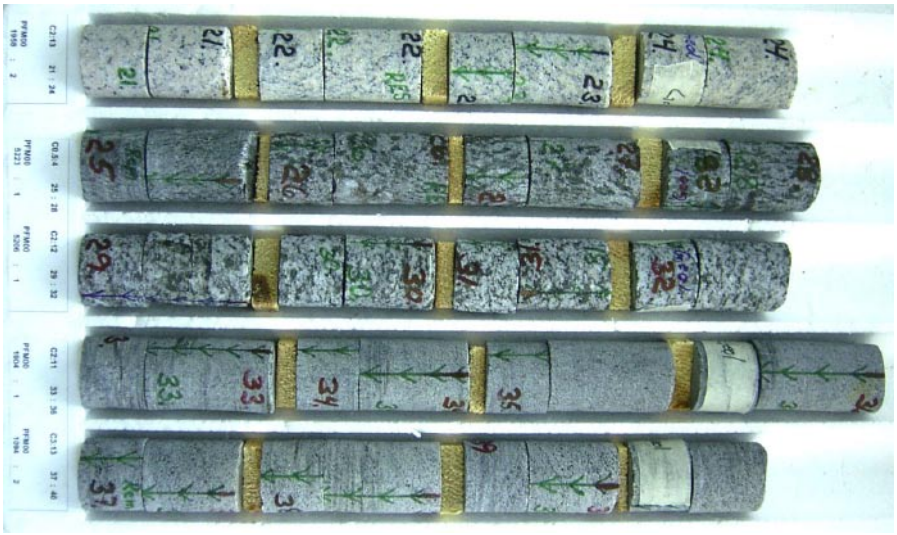

PFM001958 Rock_no: 2 **PFM005223** Rock_no: 1 **PFM005206** Rock_no: 1 **PFM001904** Rock_no: 1 **PFM001094** Rock_no: 2

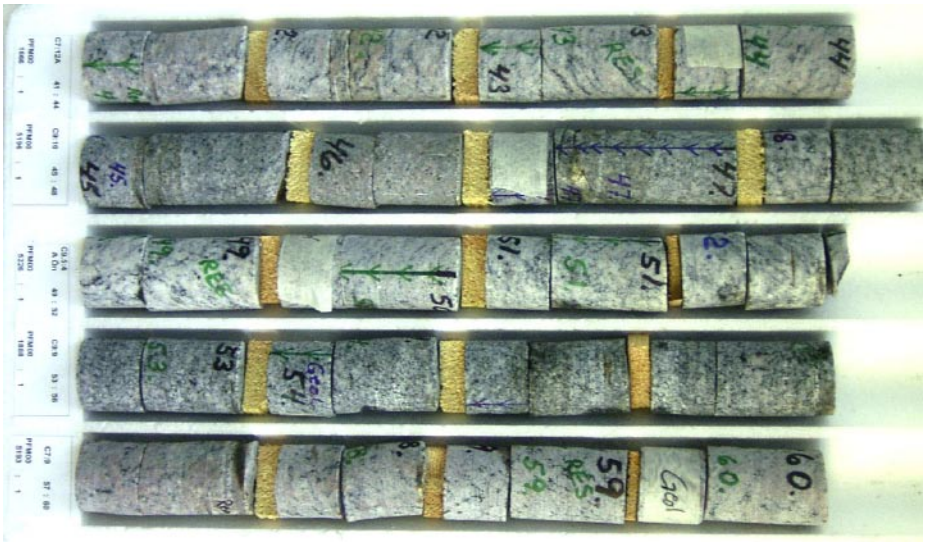

PFM001666 Rock_no: 1 **PFM005196** Rock_no: 1 **PFM005226** Rock_no: 1 **PFM001888** Rock_no: 1 **PFM005193** Rock_no: 1

PFM005193 Rock_no: 2 **PFM001022** Rock_no: 1 **PFM001618** Rock_no: 1 **PFM001616** Rock_no: 1 **PFM005288** Rock_no: 1

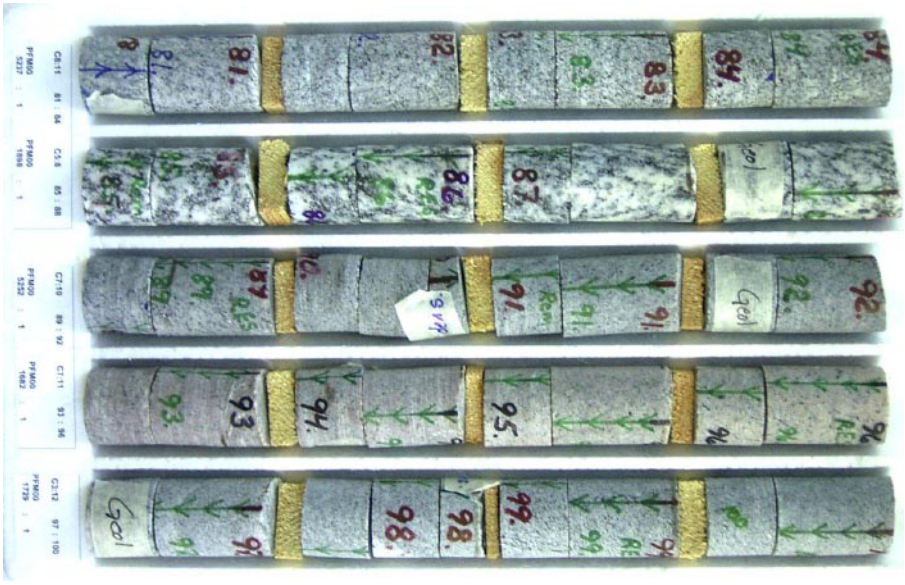

PFM005237 Rock_no: 1 **PFM001898** Rock_no: 1 **PFM005252** Rock_no: 1 **PFM001682** Rock_no: 1 **PFM001729** Rock_no: 1

PFM000214 Rock_no: 1 **PFM001640** Rock_no: 2 **PFM001654** Rock_no: 1 **PFM005215** Rock_no: 1 **PFM001728** Rock_no: 1

PFM001025 Rock_no: 1 **PFM001687** Rock_no: 1 **PFM001109** Rock_no: 1 **PFM001623** Rock_no: 1 **PFM005602** Rock_no: 1

PFM001867 Rock_no: 1 **PFM001870** Rock_no: 1 **PFM002221** Rock_no: 1 **PFM001601** Rock_no: 1 **PFM000433** Rock_no: 1

PFM000557 Rock_no: 1 **PFM000580** Rock_no: 1 **PFM002057** Rock_no: 1 **PFM000293** Rock_no: 1 **PFM000196** Rock_no: 1

Appendix 5

Gamma-ray spectrometry measurement performed by SGU (PFM002648)

Gamma-ray spectrometry measurements were carried out on 4 locations of bare soil on the Storskäret farmland in the southeast part of the candidate area, Section 7, Figure 7-2, 7-4 f and 7-5. The purpose was to investigate the radiogenic distribution and the possible source of the Th-K dominated, high intensity pattern identified from the helicopter borne gamma-ray spectrometry survey /26, Figure 4-21/, which characterizes the area around Storskäret.

The final compilation of measurements on bare soil also includes another 7 measurements on 1 location used as a calibration spot for the helicopter borne geophysical survey /5/, see Table below.

	P0	P1	P2	P3	P4	P5	P6	P7	P8	P9	P10	P11	P12	P0
K (%)	2.5	2.6	2.6	2.4	2.5	2.4	2.5	2.6	2.5	2.6	2.6	2.4	2.6	2.5
U (ppm)	1.8	1.5	1.2	1.8	1.7	2.0	1.9	2.4	2.5	3.5	3.6	4.0	4.1	4.4
Th (ppm)	9.5	11.3	9.4	9.1	10.2	9.4	9.3	10.0	9.4	10.1	10.7	10.4	11.8	9.7

Notes:

- Instrument, ExploraniumGR-320 (SGU), 240 sec measurement. Sören Byström, Hossein Shomali, SGU 2002-09-16
- At point P6 rain starts.
- Uranium is significantly affected by radon from measurement P7 and hence, only measurements P0–P6 are used in this compilation.
- Centre coordinate is approximately 1635050, 6697350 and distance between each measurement about 30 m. The location is uncertain with a 100 m error estimate.
- Survey lay out: